SURFACE MODIFICATION OF TITANIUM-BASED ALLOYS

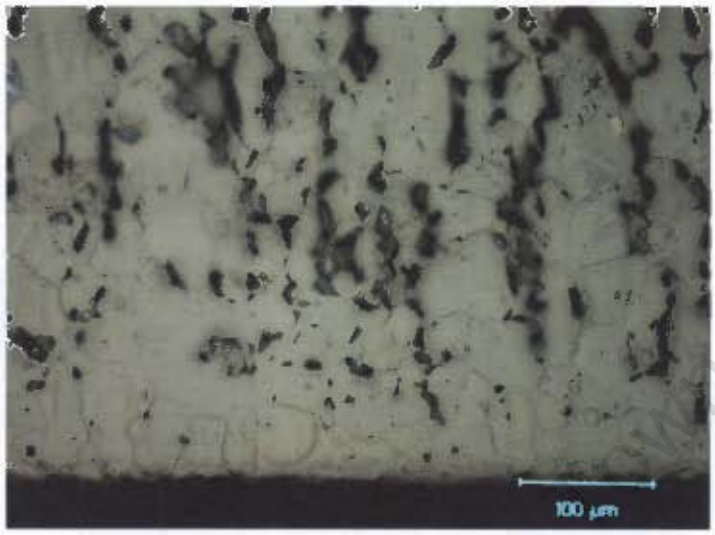

By

Sigqibo Templeton Camagu

A thesis submitted to the faculty of Engineering and the Built Environment of the University of Cape Town in fulfilment of the requirements for the degree of MSc(Applied Sciences) in Materials Engineering

Centre for Materials Engineering
Department of Mechanical Engineering
University of Cape Town
March 2007

DECLARATIONS:

1. I hereby grant the University of Cape Town free licence to reproduce for the purpose of research either the whole or any portion of the contents in any manner whatsoever of the above dissertation. I am presenting this dissertation in **FULL** fulfilment of the requirements for my degree.

2. I know the meaning of plagiarism and declare that all of the work in the document, save for that which is properly acknowledged, is my own.

Signature:. .....

Date:..... 29 MARCH 2007 .....

Acknowledgements

I am particularly grateful to my supervisor, A/Professor R D Knutsen for his valuable suggestions and relentless efforts which have made this work possible. Under his supervision and direction the quality of this work improved greatly.

I would also like to express much gratitude and appreciation to the following people who assisted me in one way or the other during the course of the project work.

- Glen Newins and the workshop staff for their technical assistance in machining the test pieces.
- Mrs P Park–Ross for her technical and logistical assistance in the laboratories.
- Mrs N S Africa for all the administrative assistance.
- Mrs F D Young for helping us to maintain a clean working environment.
- Miss Nandipha Naki for her assistance in keeping the working place neat as well as her friendly chats.
- The staff and students of the Centre for Materials Engineering for their constant words of encouragement.
- The NRF for the financial support of the research and the UCT/CSIR for supporting me during this research.

I would also like to thank my mother and my family for their encouragement throughout my life.

To Nomonde (my wife), thank you for your love, prayers and constant support during the course of this work.

The greatest of all the thanksgiving goes to God Almighty for giving me the strength and energy throughout the course of this study.

Abstract

Two routes of Oxygen Diffusion Hardening (ODH) have been investigated on two alloys of titanium, Ti-6Al-4V and Ti-6Al-7Nb (by weight). The first route involves a controlled atmosphere where argon saturated with water was used to transport water into the test pieces at elevated temperatures. The controlled atmosphere would encourage the generation of mono-atomic oxygen through the dissociation of water vapour, and therefore change the kinetics of physical absorption and diffusion of oxygen into titanium. The second route of ODH investigated was the Oxygen Boost Diffusion Hardening (OBDH). The oxygen boost diffusion hardening process was carried out in two steps. The first step was oxidation of the samples in air at elevated temperatures and the second step was to further diffusion treat the pre-oxidised test pieces in a vacuum or argon. Various temperature and time combinations were used on both steps of OBDH.

The results revealed that the ODH heat-treatment in a controlled saturated argon environment was unsuccessful in developing a significant oxygen diffusion hardened layer.

The OBDH process can be carried out to modify the surface properties of titanium and alloys. Both steps of this process play a vital role in achieving a thick modified layer for improved tribological properties of titanium and alloys. Performing the oxidation step of OBDH heat-treatment at higher temperatures results in higher surface hardness and deeper diffusion zone than carrying the oxidation step at lower temperatures for longer times provided there is no peeling of the oxide scale during the high temperature oxidation. The Ti-6Al-4V achieves higher surface hardness than the Ti-6Al-7Nb upon the same OBDH heat-treatment.

The second step of the OBDH can also be carried out in an argon environment instead of vacuum. Carrying out the second step in an argon atmosphere allowed for higher surface hardness and thicker hardened zone than carrying the same step in vacuum. The effect of the OBDH on the underlying microstructures of two alloys under investigation is the depletion of the β phase on the modified surface as a result of the

diffused oxygen which stabilises the α phase. Although higher surface hardness was achieved for the Ti-6Al-4V alloy than the Ti-6Al-7Nb alloy after the same heat-treatment, the Ti-6Al-7Nb alloy achieved higher wear resistance due to more adherence of the oxide scale after the oxidation step. Despite achieving higher surface hardness and thicker hardened zone upon carrying out the second step of OBDH in an argon atmosphere than in vacuum, samples which underwent the second step of OBDH heat-treatment in vacuum exhibited higher wear resistance. Performing a twin cycle OBDH heat-treatment results in even higher surface hardness and higher wear resistance despite the severe scaling of the alloys upon the heat-treatments.

Table of Contents

Glossary

Ti64	Ti-6Al-4V (weight percent)
Ti67	Ti-6Al-7Nb (weight percent)
ODH	Oxygen Diffusion Hardening
PTFE	Polytetrafluoroethylene
UHMWPE	Ultra-High-Molecular-Weight Polyethylene
TJR	Total Joint Replacement
HCP	Hexagonal Close Packed
BCC	Body Centred Cubic
Ms	start of Martensite
PVD	Physical Vapour Deposition
OBDH	Oxygen Boost Diffusion Hardening
rpm	revolutions per minute
SIMS	Secondary Ion Mass Spectrometry
HRC	Rockwell hardness C
Hv	Vickers Hardness
J	Flux of mass transfer
D	Diffusion coefficient
Q	Activation energy of dependence

Chapter One

Introduction

1.1 Background

Total joint replacements have been widely accepted in the past 14 years[1,2]. Destructive joint diseases including osteonecrosis, rheumatoid arthritis, osteoarthritis and severe pathologic fractures have led to materials being used as replacements to the bone[2]. In many instances arthritis destroys the joint and the patient will experience pain. X-ray pictures of the joint can reveal that arthritis is destroying the joint. The pictures in figure 1.1 show a normal hip and a hip that is degraded by arthritis.

Figure 1.1: X-ray picture of a hip joint[3].

a) Normal hip. **b) Hip with arthritis**

In figure 1a, the space between the head of the femur and the acetabulum is due to the cartilage not showing up on x-ray. There is very little space in figure 1b which is indicative of the degraded cartilage.

1.2 Motivation of the Research

The use of implants in the body poses lots of challenges. Once the implant has been used to replace a bone in the body it cannot be readily monitored or replaced. This comes not only with short term challenges such as strength requirements and manufacturing but also long term requirements such as resistance to fretting, retaining of the strength for a long time and compatibility. The implant has to perform such a specialised and complex function such that more stringent requirements are needed from the constructional material[4]. The requirements of the implant material are summarised in table 1.1.

Table 1.1: Requirements of the implant materials[4].

Compatibility	Mechanical Properties	Manufacturing

• Tissue reactions
• Changes in properties
  • **Mechanical**
  • **Physical**
  • **Chemical**
• Degradation leads to
  • **Local deleterious changes**
  • **Harmful systemic effects**
	• Elasticity
	• Yield stress
	• Ductility
	• Time dependent deformation
	  • **Creep**
	• Ultimate strength
	• Hardness
	• Wear resistance
		• Fabricating methods
		• Consistency and conformity to all requirements
		• Quality raw materials
		• Superior techniques to obtain excellent surface finish or texture
		• Capability of material to get safe and efficient sterilisation
		• Cost of product

The lack of material that would be tolerated by the body as well as possess the required properties has been the major drawback in orthopaedic surgery. Engineers have played a vital role in developing materials that can be used as replacements to the bone. Ti-6Al-4V has been used extensively for metallic implants. Ti-6Al-7Nb has been developed as an alloy that has better properties than the standard Ti-6Al-4V for metallic implants. Can the shortcomings of these two alloys be altered to ensure that the superior properties that titanium alloys have in the biomaterial field are not lost?

1.3 Objectives

Various methods of surface modification have been employed to improve the wear resistance of titanium-based alloys. All these techniques have not been overly successful. Corrosion attack is exacerbated at the coating-substrate interface on the coated materials. Loosely bound surface oxide on oxidised material has eliminated thermal oxidation as a surface treatment. Modified surfaces of less than 2 μm achieved through ion implantation has also proved rather less successful. Nitriding titanium and alloys has resulted in components with nodular surfaces. A further activity is then required to rehabilitate the surface of the nitrided components. Diffusion treatments have recently been developed to overcome various problems encountered with the techniques mentioned above. High reactivity of titanium towards oxygen, nitrogen and carbon forms the basis of the diffusion treatments. Instead of forming a thin poorly adherent ceramic layer O, N, and C diffuse into the interstitial sites of the titanium matrix forming a solid solution which causes obstruction of the dislocation movement resulting in a harder and more wear resistant metal surface. The techniques used to improve the tribological properties of titanium are outlined in detail in chapter two.

The aim of this research is to modify the surfaces of Ti-6Al-4V and Ti-6Al-7Nb for medical implants via Oxygen Diffusion Hardening (ODH). The oxygen diffusion hardening process should be reasonably obtainable, result in a thicker modified surface that is compatible with the component substrate. As the modification process is done on net-shaped components there should be no dimensional changes on the components after the ODH process and the surface integrity of the hardened component should be preserved. The ODH process should result in improved wear resistance on the titanium test pieces.

1.4 Thesis Layout

The work conducted during this research is presented in various chapters. The first chapter has been used to introduce the research. The second chapter will then review the work that has been done which is related to this research. The experimental

techniques used to conduct this research are outlined in chapter three. The results obtained from the experiments are presented and discussed in chapter four. Conclusions drawn from the results are stated in chapter five and the recommendations for future work are listed in chapter six.

Chapter Two

Literature Review

2.1 Materials Used in Total Joint Replacement.

There are various materials that have been used as replacements to the bone in orthopaedic surgery. These materials fall into two groups, surface-modified metallic materials and ceramics. Metallic alloys used in joint replacements include, cobalt alloys, austenitic stainless steels and titanium alloys[5]. To avoid a galvanic couple it is useful to use identical metals. This concept was used as the original hip prosthesis components were manufactured from stainless steel components[2,6]. It was soon discovered that metal-on-metal artificial joints was not the best tribological design due to non-optimum fit between the articulating surfaces which results in excessive wear[6,7,8].

As an alternative to the metal-on-metal joints, Sir John Charnely developed a concept of low friction arthoplasty in the 1960s[6]. In his work he designed a small-diameter metallic femoral head articulating with a polymeric acetubular cup. The polymeric acetubular cup was originally made from polytetrafluoroethylene (PTFE) which was later replaced by ultra-high-molecular-weight polyethylene (UHMWPE)[6,9]. Although this design was widely accepted (with UHMWPE being the dominant orthopaedic material for 30 years), wear of UHMWPE when rubbing against metal femoral heads has been observed[6]. Various materials combinations were considered where it was concluded that the ceramic in the ceramic/UHMWPE prostheses caused less wear to the UHMWPE compared to titanium and cobalt based alloys[6,10,11,12,13]. Ceramic materials involve the use of alumina and zirconia types[5]. Various materials combinations used in total joint replacements (TGR's) are shown in table 2.1.

Table 2.1: Materials combinations in TGR's.[6]

Femoral Component	Hip/tibial component	Results
Co-Cr-Mo	Co-Cr-Mo	Early loosening rate and limited use. New developments show lowest wear rate.
Co-Cr-Mo	UHMWPE	Widely employed, low wear
Alumina/zirconia	UHMWPE	Very low wear rate. Zirconia more impact resistant.
Alumina	Alumina	Minimum wear rate.
Ti-6Al-4V	UHMWPE	Reports of high UHMWPE wear due to a breakdown of titanium surface.
Surface coated Ti-6Al-4V	UHMWPE	Enhanced wear resistance to abrasion. Only thin treated layer achieved.

Reports on possible harmful effects of UHMWPE such as sterilisation as well as the development of the metal-on–metal technology, through optimisation of cobalt based alloys, manufacturing process and prostheses geometry has seen metal-on-metal prostheses being the most widely used in Europe[6,14]. Of all the possible joint replacement materials, titanium alloys have received the most attention in recent times. This is due to inherent properties of titanium that are very attractive to orthopaedic surgery.

2.2 Titanium Alloys in Orthopaedic Surgery

Titanium is a transition metal with physical properties that are shown in table 2.2:

Table 2.2 Physical properties of titanium[15]

Physical Property	Value
Lattice Parameter(α Ti)	a = 2.95Å b = 4.68Å
Young's Modulus (polycrystalline titanium)	107 GPa
Density	4.505 gcm^{-3}
Latent heat of ($\alpha \Leftrightarrow \beta$) transformation	678 $cal.mol^{-1}$
Melting temperature	1668°C
Latent heat of fusion	5 $Kcal.mol^{-1}$
Latent heat of evaporation	112.5 $Kcal.mol^{-1}$
Specific heat	0.1248 cal/°C/g
Thermal expansion (at 15°C)	$8.35x10^{-6}$/°C
Resistivity(at room temperature)	$42\text{-}63x10^{-6}$ohm.cm
Atomic weight	44.88g
Atomic number	22

Although pure titanium has superior corrosion resistance, titanium alloys are more useful than pure titanium in applications where mechanical strength is required. Titanium and its alloys show very high resistance to corrosion attack. This is due to the passivity of the metal's oxide which provides resistance to contamination below

535°C[16]. Titanium alloys have shown excellent biocompatibility. Biocompatibility means the metal is non-toxic and ions released by the metal do not have adverse effects on the surrounding body tissue. Chemistry and texture of this metal mediate the biomaterial-tissue interaction[17,18,19,20,21,22,23]. Lavos-Valereto et al.[24] evaluated the growth and viability of cultured osteoblast-like cells on Ti-6Al-7Nb alloy with or without plasma-sprayed hydroxyapatite coating. The conclusions drawn from the cell viability and structural studies reveal that Ti-6Al-7Nb has relevant biological and physical properties as an implant material[24]. Another important property of this metal is its high strength-to-weight ratio. Superior specific mechanical properties are achievable as a result of strengths up to 1400MN.m^{-2} combined with density of 4.505gcm^{-3} [16].

2.2.1 Structure and Properties of Titanium and its Alloys

High chemical reactivity has delayed the development of titanium due to the difficulty associated with melting, casting into ingots and hot working of this metal[25]. Special high-stability refractories such as zirconia, thoria, and yttria are used during the casting instead of the conventional silica and zirconium silicate moulds[26]. Conventional refractories result in components with unacceptable surface finish and gross porosity[26]. Low density, high thermal stability and high strength make titanium a candidate for aerospace and structural application. Indeed initial work on the metal has been based on titanium being a possible replacement to aluminium in aerospace applications due to titanium's superior thermal integrity.

Titanium exhibits a hexagonal close packed (HCP) alpha (α) phase at room temperature which transforms into a body centred cubic (BCC) beta (β) phase at 880°C[25]. The temperature at which this allotropic phase transformation occurs is known as the transus temperature[27]. Pure titanium is restricted to applications that involve moderate loads. The mechanical properties of pure titanium are shown in table 2.3.

Table 2.3: Mechanical properties of commercially pure titanium [25].

Material	Chemical Analysis, percent	Tensile Strength MPa	Yield Strength MPa	Percent Elongation	BHN
Ti	99 Ti	262 to 690	151 to 586	17 to 30	115 to 220

Titanium-based alloys are employed in applications where high mechanical strength is required[28]. A wide range of physical and mechanical properties are achievable by addition of alloying elements[27]. Addition of these elements alters the transus temperature. Some elements stabilise the α phase thereby giving the "all α" alloys. Other elements will stabilise the β phase resulting in the "all β" alloys[28]. A β-alloy will contain enough β stabilisers such that 100% β is retained upon quenching above β transus. The alloy therefore has a beta stabilising content to an extent that the chemical composition lies above β_c, in figure 2.1.

Figure 2.1: Pseudo-binary phase diagram of Ti-β stabilizer[6].

Addition of controlled amounts of α and β stabilising elements results in an α-β alloy at room temperature. Alloying solutes such as manganese, chromium, iron, copper, tantalum, molybdenum, niobium and vanadium stabilize the β phase and lower the

temperature of transformation from β to α[27]. Aluminium is the most notable alloying element that stabilises the α phase of titanium[28]. Other elements that stabilise the α phase include carbon, oxygen and nitrogen[6]. Tin and zirconium are neutral solutes that have little effect on the transformation temperature[27]. Depending on the microstructure that an alloy exhibits it will have certain properties. Near α and α titanium alloys have superior corrosion resistance with limited application on medical implants due to their low ambient temperature strength[6]. The α + β alloys exhibit higher strength due to the presence of the two phases. The β alloys and metastable β alloys exhibit high strength, good formability as well as high hardenability[6]. The β alloys have been earmarked as the alloys that will be very useful in total joint replacement. Combination of low elastic modulus and superior corrosion resistance are the unique properties that these alloys have presented to the science of orthopaedic surgery[6].

2.2.1.1 Ti-6Al-4V

Ti-6Al-4V is the alloy that has been widely used in surgical implants. It is the most commonly used alloy due to its high strength, workability and good fatigue resistance, good corrosion resistance and high biocompatibility[28]. Although this alloy was initially designed for aerospace application it is used extensively in surgical implants, pressure vessels, aircraft turbine and compressor blades and disks[6]. Aluminium is an α phase stabiliser while vanadium is a β phase stabiliser. The effects of the two solutes on phase transformation of the titanium metal are depicted by the phase diagrams in figure 2.2a-b.

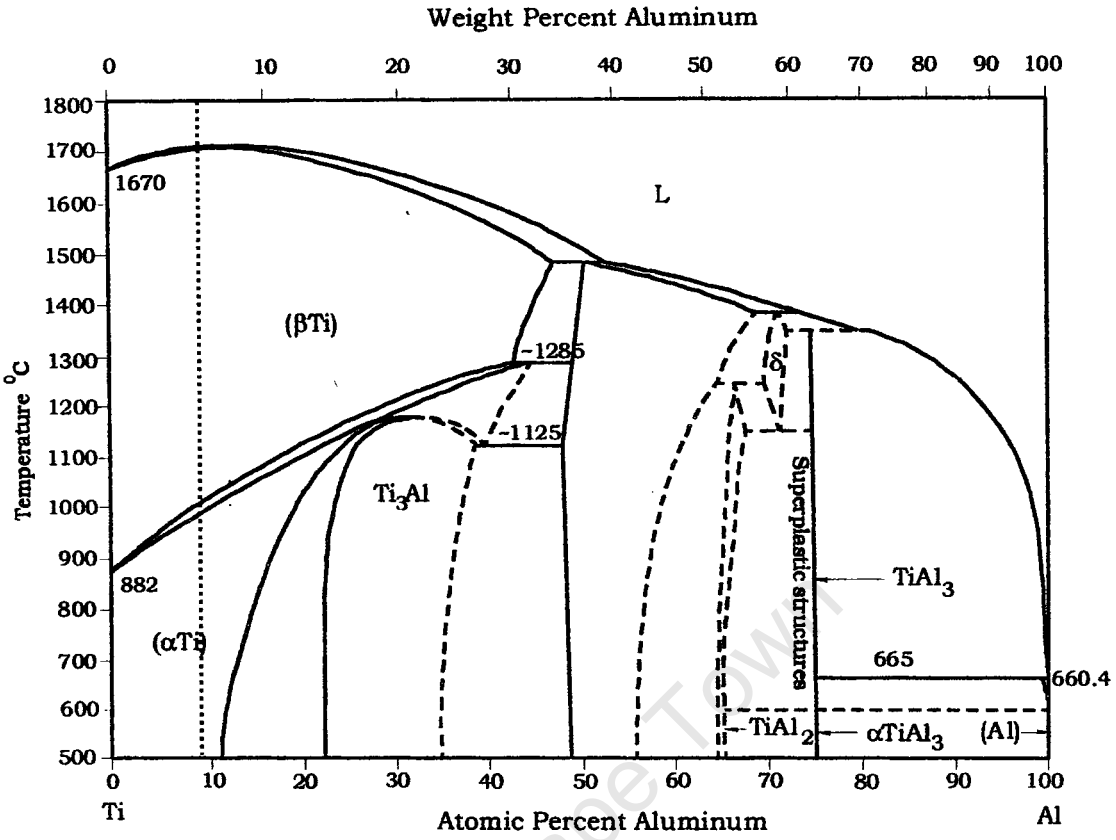

Figure 2.2a: Ti-Al binary phase system[29,30].

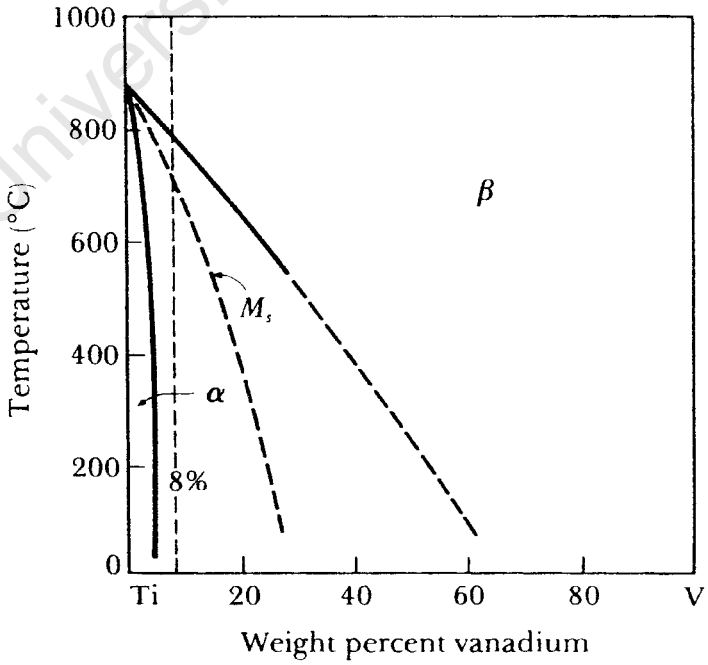

Figure 2.2b: Ti-V binary phase diagram[16].

Addition of controlled amounts of the two elements results in the stability of alpha and beta phases at room temperature. The annealed microstructure of the alloy shows the dark β phase at the grain boundaries of the white α phase as shown in figure 2.3a.

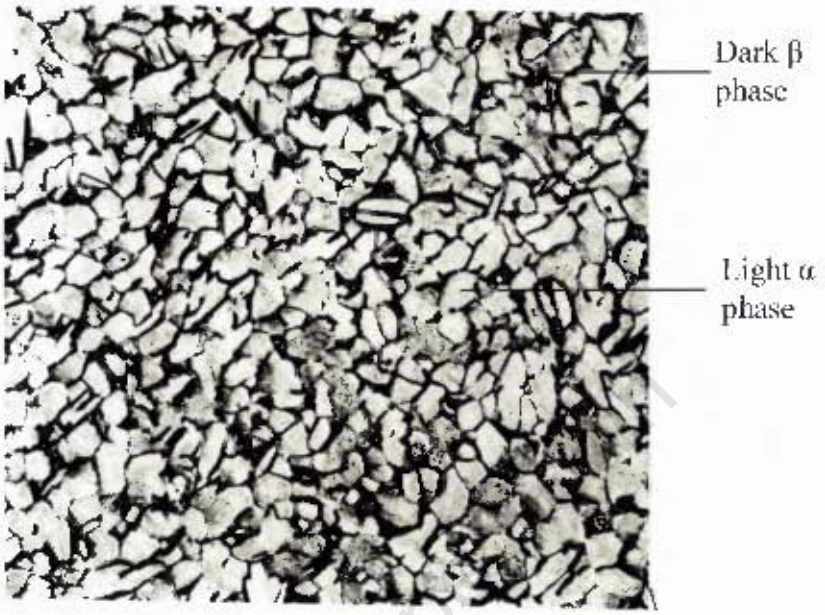

Figure 2.3a: Ti-6Al-4V bar held for 1 hr at 956°C and furnace cooled[31].

The two binary systems of Ti-Al and Ti-V indicate that titanium dissolves about 7% aluminium while complete solubility is noted for the titanium-vanadium binary system.

2.2.1.1.1 Heat-Treatment of Titanium Alloys and Mechanical Properties of Ti-6Al-4V.

Ti-6Al-4V exhibits a β transus temperature at 890°C according to Shivpuri et al.[32]. This is different from the reports made by Kerr et al.[33]and Ilyn et al.[34] who have studied the alteration of the β transus temperature with the additions of hydrogen on this alloy. Both these studies suggest a β transus temperature of around 1000 °C for this alloy. At this temperature α and β phases transform into an "all β" system. There are several heat treatments that are used for titanium alloys. Titanium castings that are heat treated yield products of comparable or even higher mechanical properties to those of wrought products[26]. When the alloy is slowly cooled from the all β region, the α phase emerges in the shape of plates below the β transus temperature with the

crystallographic morphology that is related to the parent β phase. The etch effect on the metal reveals white plates that correspond to the alpha phase while the thin dark regions between the alpha plates are the beta phase in the typical Widmansttäten structure. Different cooling rates from various temperatures result in distinct microstructures and mechanical properties. The α, α' and the β phases are observed in various volume fractions and combinations owing to annealing temperatures and cooling rates. The α' phase is formed during the martensitic transformation from quenching above the beta transus temperature. As the alloy crosses the Ms (start of martensite) line, the β microstructure transforms into titanium martensite. The basket weave structure of the air-cooled microstructure is shown in figure 2.3b.

Figure 2.3b: Ti-6Al-4V, forged at 1038°C above the beta transus, air cooled, annealed for 2 hr at 704 °C, and air cooled showing a Widmanstätten structure[31].

When titanium martensite is reheated tempering will take place as β precipitates from the supersaturated α'. When highly alloyed α-β alloys are quenched from the β field, β' which is supersaturated in titanium is formed. When this supersaturated structure is aged α will start to precipitate in a Widmanstätten structure shown in figure 2.3b. Figure 2.4 provides a schematic for the two heat treatment paths.

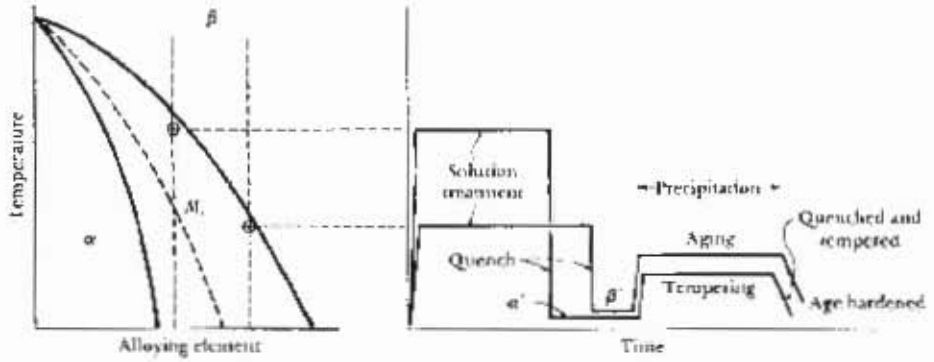

Figure 2.4: Heat treatment of the alpha-beta titanium alloys[25].

Volume fraction (%) of phases present upon different heat-treatments in a study conducted by Jovanovic et al.[26] is shown in table 2.4.

Table 2.4: Volume fraction (%) of phases present upon different heat-treatment[26].

T (°C)	Water-Quenching	Air-cooling	Furnace-cooling
1100	1.3 (β)	14.7 (α)	95 (α)
	$\acute{\alpha}$ = 98.7	β+ α_{AC} = 85.3	β– rest
1050	5 (β)	34.5 (α)	97 (α)
	$\acute{\alpha}$ = 95	β+ α_{AC} = 65.5	β= rest
1000	7.8 (β)	50.9 (α)	90 (α)
	$\acute{\alpha}$ = 92.2	β+ α_{AC} = 49.1	β– rest
950	42.2 (α)	72.2 (α)	95 (α)
	$\acute{\alpha}$ ≈ 50-57.8		
	β ≈ 8	β+ α_{AC} = 28.8	β= rest
900	61.3 (α)	81.3 (α)	95 (α)
	$\acute{\alpha}$ ≈ 26.9		
	β ≈ 10	β+ α_{AC} = 18.7	β– rest
850	80 (α)	84.5 (α)	95 (α)
	$\acute{\alpha}$ ≈ 10		
	β ≈ 10	β+ α_{AC} = 15.5	β– rest

where α_{AC} means acicular α phase and $\acute{\alpha}$ is the martensite phase.

Elemental composition analysis and mechanical properties for wrought and cast Ti-6Al-4V is shown in tables 2.5a and b.

Table 2.5a: Elemental composition specifications for cast and wrought Ti-6Al-4V alloys[5].

	Weight (%)							
Standard	Ti	Al	V	N	C	O	H	Fe
ASTM F1108 – 97 (cast)	Balance	5.5 - 6.75	3.5 - 4.5	0.05 max	0.10 max	0.20 max	0.015 max	0.30 max
ASTM F136 – 96 (wrought)	Balance	5.5 - 6.75	3.5 - 4.5	0.05 max	0.08 max	0.20 max	0.012† max	0.25 max

† Section sizes of 0.813 mm and under may have a hydrogen content up to 0.0150 wt %

Table 2.5b: Mechanical properties of cast and wrought Ti-6Al-4V alloys[5].

Standard	Minimum Tensile strength (MPa)	Minimum 0.2% proof strength (MPa)	Minimum % elongation	Minimum % reduction on area	Hardness (Rockwell C)
ASTM F1108 – 97 (cast)	860	758	8	14	Unspecified
ASTM F1472 -93 (wrought)	930	860	10	20 – 25	Unspecified

The elemental composition analysis and mechanical properties for other wrought standards of this alloy are shown in appendix B.

2.2.1.2 Ti-6Al-7Nb

There has been a decline in use of Ti-6Al-4V alloy in orthopaedic implants due to high incidence of aseptic loosening[5]. It turns out that titanium has poor tribological properties. The creation of debris due to the action of wear that leads to tissue blackening has been reported[5]. Poorly adhering surface oxide layer which continually detaches from the metal is believed to be the result of the debris formation between the articulating surfaces.

Following the decline in the use of Ti-6Al-4V alloy in orthopaedic surgery, new alloys of the titanium metal have been developed. Initially the reason for the drop in application of this metal alloy was high incidence of aseptic loosening. Recent studies have revealed another drawback associated with the use of the alloy in implant surgery. According to Oliveira et al.[28], studies conducted by Ito et al. and Okazaki et al. concluded that vanadium is toxic in the human body. Similar to other toxic metals vanadium can accumulate in the human body organs, such as liver, bone and kidneys. The alternative was found in replacing vanadium with niobium in the titanium $\alpha + \beta$ alloy type. Niobium stabilises the β phase in the alloy as depicted by the Ti-Nb binary system shown in figure 2.5.

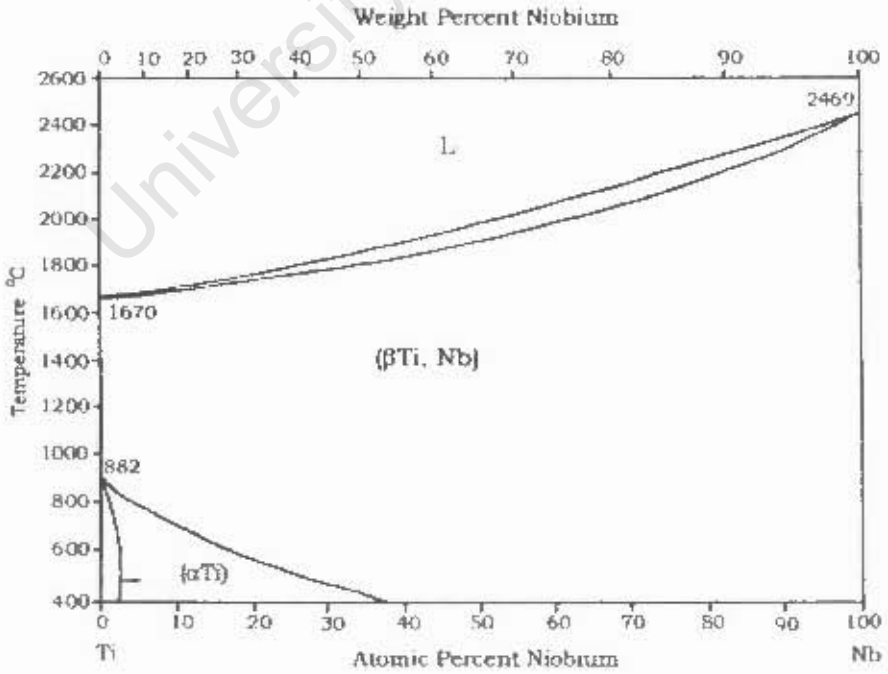

Figure 2.5: Ti-Nb binary phase system[35].

According to a tissue reaction analysis, niobium is classified into a vital class of materials while vanadium belongs to a toxic class[28]. Ti-6Al-7Nb commercially known as protasul-100 alloy has been developed as a possible replacement to Ti-6Al-4V in the field of metal implants. This alloy has an α/β equiaxed structure with 10-12 % β phase[36]. The elemental composition specifications and mechanical properties of protasul-100 are shown in table 2.6a and b.

Table 2.6a: Elemental composition specifications for Ti-6Al-7Nb alloy[36].

	Weight (%)						
Ti	Nb	Al	Ta	Fe	N	O	C
Balance	6.50-7.50	5.50-6.50	0.50 max	0.25 max	0.05 max	0.20 max	0.08 max

Table 2.6b: Properties of Ti-6Al-7Nb alloy[36].

Property	Density	0.2% proof stress	Tensile strength	Elongation on 5D	Reduction of area	Young's modulus	Fatigue strength	Hardness Hv
Value	4.52 gcm^{-3}	Min. 900MPa	Min. 1000Mpa	Min 12%	Min 35%	105 GPa	±500MPa	360

As mentioned in the introduction, there are various ways that have been employed to modify the surface of titanium and its alloys.

2.3 Techniques Used to Modify the Surface of Titanium Alloys

Most of these techniques are based on high reactivity of titanium with respect to elements such as oxygen, nitrogen and carbon[37]. The high reactivity of this transition metal can be attributed to its electronic structure ($1s^2$, $2s^2$, $2p^6$, $3s^2$, $3p^6$, $3d^2$, $4s^2$). There is a stable shell of eight electrons and four ($3d$ + $4s$) electrons that are held loosely[25].

2.3.1 Coating of Titanium Alloys

Improved wear resistance can be achieved by producing components with thick coatings. These coatings can be introduced by Physical Vapour Deposition (PVD), Chemical Vapour Deposition (CVD) and plasma spray. Achieving implants of consistent coating that influences physical-chemical behaviour is very challenging and in many instances spalling and delimination of the coating is experienced[38]. The shortcoming of the process is the exfoliation as a result of corrosive attack at coating substrate interface. This effect (exfoliation) is worsened by the high porosity of the coating.

2.3.2 Thermal Oxidation

Titanium components are thermally oxidised at elevated temperatures (850°C) in air[39]. The result is a thin oxide layer that is formed on the surface of the titanium alloy. The thin oxide layer inhibits further reaction and therefore no further oxygen molecules can diffuse into the surface of the component. Severe scaling is experienced when temperature is increased or longer heat-treatments are performed in an attempt to increase the depth of the modified layer. The scaling of the poorly adherent oxide layer can be attributed to the high value of the Pilling-Bedworth ratio for titanium[39,40]. The Pilling-Bedworth ratio, R of a metal oxide is defined as the ratio of the volume of the metal oxide which is produced by the reaction of metal and oxygen, to the consumed metal volume [41].

$$R \equiv \frac{V_{metal\ oxide\ produced}}{V_{metal\ consumed}} = \frac{Md}{amD} \text{ -------- Eqn (1)}$$

D and M are the density and molecular weight of the metal oxide that has a composition: $(metal)_a$ $(oxygen)_b$ while m and d are the atomic weight and density of the metal. When R is less than one, the oxide cannot cover the whole surface as it is porous and therefore non-protective. Compressive stresses exist in metal oxides with large R. The result is buckling and spalling of the metal oxide. According to Corrosion Doctors Organisation[41], Chalmers and McKay of Harvard University separated protective metal oxides from non-protective metal oxides and titanium forms a non-protective metal oxide. The rest of the metals they separated are shown in appendix C.

The nature of oxides that form on titanium and its alloys are shown in table 2.7.

Table 2.7: Nature of oxides formed on titanium and its alloys[6].

Material	Oxide					
	TiO_2	Al_2O_3	Nb_2O_5	V_2O_5	MoO_3/MoO_2	ZrO_2
cp Ti	x					
Ti-6Al-4V	x	x		x		
Ti-5Al-2.5Fe	x	x				
Ti-6Al-7Nb	x	x	x			
Ti-15Mo-5Zr-3Al	x	x			x	x

The difference between V_2O_5 formed in Ti-6Al-4V and Nb_2O_5 Ti-6Al-7Nb is the fact that Nb_2O_5 is chemically much more stable, less soluble and more biocompatible in comparison to V_2O_5[42,43]. The selected physico-chemical properties of titanium oxides and oxides of other metals used as alloying elements in titanium in table 2.8 show the superiority Nb_2O_5 of over V_2O_5 in metallic implants.

Table 2.8: Physico-chemical properties of titanium oxide and of oxides of other metals used as alloying elements in titanium alloy[42].

Element	Most stable oxide	Typical tissue response
Ti	TiO_2	Inertness
Al	Al_2O_3	Sequestration
Nb	Nb_2O_5	Inertness
V	V_2O_5	Toxicity
Zr	ZrO_2	Inertness
Ta	Ta_2O_5	Inertness
Fe	Fe_2O_3	Sequestration
Cr	Cr_2O_3	Toxicity
Co	Co_2O_3	Toxicity

Recently the thin oxide layer has been supported by an oxygen diffusion zone as means of improvement to the easy process of thermal oxidation. Four fifths of air consists of nitrogen[15,44]. It is therefore worth mentioning that during oxidation in air there is nitrogen intake as well. Dong and Li[39] detected nitrogen pile-up in the titanium oxygen interface of Ti-6Al-4V specimens oxidised in air as shown in figure 2.6. However, nitrogen plays a minor role in the scaling of titanium in air as a result of slower diffusion rates of nitrogen in titanium and titanium nitride as well as the instability of titanium nitrides with respect to the oxides[15]. Another atmospheric gas that takes part in the reaction is water vapour[15].

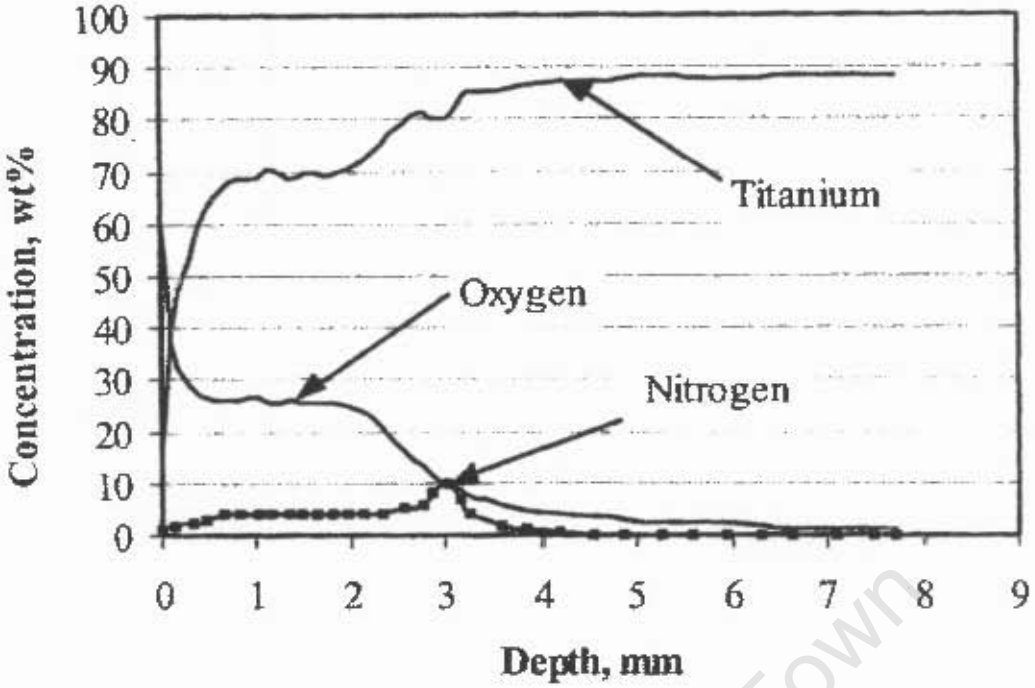

Figure 2.6: Composition profile showing nitrogen pile-up at the interface between the oxide layer and the substrate during oxidation of Ti-6Al-4V[39].

A series of experiments shown in table 2.9 conducted by Dong et al.[45] indicate that thermally oxidised specimens of Ti-6Al-4V contain a hardened oxygen diffusion zone underneath the thin surface compound layer. A hardened surface layer with an outer compound layer and inner diffusion layer can be achieved[37,45].

Table 2.9: Oxide layer thicknesses and diffusion zone depths resulting from various oxidation heat treatments in air[45].

No.	Time (hr)	Temp. (°C)	Thickness of the oxide layer (μm)	Depth of the diffusion hardened zone (μm)
1	50	600	1.4	10.6
2	100	600	2	14
3	3	630	0.2	4
4	10	650	1	8
5	2.5	700	1	10
6	20	680	8	20
7	8	700	6	15
8	20	700	10	27
9	48	700	15	45

2.3.2.1 Kinetics of Reactions of Titanium as well as the Nature of Scale Formed during Oxidation in Air

Morton and Baldwin[46] carried out their study of the scaling of titanium in air on sintered magnesium-reduced titanium using a gravimetric technique[15,46]. They concluded that at temperatures between 250 and 700°C the increase in weight, w, of a specimen heated in air for time, t, obeyed, after initial deviations a modified parabolic law of the form[39,46]:

$$(w - w_0)^2 = kt \quad \text{-------- Eqn (2)}$$

where w_0 and k are constants for any given temperature. The scaling rate

$$dw/dt = k/2(w - w_0) \quad \text{-------- Eqn (3)}$$

is controlled by the amount of gas absorbed in excess of a certain amount, w_0, which is fixed for each temperature. The quantity k was found to be more temperature dependent than w_0. After a comparable short time of heating the magnitude of w is much greater than that of w_0 hence the quantity w_0 has not been found to have a very marked effect on the form of the isothermal gas-absorption / time curves. Morton and Baldwin [46] discovered discontinuities on the absorption isothermals occurring after heating periods which became shorter at higher temperatures. According to Morton and Baldwin the discontinuities took the form of a sudden increase in the rate of gas absorption, which continued for a short period and then gradually fell off again until the isothermal reverted to a parabolic form, the new parabola corresponding to a value, k_2, of the constant, k, different from that governing the earlier parabolic section of the curve, k_1[15]. Values of $(k_1)^{1/2}$ and $(k_2)^{1/2}$ plotted by Baldwin and Morton from their experimental curves logarithmically against the reciprocal of the absolute temperature are shown in figure 2.7. Similar data obtained from the experiments of Gulbransen and Andrew[47,48] on the scaling of titanium in oxygen are included for comparison.

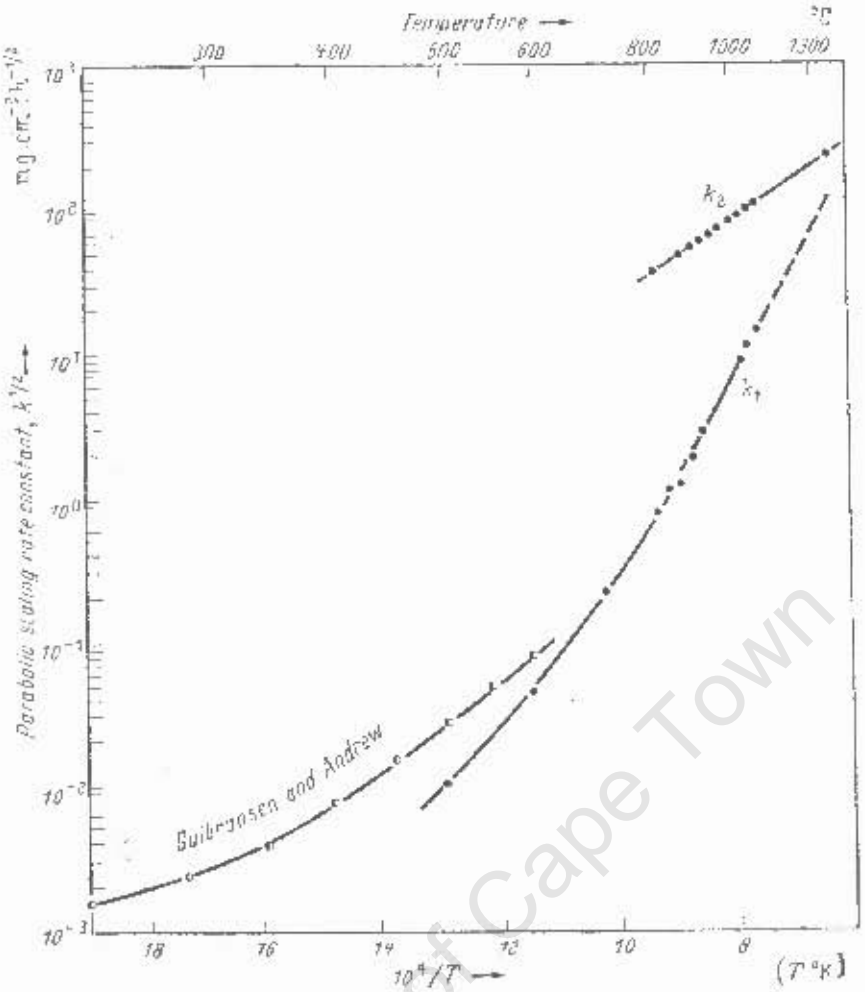

Figure 2.7: Values of $(k_1)^{1/2}$ and $(k_2)^{1/2}$ obtained by Morton and Baldwin[46] from experimental curves of the increase in weight of titanium on heating in air as a function of temperature and a similar data obtained from the experiments of Gulbransen and Andrew[47, 48] on the scaling of titanium in oxygen.

The early parabolic section of the isothermal curve for the oxidation (250°C-700°C) of titanium in air corresponds to a value (k_1) of the constant k and the later stage of oxidation (800°C-1000°C) parabolic isothermal corresponds to a value (k_2) of the constant k[15]. As suggested by figure 2.7, the relationship between $\frac{1}{2}\ln k_1$ and $\frac{1}{T}$ is not linear, hence Morton and Baldwin did not attempt to evaluate the activation energies of the processes operative during the two stages of their oxidations[15].

Morton and Baldwin[46] have published the sketches of the scale formed on heating titanium in air depicted in figure 2.8.

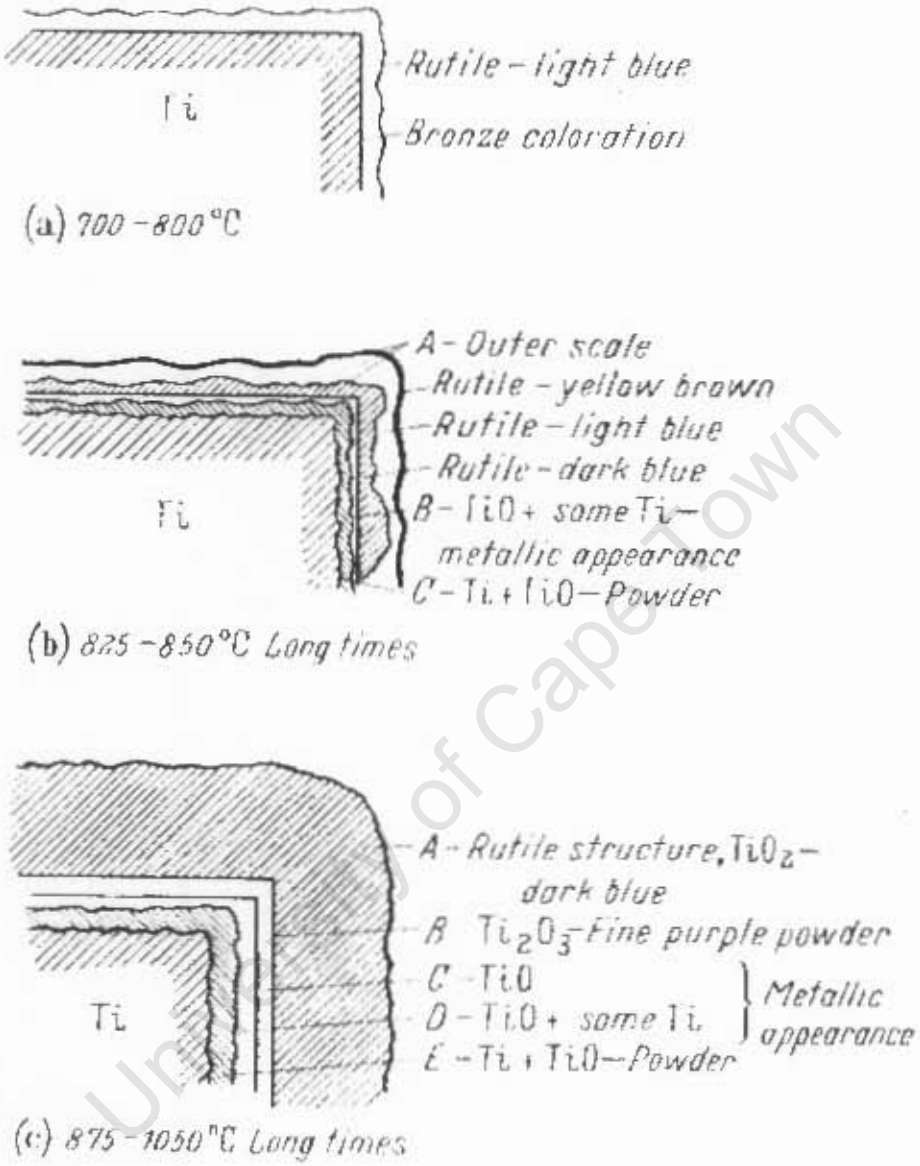

Figure 2.8: The appearance of the scale observed by Morton and Baldwin[46] to form on commercial titanium after heating in air.

It has been established by Finlay and Snyder[49] as well as Bumps, Kessler and Hansen[50], that in addition to the solid solution of oxygen in titanium, at least three intermediate phases, TiO, Ti_2O_3 and TiO_2 exist with other phases, Ti_3O_2 and Ti_3O_5 that are possible to form[51]. Some of these phases are shown in the Ti-O binary system in figure 2.9.

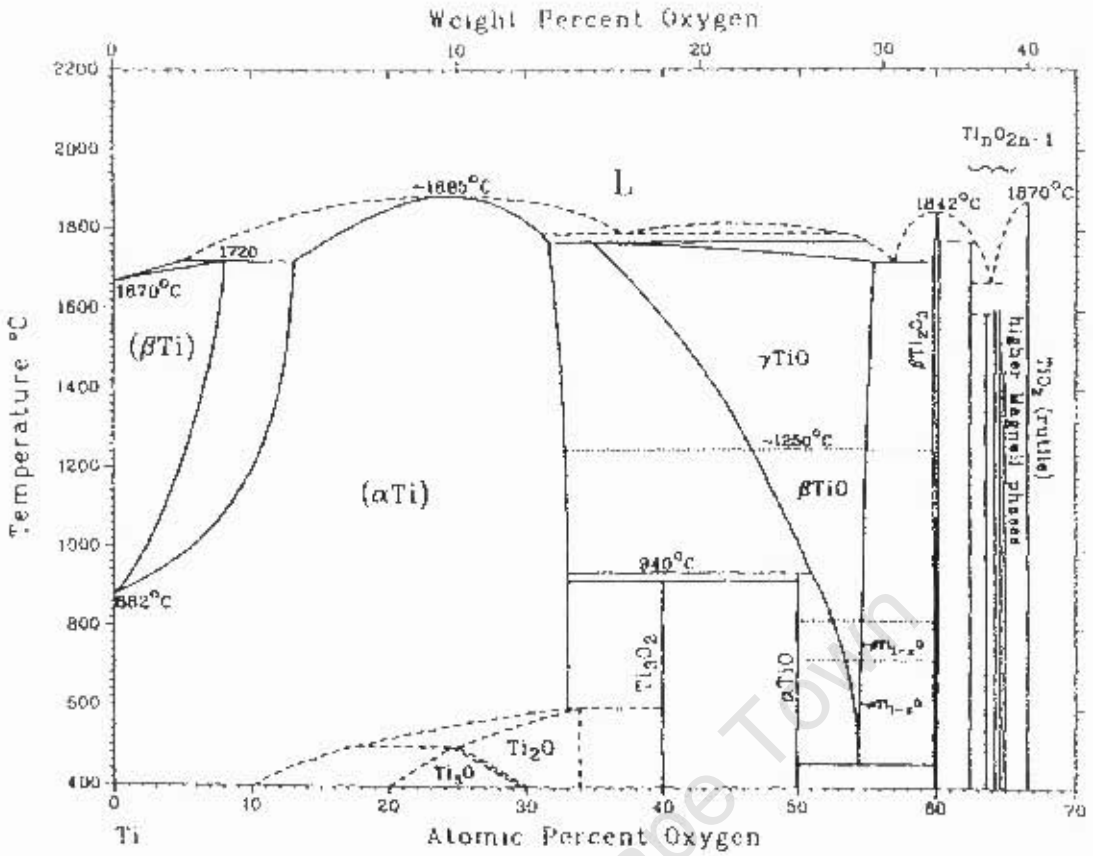

Figure 2.9: Phase diagram of the Ti-O system[52].

Therefore the reaction of oxygen with titanium as a dynamic process would be expected to be an extremely complex process since at least five and possibly more distinct layers are likely to be found between the uncontaminated core of an oxidised sample of titanium and the outer surface layer[15]. The oxidation reactions of titanium are therefore not fully understood. It has been established though that the greater part of the scale which is in direct contact with the atmosphere is rutile, and since it is observed in general that the thickness of the scale increases with time, it may be assumed that the rate of diffusion of oxygen through the coherent outer layers of rutile is the process controlling the reaction rate under all conditions which are of practical importance and thus any reduction of the rate of diffusion of oxygen in rutile would be expected to decrease the rate of scale formation[15].

2.3.3 Ion Implantation

This involves firing of atoms into a titanium surface. This process can be carried out at ambient temperatures as it requires no heating up of the substrate. The process is

independent of the solubility of elements that are fired at titanium substrate and there are no dimensional changes on the substrate. In practice this is quite a complicated activity. For complex geometry components, the line of site constraints requires target manipulation and careful dose control[40]. High energy implanters and post-implant annealing are used to increase the very shallow modified depths achieved by ion implantation. Nitrogen ion implantation is the most widely used surface treatment of titanium components. Streicher et al[36] conducted the study of N^+ implantation on Ti-6Al-7Nb. An increase in hardness was observed to a depth of less than 1 μm. Figure 2.10 shows that the depth of maximum N^+ concentration with the investigated variations was below 100nm.

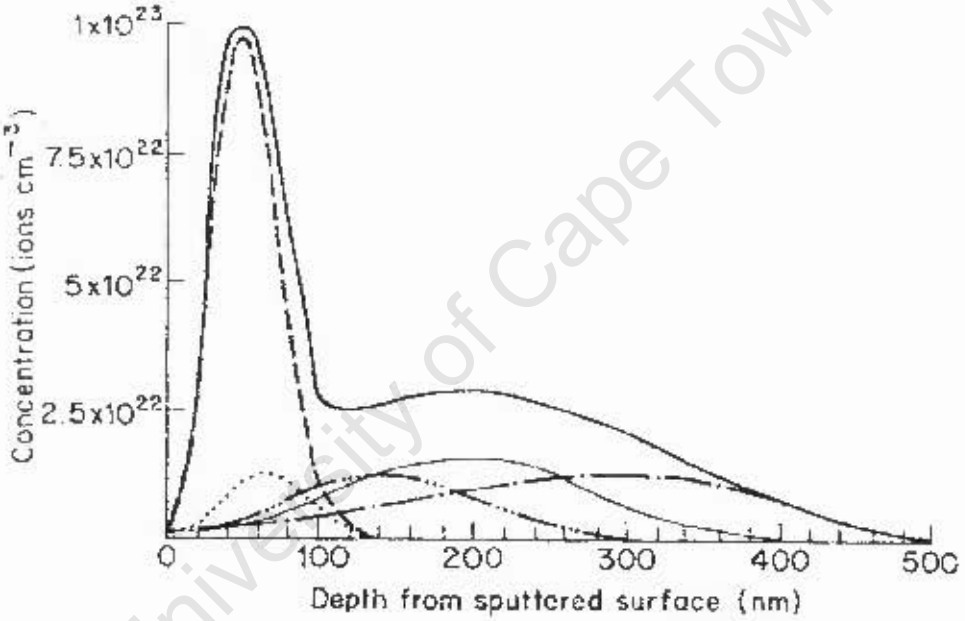

Figure 2.10: Nitrogen ion profile for a five-fold implantation treatment of Ti-6Al-7Nb with cumulative profile for different energy implanters[36].

2.3.4 Nitrogen Diffusion Hardening

Introducing nitrogen (N_2) into the interstitial sites of the titanium lattice can improve the hardness of titanium substantially. Thermo-chemical nitriding processes such as gas and salt bath nitriding have been used. Higher mean roughness values and increasing nodular surfaces of titanium components treated by these traditional nitriding processes have been reported[48]. Recently plasma nitriding has been

introduced to overcome various existing problems that are associated with traditional nitriding processes. During this process sputtering removes the reactive layer. Increased process rates are made possible by high temperature processing[40]. Distortion of components treated at high temperatures has been reported[40].

2.3.5 Oxygen Diffusion Hardening

This is a process by which oxygen atoms diffuse into the titanium component at elevated temperatures. Controlled diffusion can result in a net of flux of atomic movement into the substrate[36]. The movement of these foreign atoms into the titanium substrate does not change the dimensions of the substrate. The much smaller oxygen atoms occupy the interstitial sites of the titanium matrix. There are four factors that affect the process of oxygen diffusion into the surface of titanium. The temperature at which the diffusion is carried out, time allowed for the diffusion process, partial pressure of the oxygen as well as the solutes (other elements) dissolved in the titanium matrix[1]. The study conducted by Poggie et[1] al showed that zirconium is essential to oxygen diffusion and surface hardening of Ti-Nb-Zr alloys at 500°C. In the study Ti-Nb-Zr samples were hardened by linear ramp-up to 500°C over two hours and six hours at 500°C and finally cooled to room temperature in one hour. The hardness values measured on the treated alloys are shown in figure 2.11.

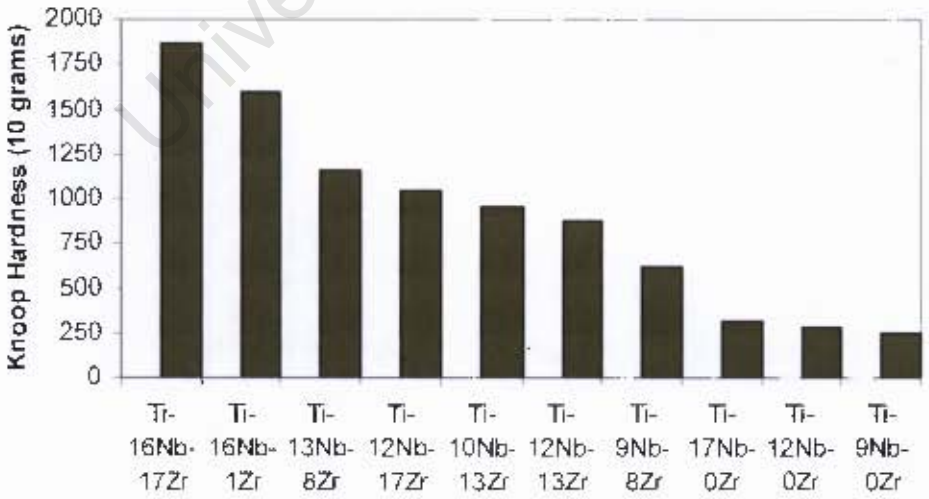

Figure 2.11: Knoop hardness values (10g) for the surfaces of the Ti-Nb-Zr alloys oxygen hardened in air[1].

Higher hardness is achieved by an outermost oxide layer below which is the interstitial oxygen hardened metal. Semlitsch et al.[36] have successfully hardened Ti-6Al-7Nb through oxygen diffusion hardening. Figure 2.12 shows that a hardness of more than twice the hardness of the bulk material can be achieved on the surface of the alloy.

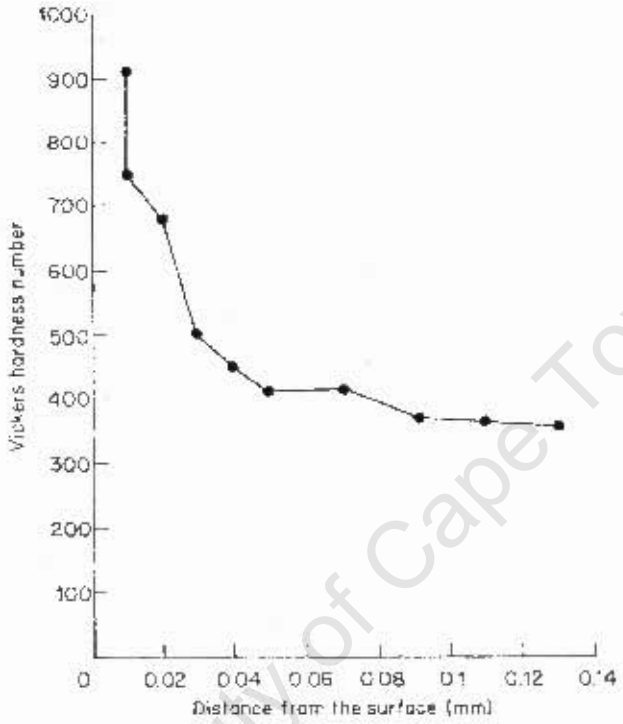

Figure 2.12: Hardness profile of Oxygen diffusion hardening – treated Ti-6Al-7Nb[36].

Figure 2.13 shows the reduction of the β phase near the surface which indicates the effect of oxygen as the α phase stabiliser on the alloy.

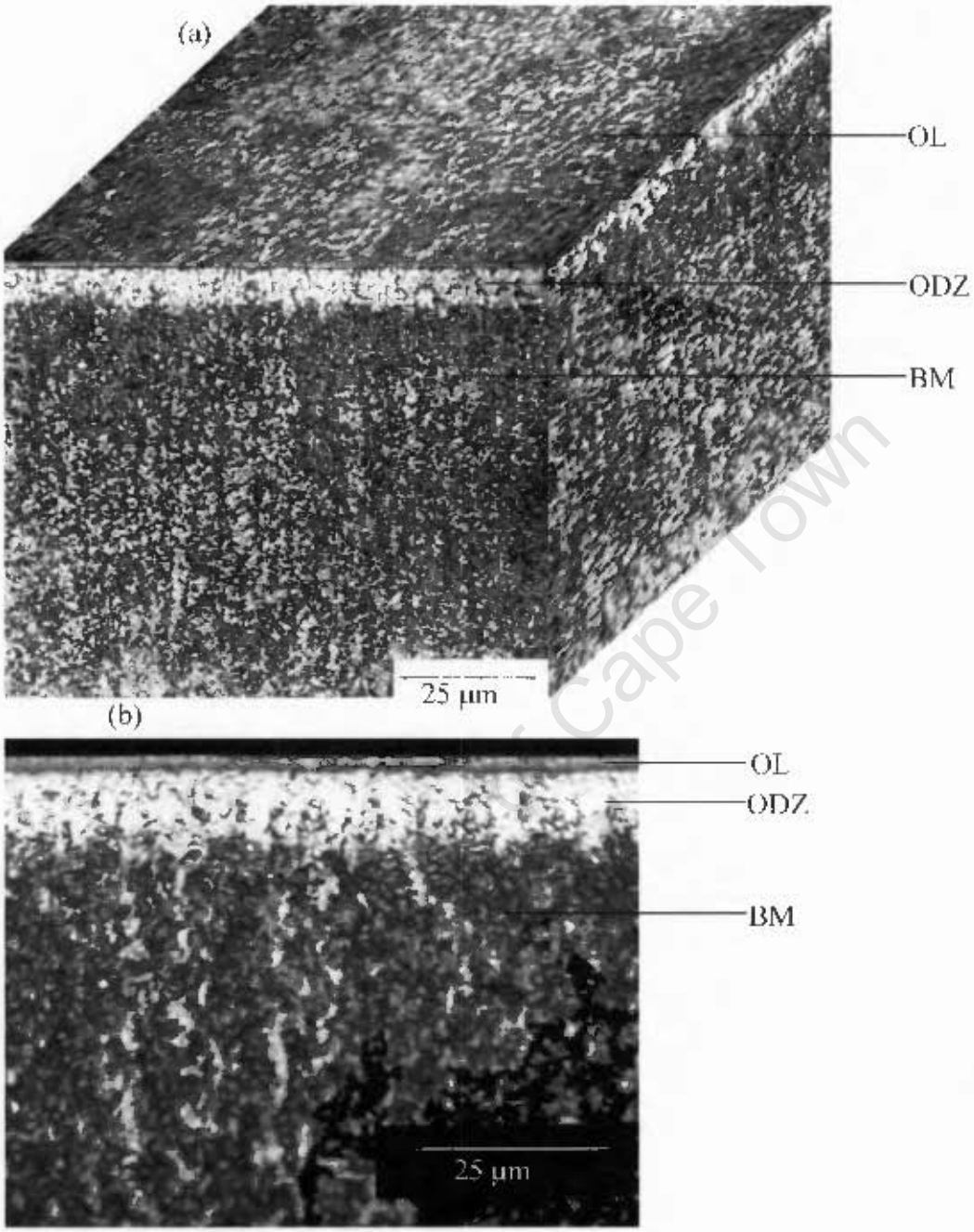

Figure 2.13: (a) 3-D and (b) 2-D section optical micrographs of the Ti-6Al-4V oxidised for 60 h (OL: oxide layer, ODZ: oxygen diffusion zone, and BM: base metal[53]

The effect of oxygen on room temperature tensile properties and hardness of titanium shown in figure 2.14 was constructed by Jaffee, Ogden and Makuth[54] as well as

Finlay and Snyder[49]. The diagram shows the increase of various mechanical properties and the reduction in elongation.

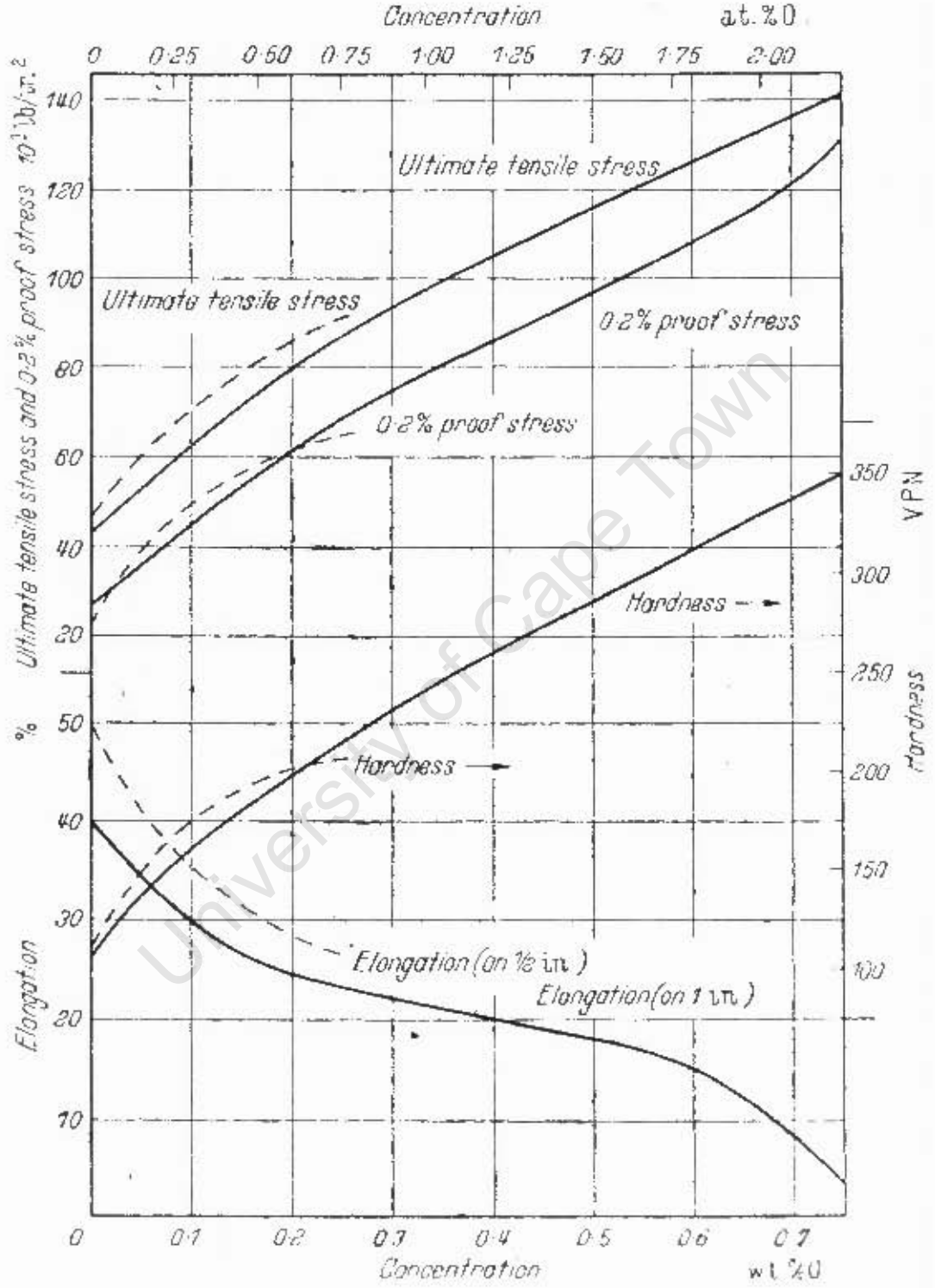

Figure 2.14: Effect of oxygen on room-temperature tensile properties and hardness of titanium[49,54].

Diffusion treated metals are more favoured than coated metals due to the problems associated with coating-substrate interface. The difference in the structure of the coating and that of the substrate results in a mismatch of properties at the interface. The diffusion zone beneath the compound layer results in a smoother hardness transition between the outer compound layer and the substrate beneath[1]. This phenomenon is depicted by the schematics of a coated metal and a diffusion hardened metal in figure 2.15.

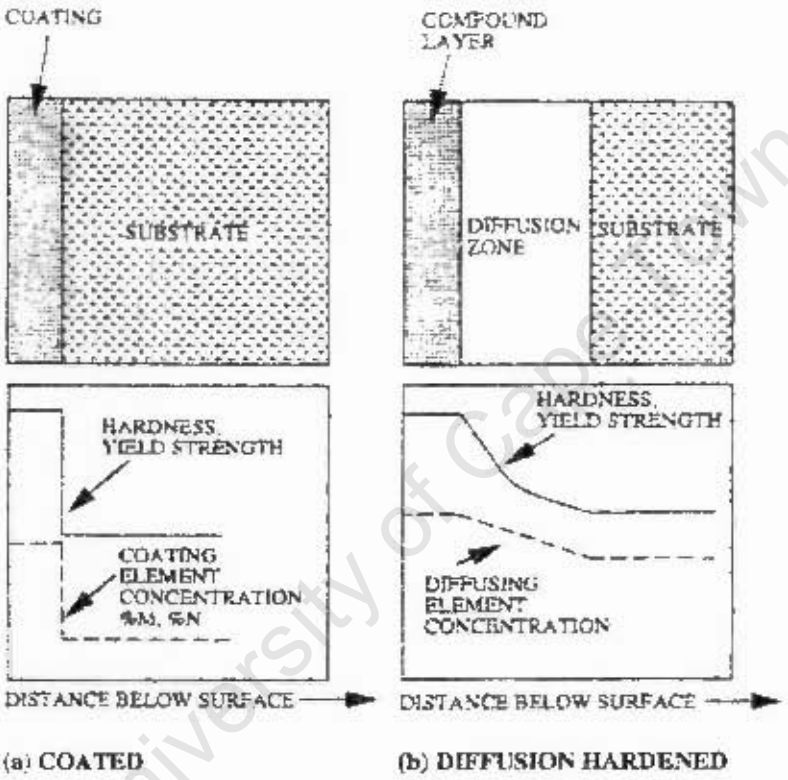

Figure 2.15: (a) a PVD (physical vapour deposition) ceramic coated metallic alloy, (b) a diffusion hardened metallic alloy[5].

2.3.6 Deep Case Hardening of Titanium Alloys with Oxygen.

A short heating time of the titanium components results in a surface layer which contains dissolved oxygen at a concentration that diminishes gradually with the increase of distance from the metal surface[15]. High Pilling-Bedworth ratio of the titanium alloys which results in severe scaling that compromises the quality of surfaces has ruled out thermal oxidation as a surface treatment to improve tribological

properties of titanium. In recent studies, a new thermal oxidation process whereby an adherent thin oxide film supported by an oxygen diffusion zone has been developed. The two-step process is referred to as deep case hardening of titanium alloys with oxygen or Oxygen Boost Diffusion Hardening (OBDH)[39,55]. The first step involves heating the metal in air. In the event that the compound layer is found unsuitable it can be broken down by further heat-treating the pre-oxidised specimen at elevated temperatures in vacuum or under inert gas atmosphere allowing for the coherent oxide layer to be re-absorbed by the metal leaving only a metal-gas solid solution[15,39,55]. Controlling the parameters of this process such as the time of heating, temperature and gas pressure can produce surface layers of any desired hardness whereby the bonding of the hardened surface layer to the core is strong since the lattices of the core material and the solid solution are fully coherent[15]. C. Boetcher[55] concluded that a post diffusion treatment applied to Timet550 (Ti-4.050Al-2.075Sn-0.415Si-0.035Fe-4.140Mo-0.010C, with 1800 ppm O and 35 ppm N) increases the effective case depth from 60 to 120 μm, thus improving the poor wear resistance associated with titanium[55]. Time allowed for the first step of the process is critical. The obtained adherent oxide layer becomes an oxygen reservoir for the second step. Figure 2.16 shows the effects of time allowed for the first step on microhardness for Ti-6Al-4V on a study conducted by Dong and Li[39].

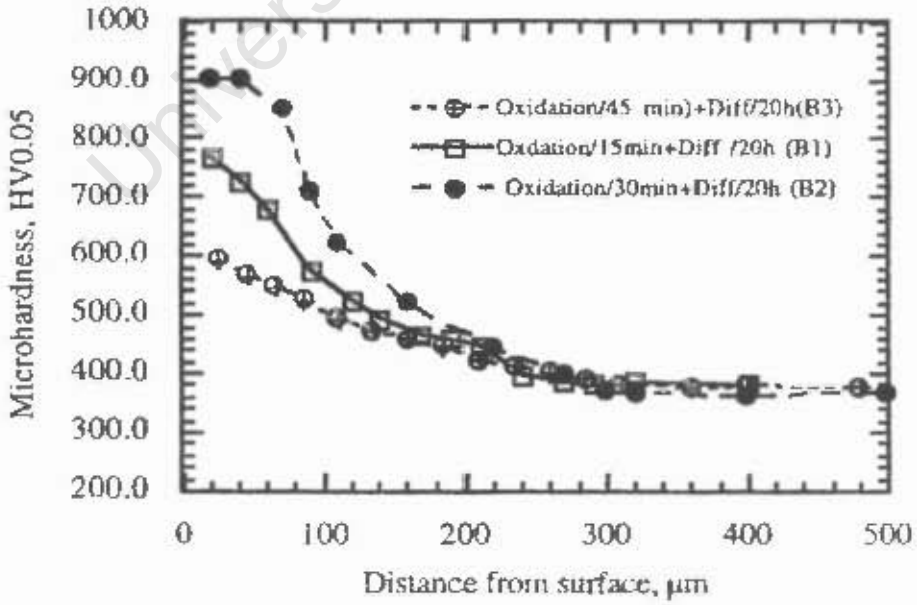

Figure 2.16: Effect of the oxidation time in step 1 on the microhardness distribution of the oxygen boost diffusion treated material[39].

Either shorter time or longer time oxidation in step one resulted in weaker effective hardening effect compared with that produced using an optimum oxidation time (30 minutes)[39]. Oxidation for a short time (15 minutes) results in a thin oxide formation which results in less oxygen for step two. Longer (45 minutes) oxidation time results in a crumbly oxide that spalls off and the result is less oxygen for step two.

Table 2.10 summarizes the surface treatments that are used in various total joint replacement metals.

Table 2.10: Treatments presently used in TGR's[5]

Substrate	Surface treatment	Commercial affiliation/sponsor	Current status
Ti-6Al-7Nb	Oxygen diffusion hardening	Zimmer, USA	C
Ti-13Nb-13Zr	Oxygen diffusion hardening	Smith and Nephew Richards, USA	IVT
Ti-6Al-4V	Nitriding	-	IVT
Co-Cr-Mo (cast and wrought)	Nitriding	Zimmer, USA	IVT
Zircadyne 705 (Zr-2.5Nb) and other zirconium alloys	Oxygen diffusion hardening or nitriding	Smith and Nephew Richards, USA	IVT
Ti-6Al-4V	PVD-TiN	Innovatique, France	CE
Ti-6Al-4V	PVD-TiN	Endotec, USA	CE
Ti-6Al-4V	DLC	Ion Tech, UK	IVVT/IVT
Various metals	DLC	Teer Coatings, UK	IVT

C = commercially available, CE = undergoing clinical evaluation, IVT = *in vitro* testing, IVVT = in vitro testing (sheep)

2.3.6.1 The Mechanism for the Oxidation and Boost Diffusion Process.

Superposition and/or competition of two fundamental processes characterise the oxidation of titanium. The two processes are: the growth of the surface oxide layers and the formation of the oxygen solid solution[56,57]. Despite the high number of oxides that form readily even at room temperature, rutile is the only titanium oxide identified in the layer with certainty between 600 and 900°C[56,57,58]. Controversy has come about whether the oxide film grows inward or outward[59]. In their work Dechamps et al.[57] argued that although in monocrystalline oxide film the diffusion coefficient of titanium is greater than that of oxygen by about 10 times, the existing defects such as strata, micropores or grain boundaries will effectively inhibit the diffusion of titanium but facilitate the diffusion of oxygen, hence the main diffusion species through the oxide is oxygen and the film grows inward[56,57,59]. Surface defects are therefore believed to be a dominating factor in the surface chemistry of oxide materials[60,61,62].

In a different view, Li et al.[63] concluded from their study of oxygen-induced restructuring of the rutile that TiO_2 (110) surfaces in an oxygen environment causes extraction of interstitial Ti atoms from the bulk and near surface region. These Ti atoms are oxidised at the surface, forming added layers of TiO_2 (110) (1x1). In the notation TiO_2 (110), TiO_2 is the substrate upon which the layer is growing on the (110) face and (1x1) indicates that the arrangement of the atoms growing on the surface corresponds to the bulk unit cell called the substrate structure. Kinetic limitations result in the formation of a metastable phase consisting of a partially incomplete TiO_2 (110) structure from the added TiO_2 layers. Li et al.[63] proposed that this structure consists of Ti atoms with a reduced coordination number. This study will then suggest the outward growth of the oxide film as well as Ti being the main diffusion species through the oxide.

The diffusivity of oxygen in TiO_2 is about 50 times the value in Ti, therefore oxidation of titanium is controlled by oxygen diffusion in the diffusion zone rather than in the oxide[64].

There are two mechanisms that have been proposed for the degradation of TiO_2 in the boost oxygen diffusion process[39]. The first mechanism involves the dissociation of the oxide at the oxide/air interface. The second mechanism is the dissolution of oxide at the oxide/Ti interface and the absorption of oxygen by titanium via the following overall reactions[39,65].

$$TiO_2(s) \rightarrow Ti(s) + O_2 \text{ -------- Eqn (4)}$$

$$TiO_2(s) + Ti(s) \rightarrow 2O \text{ (dissolved in Ti) -------- Eqn (5)}$$

Dong and Li[39] state that the first mechanism is unlikely to take place during the boost oxygen diffusion process. Even though the partial pressure of oxygen in the vacuum is very low (about 1.3×10^{-4} Pa), it is still much higher than the dissociation pressure of TiO_2 at 850°C which is calculated to be 4.39×10^{-29} Pa based on equation 4 as well as equations 6 and 7[39,66].

$$\Delta G = 910000 - 173T \text{ ------- Eqn (6)}$$

$$\Delta G = -RT \ln K = -RT \ln \left\{ \left[(\alpha_{Ti})(p_{O_2}) \right] / \alpha_{TiO_2} \right\} \text{ -------- Eqn (7)}$$

This is supported by the much deeper hardened layer after the boost oxygen diffusion process which would otherwise be thinner if the first mechanism was dominant[39].

2.4 Effect of Surface Hardening on Wear Behaviour of Titanium Alloys

As indicated in the introduction, low frictional wear resistance and tendency to seizure has restricted the wider application of titanium and titanium alloys[67]. Various surface modification techniques have been developed and their effect on tribology of titanium has been studied. Ion implanted Ti-6Al-4V showed substantially improved wear resistance[40,68]. Tribological properties of the Ti-6Al-4V can also be improved significantly by the nitriding technique according to a study conducted by Johns et al.[40] on the wear resistance of plasma immersion ion implanted Ti-6Al-4V. The

TiN/TiNO complexes on nitride and oxidised surfaces have resulted in a substantially improved resistance to wear/fretting. The linear wear rate of oxygen diffusion hardened titanium sliding against a carbon steel AISI 1045 appeared to be lower by a factor of 160, with a value of $3.0x10^{-5}$ μm / (mN) compared with untreated titanium with a value of $4.83x10^{-3}$ μm /(mN)[67]. The α-Ti(O) continuous layer in dry sliding against Co-28Cr-5W-4Fe-3Ni-1Si showed a significantly lower wear resistance than pure titanium, but only over a limited sliding distance proportional to the thickness of the hardened zone[67]. Dong and Li[39] also performed abrasive wear tests on oxygen boost diffusion treated Ti-6Al-4V samples. In their study they further conclude that oxygen boost diffusion treated components possess higher wear resistance than oxidised components with the same thermal cycle. The abrasive wear resistance test showed a higher mass loss for the untreated material followed by oxidised and the least mass loss was noted for the diffusion treated samples shown in figure 2.17.

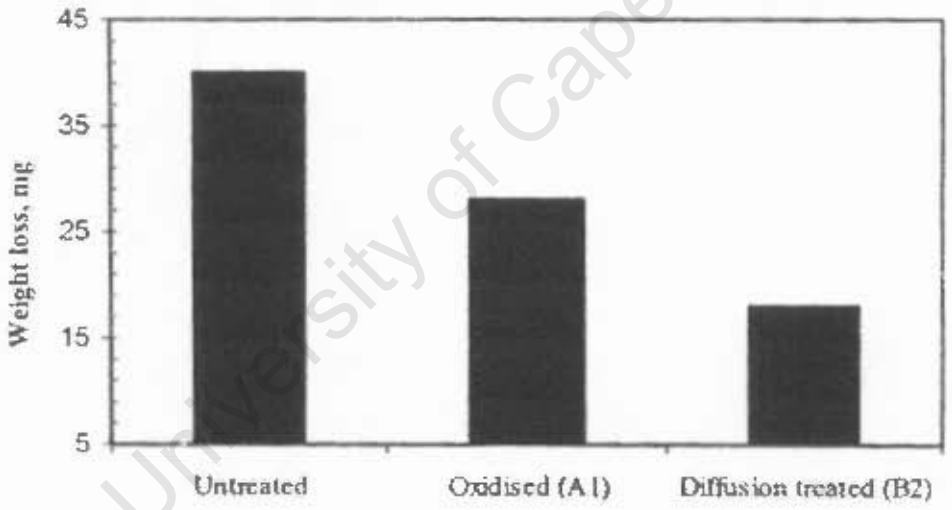

Figure 2.17: Abrasive wear resistance of the oxygen boost diffusion treated, oxidised and the as-received material[39].

Chapter Three

Experimental Procedure

3.1 Materials

The materials used were:

1. Timetal 6-4 in the form of hot rolled and annealed bar of 25 mm diameter was supplied by Goodfellow, Cambridge LTD, Huntington. This "all purpose" alloy is the most widely used[39]. Its medium to high strength, workability, good fatigue resistance, good corrosion resistance and high biocompatibility has landed it to a position where it accounts for about 50-60% of world tonnage production of titanium[6,28,39]. This alloy has a nominal composition of 6wt% Al, 4 wt% V and balance Ti, hence the designation Ti-6Al-4V (Ti64). Cylindrical coupons of 22mm in diameter and thickness of 5mm were then machined from the bulk material and used as test pieces.

2. Protasul-100 (Ti-6Al-7Nb) in the form of hot rolled and annealed bar of 22 mm diameter was supplied by Biomaterials, Bar Lane Industrial Estate, North Yorkshire. Following the decline in the use of Ti-6Al-4V as an implant due to aseptic loosening and the toxicity of vanadium in the human body new titanium alloys were then specifically developed for biomedical applications[1,5,6]. Ti-6Al-7Nb is among the first alloys that were tailored to replace Ti-6Al-4V while maintaining the desirable properties such as high resistance to corrosion, α-β grain structure as well as mechanical properties that are comparable with those of Ti-6Al-4V[6,29]. This alloy has a nominal composition of 6 wt% Al, 7 wt% Nb and balance Ti, hence the designation Ti-6Al-7Nb (Ti67). Cylindrical coupons of 22mm in diameter and thickness of 5mm were then machined from the bulk material and used as test pieces

3.2 Heat-treatments

Test pieces from both alloys were subjected to the same heat treatment processes. The oxygen diffusion hardening process was carried in two ways.

3.2.1 Water saturated Argon Environment

This method of Oxygen Diffusion Hardening was done by Poggie et al.[1] on Ti-13Nb-13Zr (by weight) samples. According to their experimental set up, this heat-treatment was performed in a controlled atmosphere, positive pressure in a convection furnace. A bottle of water containing two openings was set to receive through one of its openings the argon gas supply. Subsequently the argon gas saturated with water would exit the bottle via the second opening into the furnace. The opening on the furnace would allow for a continuous flow of saturated argon into and out of the furnace, while maintaining a positive pressure of at least two inches of water above standard atmospheric pressure[1]. The objective of this controlled atmosphere is to generate mono-atomic oxygen through the dissociation of water vapour in the furnace, and therefore change the surface kinetics of physical absorption and diffusion of oxygen into titanium[1]. The positive pressure of at least 2 inches can be measured using the manometer scale.

A similar set up outlined above was put together for this research. The experimental set up is shown in figure 3.1. The furnace with the test pieces was ramped up at 350°C per hour to 700°C and then allowed to stay at that temperature for 10 hours in the controlled atmosphere. The next set of specimens was heat-treated in the same way for 48 hours.

3.2.2 Oxygen Boost Diffusion Hardening

The oxygen boost diffusion hardening process was carried in two steps. The first step was oxidation in air at elevated temperatures and the second step was the diffusion treatment carried out in a vacuum furnace. This form of heat treatment is referred to

as oxygen diffusion hardening or deep case hardening of titanium alloys [39,55]. The first set of specimens were oxidised at 850°C for 30 minutes in air. This oxidation step is referred to as A. These pre-oxidised specimens were further diffusion treated under vacuum of about $1x10^{-4}$ Pa at 850°C (Vac 850) for 20 hours while others were diffusion treated under the same vacuum pressure at 750°C (Vac 750) for 20 hours in a cycle heat-treatment. The vacuuming step at 750°C for 20 hours is referred to as Vac-750 such that a Ti-6Al-4V test piece that has been oxidised at 850°C for 30 minutes in air followed by heat-treatment in vacuum at 750°C for 20 hours will thus be referred to as Ti64-A, Vac-750. Similar heat treatments in vacuum were done on specimens pre-oxidised at 750°C for 45 minutes (B) as well as those pre-oxidised at 600°C for 20 hours (C). A twin cycle heat treatment was carried out for the pre-oxidised samples that were heat treated in vacuum at 850°C. During the OBDH heat-treatment a sample that is oxidised in air and further diffusion treated in vacuum has undergone a cycle heat-treatment. A cycle heat-treated sample that is further oxidised and diffusion treated in the same conditions as the first cycle has undergone a twin cycle heat-treatment.

Key for the OBDH Samples

Example: Ti64-A,Vac-850

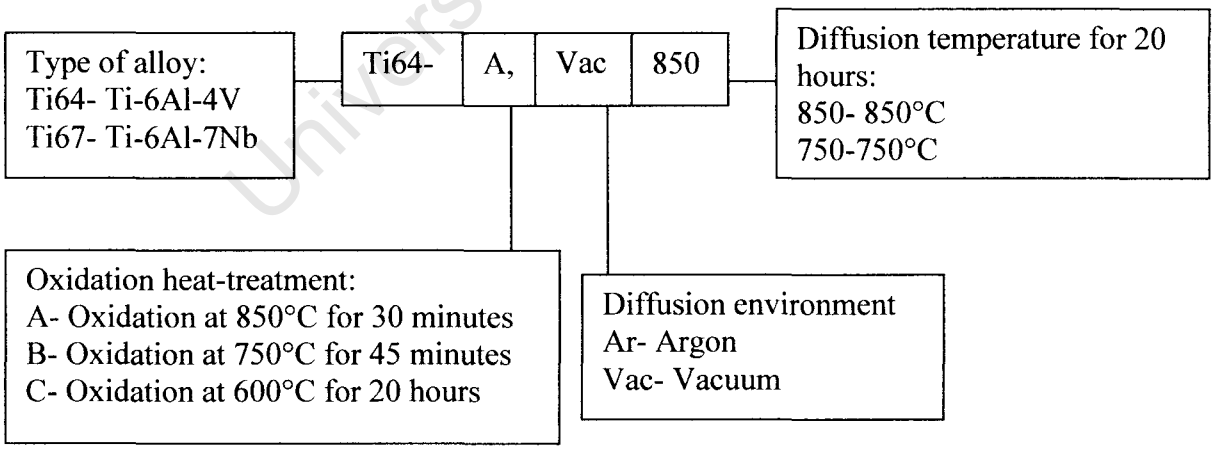

The second set of specimens was heat-treated in the same way except for the second step which was carried out in argon instead of the vacuum environment. The heat-treatment vacuum furnace would be pumped down at room temperature to a pressure of about $1x10^{-4}$ Pa. Argon was then purged into the furnace at room temperature until

the pressure gauge reads 8.27×10^4 Pa. As the furnace heats up argon will expand until 9.33×10^4 Pa at 850°C (Ar-850). For the diffusion treatments at 750°C (Ar-750), argon was purged at room temperature until the gauge registers 8.60×10^4 Pa and that would expand to 9.33×10^4 Pa once 750°C is attained. This pressure of 9.33×10^4 Pa used during the diffusion in the argon environment was chosen because lower pressures will be closer to vacuuming conditions while room temperature pressure (10.13×10^4 Pa) and pressure above that will break the seal of the furnace and allow the air to leak into the furnace. A twin cycle heat treatment was carried out for the pre-oxidised samples that were heat treated under argon environment at 850°C. All the diffusion heat treatments were carried out on the vertical vacuum furnace which is shown as component in figure 3.1. A flow chart for the performed heat treatments except the twin cycle heat treatments is shown in figures 3.2 (a) and (b).

Figure 3.1: Experimental set-up for water saturated argon environment heat treatment process with (1) high temperature vacuum furnace, (2) manometer, (3) water bottle and (4) gas cylinder (with Argon)

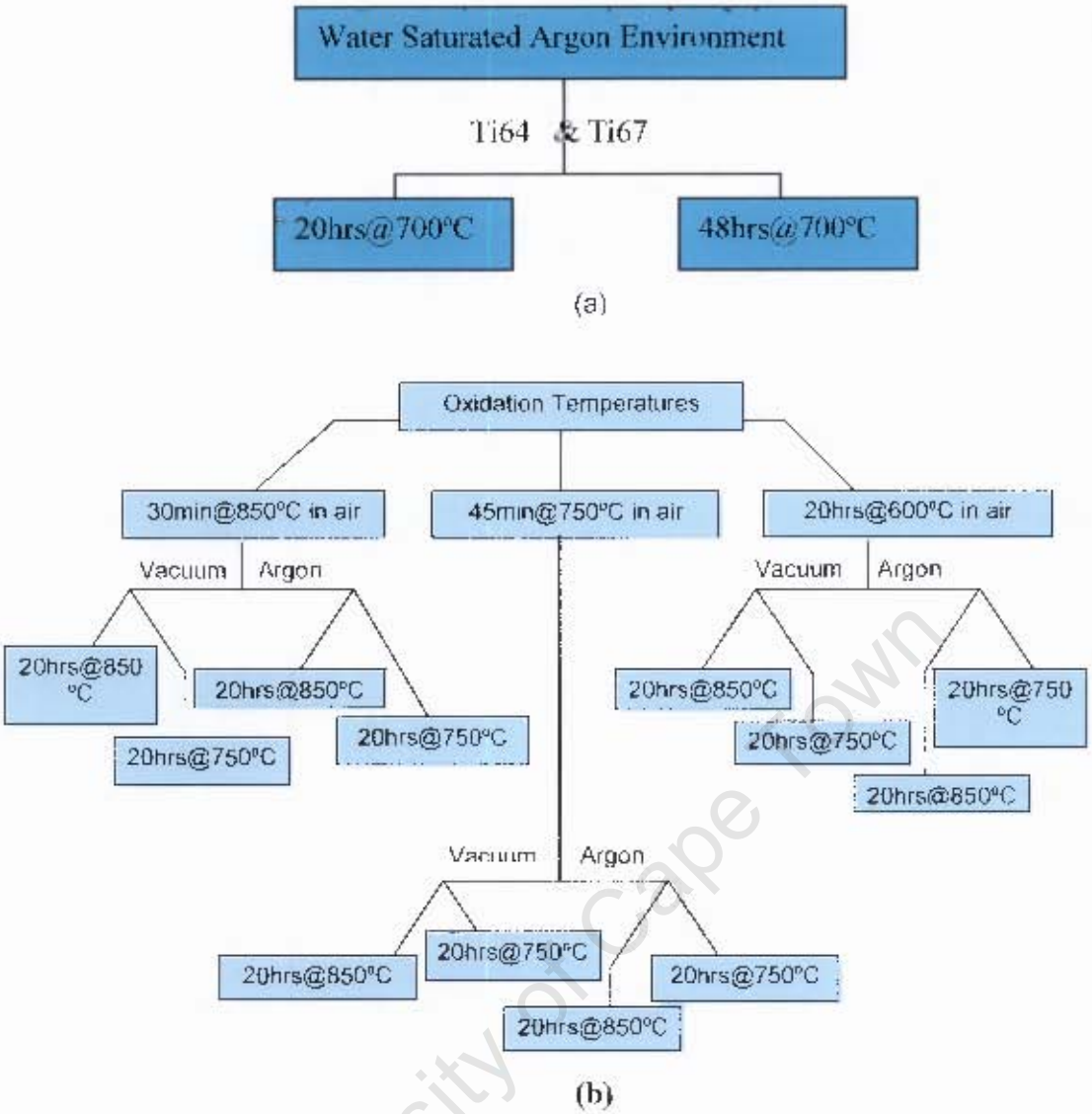

Figure 3.2: (a) WSAE and (b)OBDH heat-treatment procedure.

3.3 Characterisation of the Oxygen Diffusion Layer

Various characterisation techniques were used to study the effect of the oxygen diffusion hardening.

3.3.1 Hardness Measurement

Microhardness measurements were done on both alloys in the as-received state. Microhardness was then measured on the oxidised circular coupons as well as on the diffusion treated ones. Specimens were sectioned normal to the flat surface using a precision cutting machine shown in figure 3.3.

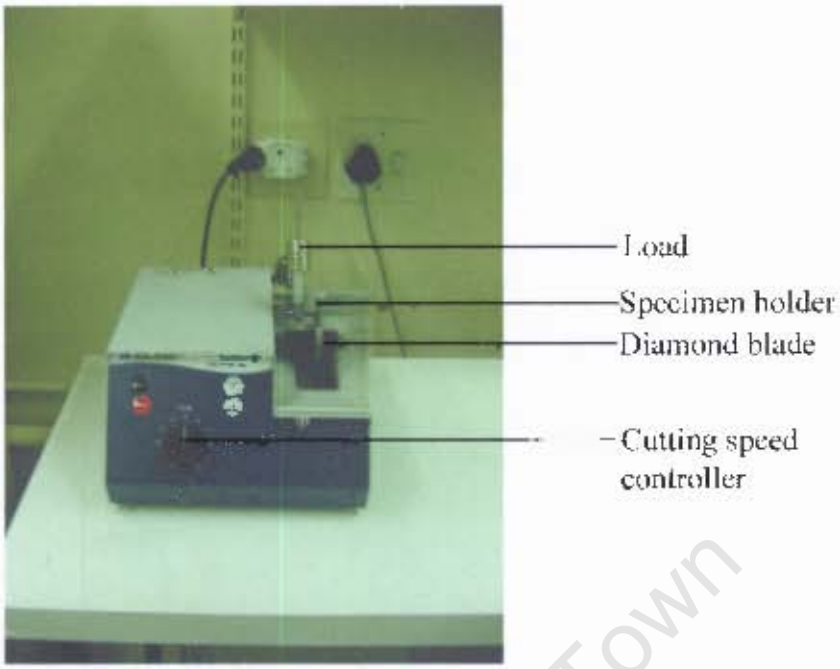

Figure 3.3: Isomet low speed saw used for precision cutting of the specimens.

Specimens were prepared for microhardness measurements in the following way: Firstly the specimens were mounted in Durofast resin using the Struers lab-press 3. Metalog method B from Struers Metalog Guide was used to grind and polish the specimens. The first step in the guide is grinding the specimen with the MD-Primo 220 grit pad at 300 rpm using water as a lubricant on the automatic polisher applying a force of 120N until the specimen is plane. The second step is further grinding of the specimen using the MD-Largo pad at 150 rpm using the diamond paste suspension with a grain size of 9 microns applying a force of 180N for 5 minutes. The final step is the polishing step that uses the MD-Nap pad at a speed of 150 rpm under a force of 60N for 2 minutes. The lubricant used in this final step is a mixture of 96 ml of the OP-U solution, 2 ml hydrogen peroxide and 2 ml of ammonia. After this step the specimens are ready for microhardness measurements and etching to reveal the underlying microstructure.

The Zwick microhardness tester shown in Figure 3.4 was used to measure the hardness on all the specimens.

Figure 3.4: Zwick hardness tester.

A load of 50 grams was used in the microhardness measurements. The hardness on the heat treated specimens was measured from the surface into the bulk of the specimen. Ten hardness measurements were taken at each fixed distance from the surface and an average hardness value as well as the standard deviation (for the particular distance) was computed from the ten values. A set of ten hardness measurements were taken at 13, 20, 45, 70, 100, 130 and 160 µm below the surface for the cycle heat-treated samples. An additional three distances of 200, 300 and 400 µm were included for the twin cycle heat-treated samples. The flow chart of heat treatment with sample preparation for hardness for one specimen is shown in figure 3.5.

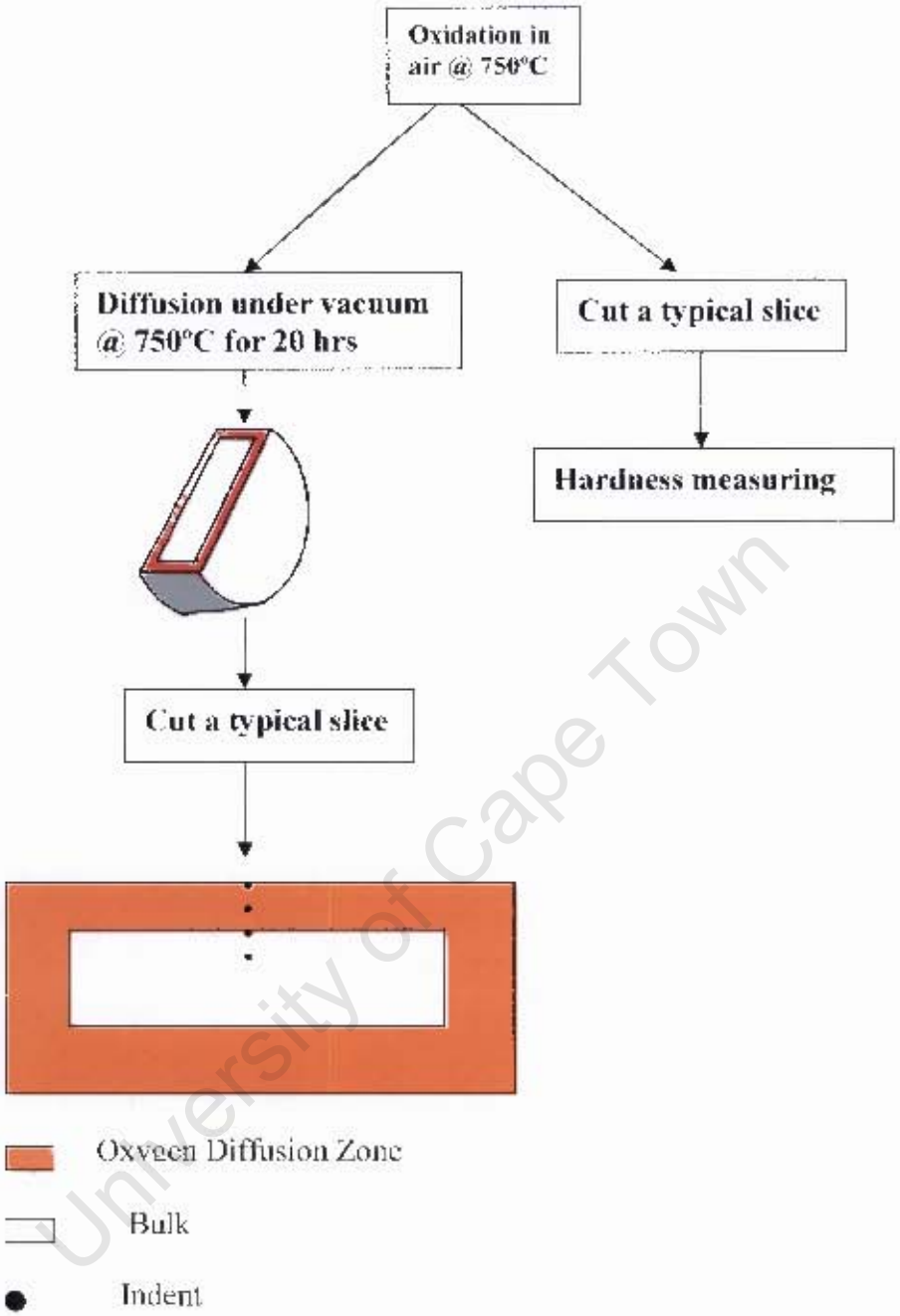

Figure 3.5: The flow diagram on the preparation of the test pieces for microhardness testing.

3.3.2 Metallographic Studies

A solution of 10 ml hydrogen fluoride, 30 ml nitric acid and 50 ml of water was used to etch the test pieces that were prepared in the same way as those prepared for microhardness measurements. The samples were dip-etched in the solution for 15-20 seconds. The revealed microstructure was then examined under the light microscope.

3.4 Wear Testing

There were three types of wear apparatus that were available to conduct the wear experiments. Prior to testing, the test pieces were ground using the 4000 grit silicon carbide (SiC) paper to remove any loose layer on the surface. The specimens were then cleaned with ethanol in ultrasonic bath and weighed.

3.4.1 The Pin-On-Disk Set Up

This form of tribometer is a widely used standard wear testing apparatus due to its simplicity and convenience[69]. The test piece is mounted and forced against the counterface disk (mounted onto a shaft driven by an electric motor) by the lever arm system. The counterface disk has to be more wear resistant than the specimen to ensure that only the test piece undergoes mass loss during the wear experiment although it is generally accepted that the counterface will undergo some minimal wear loss. When the specimen is mounted before the experiment commences the lever arm must be balanced to ensure zero residual load. The dead weight load can be placed on the end of the arm to increase the interfacial pressure. The load at the pin-counterface interface is twice the dead weight load due to torque balance. Friction can then be measured by a load cell restraining the tangential movement of the specimen clamp or measured by a strain gauge device located on the pivot arm. The Pin-On-Disk apparatus is shown in figure 3.6.

A – Chart recorder used to measure friction

B – Disk

C – Load

D - AC control box

E - R.P.M counter

F - Speed dial

G - Counter

Figure 3.6: The Pin-On-Disk set up.

There are various variables that can be altered to achieve the desired testing conditions. These include the load, the sliding velocity and the sliding distance. The load and the sliding velocity were fixed at 36.32N and 1.5 ms^{-1} respectively. The sliding distance was interrupted at regular intervals to measure the mass loss. The cumulative mass loss can thus be plotted against the sliding distance. The test was conducted without the use of a lubricant. The counterface of the cast iron with a hardness of 59 HRC (675Hv) was found to exhibit severe wear when the surface treated samples were tested. This compromised the integrity of the results and meant that the results of the surface treated samples could not be compared and contrasted with those of the untreated samples as there was no wearing of the counterface when the untreated samples were tested. The image of the worn cast iron counterface disk is shown in figure 3.7.

(a) (b)

Figure 3.7: (a) A severely worn cast iron counterface after pin on disk experiment against an OBDH treated test piece and (b) magnified portion of the cast iron counterface to show the extent of wear.

3.4.2 The Pin-On-Belt Abrasion Set Up

This kind of wear testing is conducted using pin on belt apparatus. The specimen is locked into a bracket and placed in contact with an abrasive belt. The motor-driven abrasive belt moves continuously in one direction while the specimen bracket moves simultaneously across the belt. The result is that the specimen surface is always in contact with fresh abrasive. The abrasive wear testing equipment used is shown in figure 3.8.

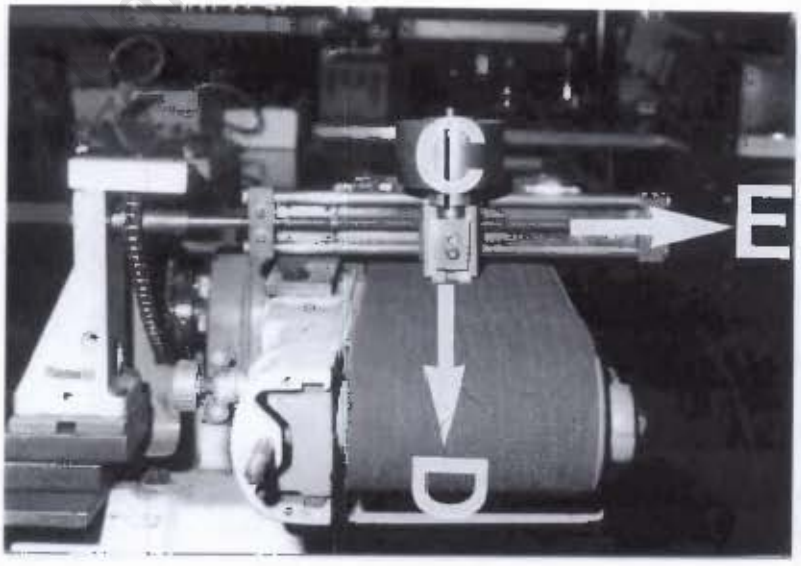

Figure 3.8: The Pin-On-Belt abrasion equipment.

The contact load, belt speed and the type of abrasive can be varied. The load was fixed at 2.5 kg while the belt speed was kept fixed at 0.6ms^{-1} and the type of abrasive used was metalite (alumina abrasive) 600 grit paper. Metalite 600 grit was convenient because a coarser grit would remove the modified layer quickly while a finer grit would take long to cause wear on the test pieces. This was a dry sliding wear test. The cumulative mass or volume loss can then be plotted against the sliding distance. Due to the relatively large surface area of the 22 mm diameter coupons there was no uniformity in the wear. A slight angle on the specimen orientation will be magnified as the test piece will lose mass at the point of contact that is experiencing the highest interfacial pressure. This disputed the integrity of the results obtained via this wear testing method. An image of the Ti67 alloy (oxidised at 750°C for 45 minutes and further boost heat-treated in argon at 850°C for 20 hours) in figure 3.9 depicts the non-uniform surface after the belt abrasive wearing.

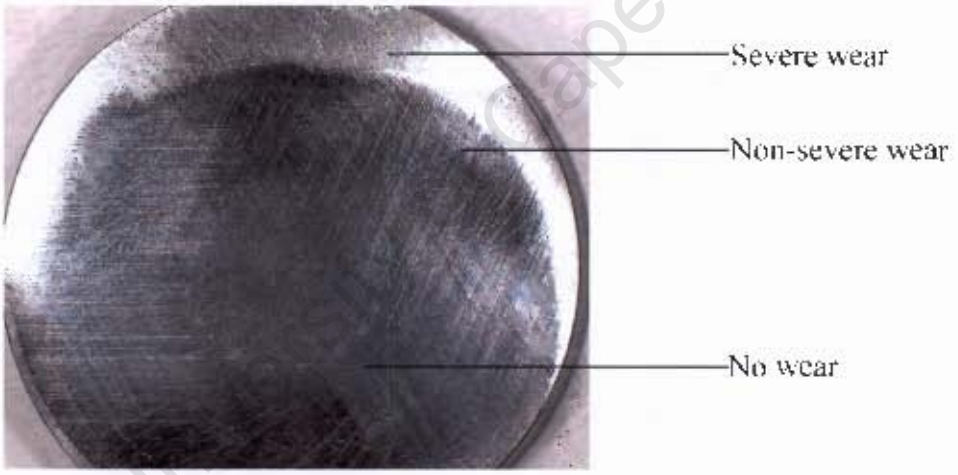

Figure 3.9: Non-uniform wearing of the OBDH treated sample upon the pin on belt abrasion wear.

3.4.3 Two-body Abrasive Wear on Automatic Grinding/Polishing Machine

The Struers Rotopol-22 base with rotoforce-4 head automatic grinding or polishing machine was used to carry out the abrasive wear test. The as-received, the pre-oxidised samples that were further heat-treated in vacuum or in argon as well as the

samples that underwent the twin cycle heat-treatment were subjected to this form of wear testing. A set of parameters were keyed into the machine. The pin specimen in the sample holder was set to run at 150 rpm in the same direction as the 800 grit SiC counterface under a load of 15N for five minutes. A constant flow of water at the centre of the rotating SiC ensured the removal of the wear debris. A fresh 800 grit SiC paper was used for each five minute test. The mass loss was measured for the untreated and surface treated samples under the above conditions. The mass loss was then plotted as a function of heat treatment.

Chapter Four

Experimental Results and Discussion

Introduction

From the various characterisation techniques employed to investigate the effect of the oxygen diffusion on the two alloys the following results have been obtained and discussed

4.1 Surface Hardening

Microhardness profiles for each heat-treated sample have been plotted. As indicated in the previous chapter a load of 50g was used on measuring the hardness on all the samples. Due to the good surface finish required for microhardness testing, the hardness resulting from the indents taken on the surfaces of the heat-treated samples could not be reported due to high percentage error. The closest distance from the surface edge of the specimens that the indents were made was at 13 μm. Getting closer to the edge increases the influence of the edge ("edge effects") on the hardness measurements. A lower load can be used to try and get even closer to the edge as well as obtain more points on the diffusion zone but the smaller the load the smaller the indent and the percentage error on the measurements is magnified.

4.1.1 Saturated Argon Environment

Upon carrying out the oxygen diffusion hardening via the dissociation of water vapour (in a controlled atmosphere of saturated argon) at 700°C for 10 and 48 hours for both alloys the microhardness of the heat-treated alloy surfaces was measured and presented in figures 4.1 and 4.2.

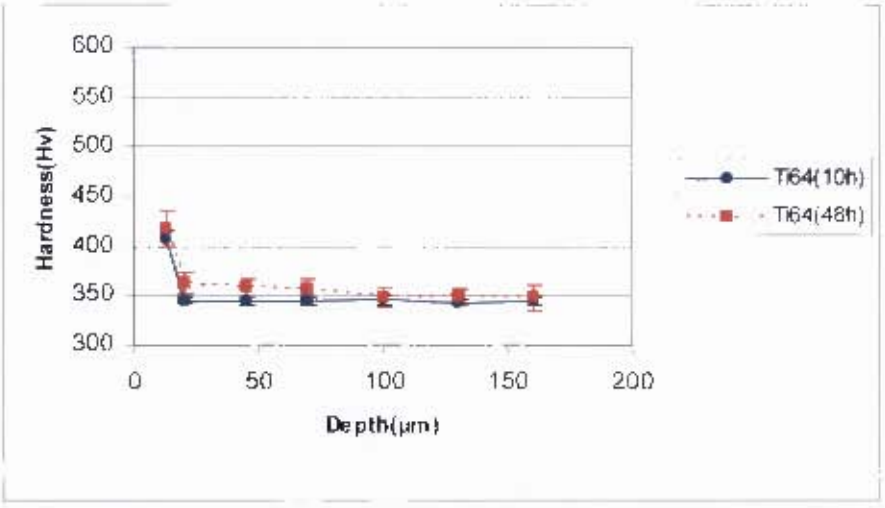

Figures 4.1: Microhardness profiles for the Ti64 alloy after ODH via the dissociation of water vapour at 700°C for 10 and 48 hours.

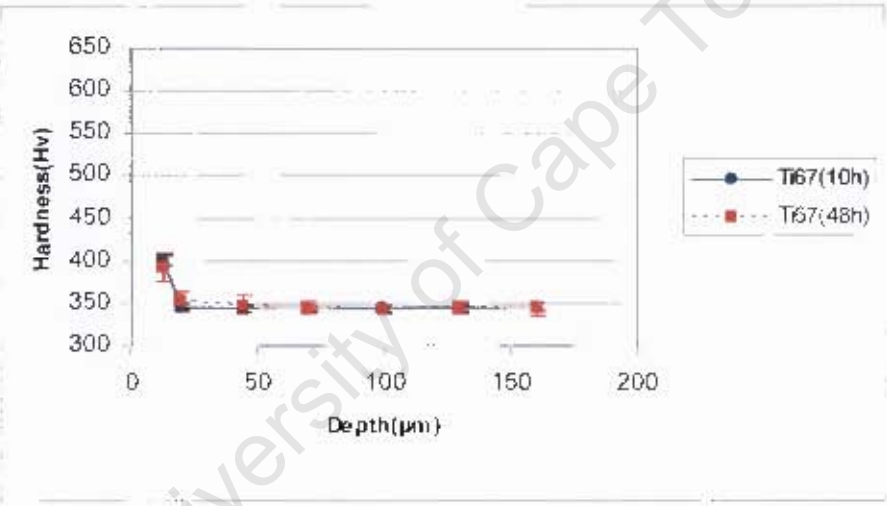

Figures 4.2: Microhardness profiles for the Ti67 alloy after ODH via the dissociation of water vapour at 700°C for 10 and 48 hours.

Inspection of the figures 4.1 and 4.2 shows an increase in hardness at 13 µm for both alloys. SIMS analysis conducted by Poggie et al.[1] on the Ti-13Nb-13Zr oxygen diffusion hardened in same controlled atmospheric conditions at 500°C for 6 hours showed the total depth of oxygen penetration to be 2-3 µm. The conditions at which the ODH was conducted in this research encouraged more diffusion of oxygen into the two alloys as more time and higher temperature were used. This results in the oxygen diffusion that will cause an increase in hardness up to 13 µm. There is no significant increase in the surface hardening of the two alloys from carrying the ODH

at 10 or 48 hours at 700°C. This suggests that increasing the time at the same temperature does not influence the kinetics of this form of ODH very much.

As an under study to this particular ODH process, an experiment was conducted to investigate the role of water vapour on the hardening of the two alloys. The controlled atmosphere experiment was set up with argon instead of the saturated argon flowing into the furnace. In other words, the water bottle was excluded from the set up as the argon was purged directly into the furnace at atmospheric pressure. The experiment was carried out at 700°C for 10 hours. The hardness profiles of the two alloys after this heat-treatment are shown in figure 4.3.

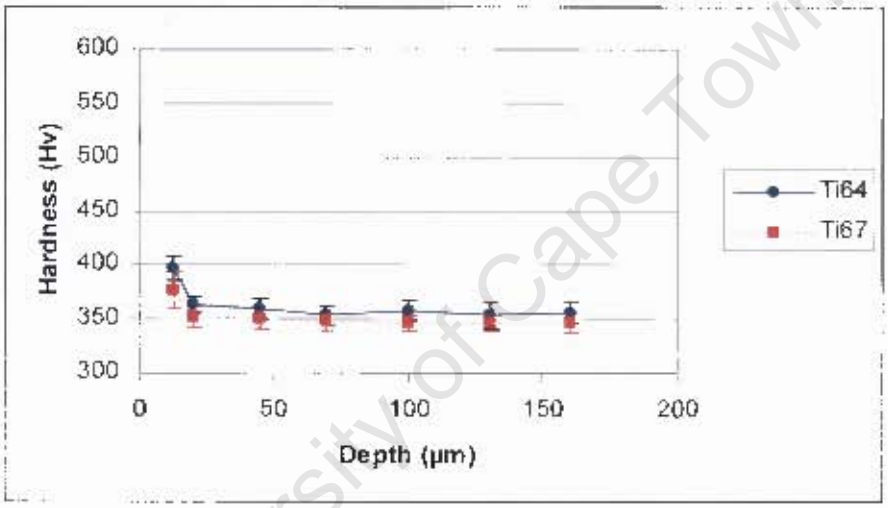

Figures 4.3: Microhardness profiles for the Ti64 and Ti67 alloys after heat-treatment in circulating argon atmsphere at 700°C for 10 hours.

It can be seen from the hardness profiles of the two alloys that the hardening that was measured at 13 µm for the ODH with the heat-treatment that involved argon saturated with water vapour has been detected for the samples with only argon. This may not necessarily discard the diffusion of oxygen during the ODH in argon saturated with water vapour but encourage the study of the reaction of titanium metal with argon or the rest of the noble gases and the resulting influence on the mechanical properties of titanium. It is possible that an oxide layer forms (due to small amount of oxygen present in the furnace) and that the hardness reflects this oxide formation. The outcome possibly points to the fact that under the present experimental conditions the saturated argon technique is not particularly effective.

4.1.2 Oxygen Boost Diffusion Hardening (OBDH)

The initial step of the OBDH process was oxidation of the test pieces in air.

4.1.2.1 Step One: Oxidation Heat-treatment in air

The hardness profiles of the two alloys after oxidation at various temperatures for various periods are shown in the figures 4.4 and 4.5.

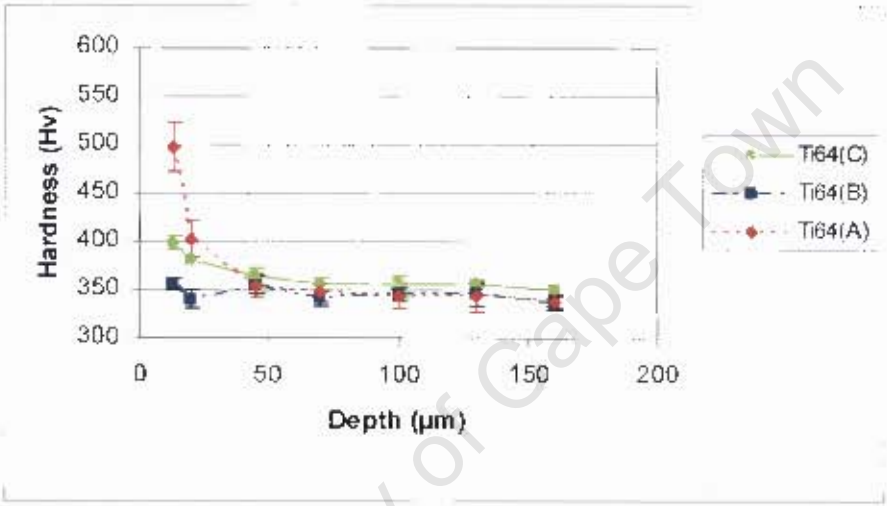

Figures 4.4: Microhardness profiles for Ti64 alloy after oxidation at 850°C for 30 minutes (A), oxidation at 750°C for 45 minutes(B) and oxidation at 600°C for 20 hours (C).

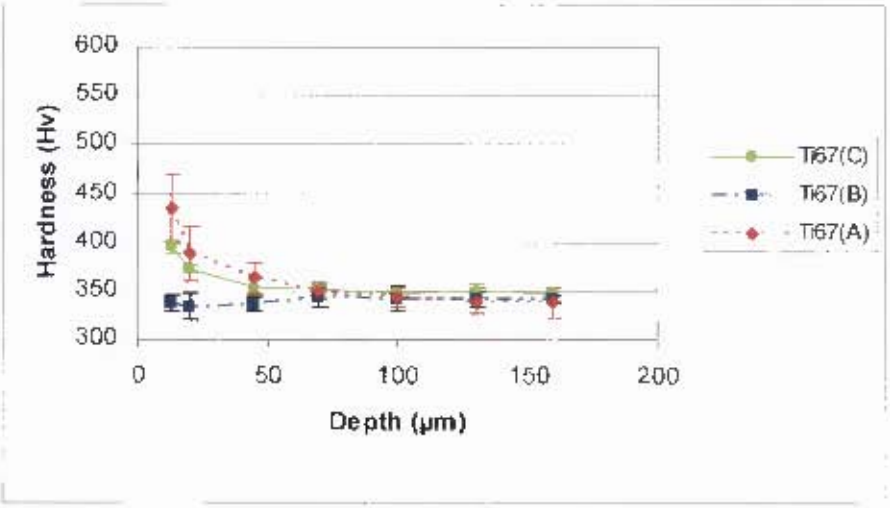

Figures 4.5: Microhardness profiles for Ti67 alloy after oxidation at 850°C for 30 minutes (A), oxidation at 750°C for 45 minutes(B) and oxidation at 600°C for 20 hours (C) in air.

Of the three oxidation conditions it is seen that oxidation in air at 850°C for 30 minutes results in the highest average hardness on the surfaces of both alloys. The Ti64 alloy shows higher surface hardness than the Ti67 alloy upon the same oxidation heat-treatments. There is also an increase in hardness at the surfaces of both alloys after oxidation at 600°C for 20 hours. There is no observed change on the surface hardness of both alloys after oxidation at 750°C for 45 minutes.

The above result indicates that oxidation at 850°C for 30 minutes results in thicker oxide formation and more diffusion zone supporting the oxide scale than the other two oxidation conditions. This is in agreement with the optimum oxidation conditions for the Ti64 alloy suggested by Dong et al.[39]. Oxidation at 600°C for 20 hours also shows an increase in hardness on the surfaces for both alloys despite the relatively low oxidation temperature. The relatively longer time has resulted in sufficient diffusion which allows for an increase in hardness at 13 µm. The change in colour for both alloys after oxidation at 750°C for 45 minutes clearly suggests that oxidation took place. The time period of 45 minutes at 750°C may not be sufficient to allow for an oxide formation and diffusion that would be detectable by means of hardness measurements at 13 µm from the surface.

The pre-oxidised samples were then further heat-treated in an oxygen-free environment. The effect of heat-treating the pre-oxidised test pieces in an oxygen deficient environment is shown by means of hardness profiles (figures 4.6-4.8) for pre-oxidised samples that were further heat-treated in vacuum at 750°C for 20 hours.

4.1.2.2 Step Two: Vacuum Boost Diffusion

Subjecting the pre-oxidised samples to further heat-treatment in vacuum has resulted in higher hardness on the surface as well as a thicker hardened zone for both alloys as shown by figures 4.6-4.8.

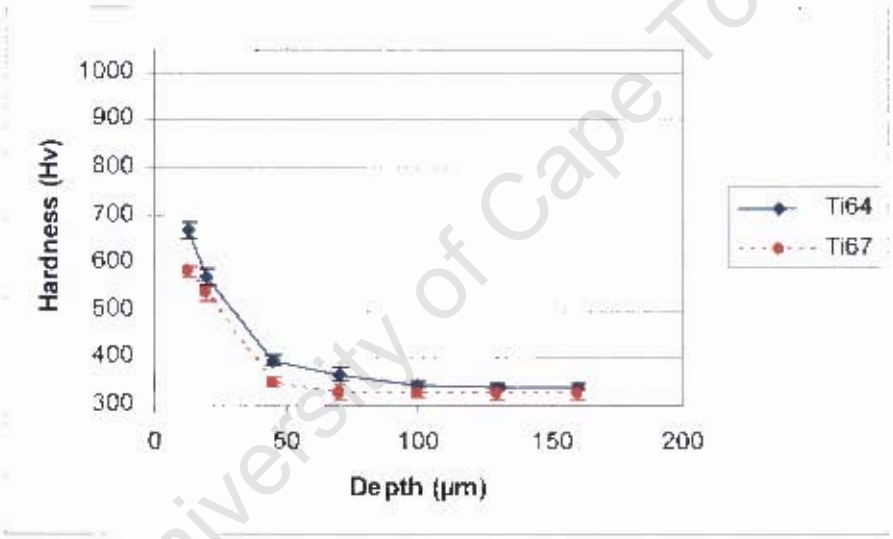

Figure 4.6: Microhardness profiles for Ti64 and Ti67 alloys- Oxidation at 850°C for 30 minutes followed by heat-treatment in vacuum at 750°C for 20 hours.

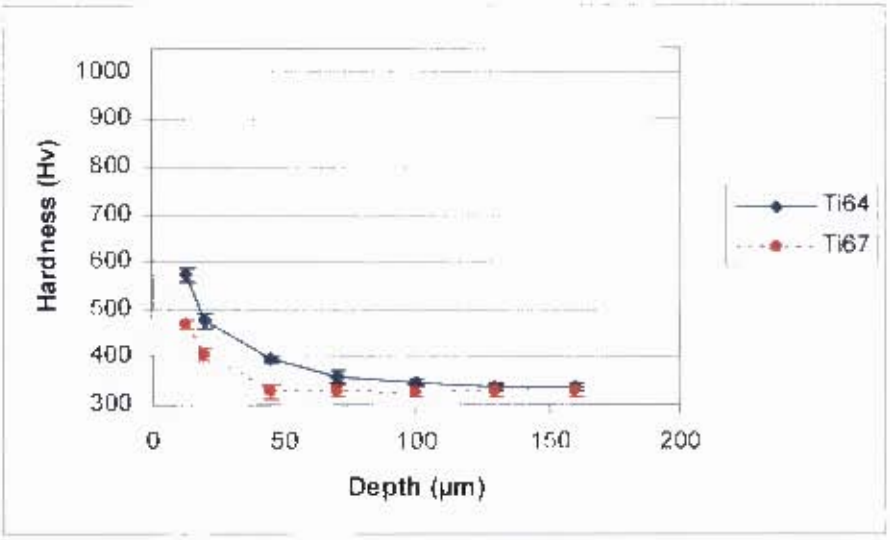

Figure 4.7: Microhardness profiles for Ti64 and Ti67 - Oxidation at 750°C for 45 minutes followed by heat-treatment in vacuum at 750°C for 20 hours.

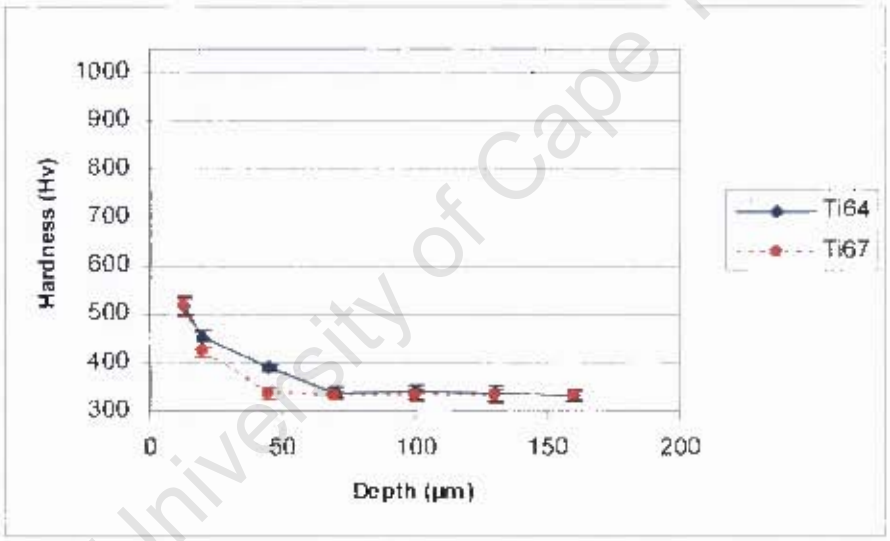

Figure 4.8: Microhardness profiles for Ti64 and Ti67 - Oxidation at 600°C for 20 hours followed by heat-treatment in vacuum at 750°C for 20 hours.

Both alloys have showed an increase in hardness which declines gradually with increasing depth from the surface into the bulk of the surface treated samples. Highest surface hardness is measured for sample pre-oxidised at 850°C for 30 minutes for both alloys. As concluded by Dong et al. [39], the oxidation step is vital for OBDH as the oxide formed during this step acts as an oxygen reservoir for the second step. It is the rutile formed during the oxidation step that breaks down in the oxygen and nitrogen free environment and oxygen is released to diffuse further into the titanium

component and forming an oxygen diffusion zone beneath the oxide scale. Oxidation at higher temperatures results in optimum oxide formation which is essential for the second step. Morton and Baldwin [47] discovered that discontinuities on the gas absorption isothermals which occurred after heating titanium for short periods at high temperatures took the form of a sudden increase in the rate of gas absorption. As indicated before, oxidation of titanium is still not fully understood. Other studies suggest that the diffusivity of oxygen in rutile is 50 times that of titanium in rutile and therefore oxygen is the diffusing species during the "inward growth" of the oxide. Studies by Li[63] et al. have revealed that oxygen ambient causes extraction of titanium atoms from the bulk and near surface region in the "outward growth" of the oxide. This research cannot suggest which of the two processes actually takes place. One of these two processes occurs, it is clear that the process will be enhanced by high temperatures because of increased diffusion resulting in a thicker oxide formation.

While samples oxidised at 750°C for 45 minutes showed no increase in hardness at 13 μm, after heat-treatment in vacuum at 750°C for 20 hours, an increase from ≈344 Hv to 577±16 Hv is measured for the Ti64 alloy. This suggests that despite oxidation at 750°C for 45 minutes not forming a thick oxide that can be detected via microhardness testing at 13 μm from the surface, some oxide has been formed to allow for the diffusion of oxygen during the second step. Oxidation at 600°C for 20 hours might not necessarily form a thick oxide but the relatively long time encourages diffusion of oxygen into the zone below the oxide layer during oxidation, hence the hardness increase that was measured for both alloys after oxidation at 600°C for 20 hours.

Another set of the pre-oxidised samples was further heat-treated in vacuum at 850°C for 20 hours to study the effect the varying the temperature for the second step of OBDH.

4.1.2.3 Effect of Varying the Step Two Temperature

Subjecting the pre-oxidised samples to a heat-treatment in vacuum at higher temperature (850°C) for 20 hours has produced different hardness profiles to those of

pre-oxidised samples further heat-treated in vacuum at 750°C for 20 hours. Higher surface hardness and deeper modified layer is achieved for both alloys. The hardness profiles of both sets of alloys after these heat-treatments are shown in figures 4.9-4.11.

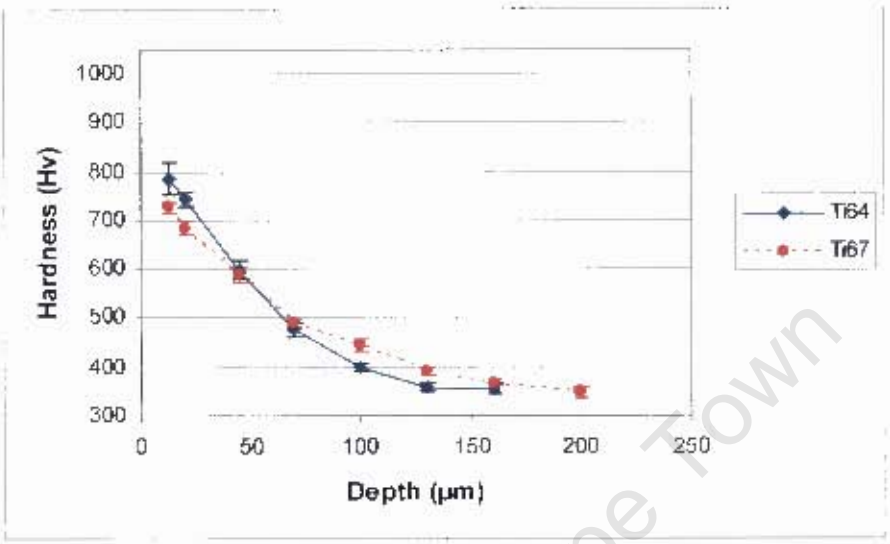

Figure 4.9: Microhardness profiles for Ti64 and Ti67 - Oxidation at 850°C for 30 minutes followed by heat-treatment in vacuum at 850°C for 20 hours.

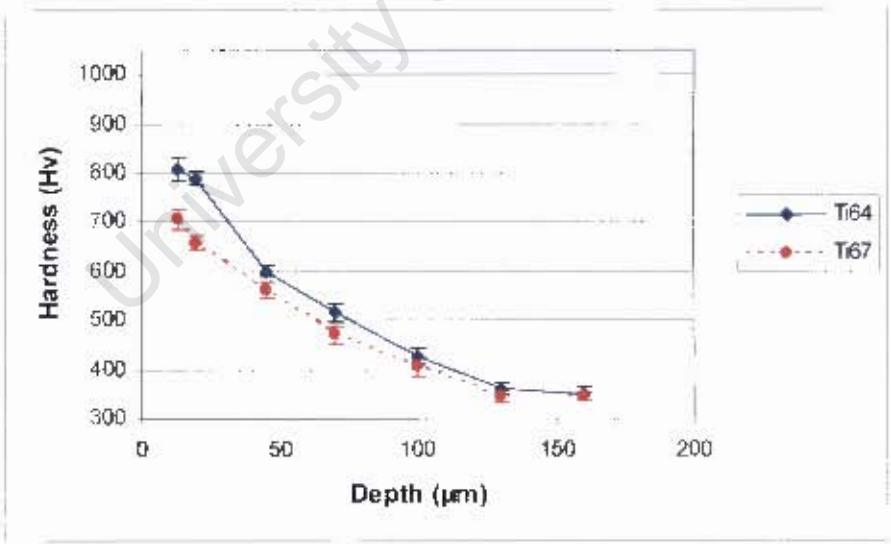

Figure 4.10: Microhardness profiles for Ti64 and Ti67 - Oxidation at 750°C for 45 minutes followed by heat-treatment in vacuum at 850°C for 20 hours.

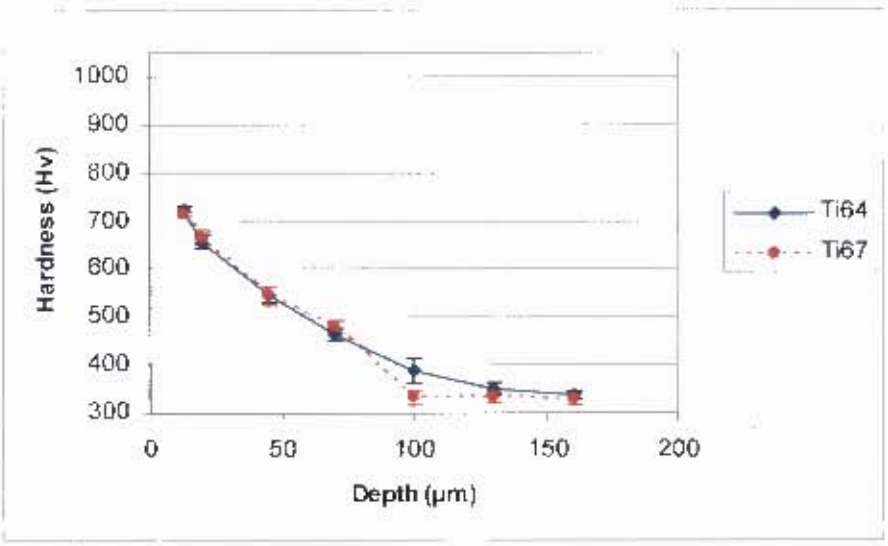

Figure 4.11: Microhardness profiles for Ti64 and Ti67 - Oxidation at 600°C for 20 hours followed by heat-treatment in vacuum at 850°C for 20 hours.

The surface hardness of the pre-oxidised samples subsequently heat-treated in vacuum at 850°C for 20 hours showed hardness values between 721±11 and 810±25Hv on the surfaces for the Ti64 alloy, while the pre-oxidised Ti64 samples subsequently heat-treated in vacuum at 750°C for 20 hours showed surface hardness values between 518±18 and 670±17. Similarly the Ti67 alloy has showed a hardness increase from between 417±14 and 574± 16 Hv to between 706±21 and 727±9 upon increasing the second step temperature from 750°C to 850°C.

Higher temperature facilitates higher diffusion rates. Both mechanisms that are suggested for the OBDH process are temperature dependent. The decomposition of the oxide into titanium and oxygen as well as the diffusion of oxygen into titanium is dependent on the temperature. Luo et al.[56] states that according to Crank[70], the diffusion of oxygen in titanium lattices follows the Fick's first and second laws.

$$J = -D\frac{\partial C(x,t)}{\partial x} \text{ -------- Eqn (10)}$$

$$\frac{\partial C(x,t)}{\partial t} = D\frac{\partial^2 C(x,t)}{\partial x^2} \text{ --------- Eqn (11)}$$

where, J is the flux of mass transfer ($kgs^{-1}m^{-2}$), $C(x,t)$ is the oxygen concentration in solution at depth x and time t, D is the coefficient of oxygen in titanium (m^2s^{-1}).

The diffusion coefficient of oxygen in titanium is strongly dependent on the concentration of oxygen and if that dependence is considered, then Fick's second law becomes:

$$\frac{\partial C(x,t)}{\partial t} = D\frac{\partial^2 C(x,t)}{\partial x^2} + \left(\frac{\partial D}{\partial x}\right)\left(\frac{\partial C(x,t)}{\partial x}\right) \text{-------- Eqn (12)}$$

Luo et al.[56] states that according to Shamblen and Redden[71], the diffusion coefficient of oxygen in titanium may take the form of:

$$D = \left[k(C)^{\gamma}\right]\exp\left(-Q/RT\right) \text{-------- Eqn (13)}$$

where k, γ is the empirical constants to be determined for each alloy, C is the oxygen concentration (wt%), Q is the activation energy of temperature dependence of diffusivity, R is the gas constant, T is the temperature. This equation of diffusivity can be inserted into the Fick's second law to describe the diffusion of oxygen in titanium lattice. The equation suggests the dependence of the diffusion process on temperature.

For the pre-oxidised test pieces that were further heat-treated in vacuum at 850°C for 20 hours, it is noticeable that the Ti64 alloy pre-oxidised at 750°C for 45 minutes shows a slightly higher surface hardness than the sample pre-oxidised at 850°C for 30 minutes. This is not the case for the Ti67 alloy. This depicts a very important difference in the thermal behaviour of the two alloys. Despite oxidation at 850°C for 30 minutes in air being suggested as optimal for the first step of OBDH of Ti64, there is incidence of spalling off of the oxide layer that sometimes occurred during air cooling from this oxidation temperature. The peeling of the oxide scale means less oxygen content is then made available for the second step of OBDH. The Ti67 alloy showed no signs of scaling after oxidation at 850°C for 30 minutes. This alloy derives its thermal stability from the formation of Nb_2O_5 which is much more stable than V_2O_5 formed in the Ti64 alloy as concluded by Chuanxi et al.[43].

The other set of pre-oxidised samples were further heat-treated in an argon atmosphere at the same temperature and time as those samples subsequently heat-treated in vacuum. This was to understand whether it is the action of vacuum or the absence of oxygen that is responsible for the decomposition of the oxide film during the second step.

4.1.2.4 Step Two: Argon Boost Diffusion

The hardness profiles of the pre-oxidised samples further heat-treated in an argon atmosphere of 9.33×10^4 Pa at 750°C for 20 hours are shown in figures 4.12-4.14.

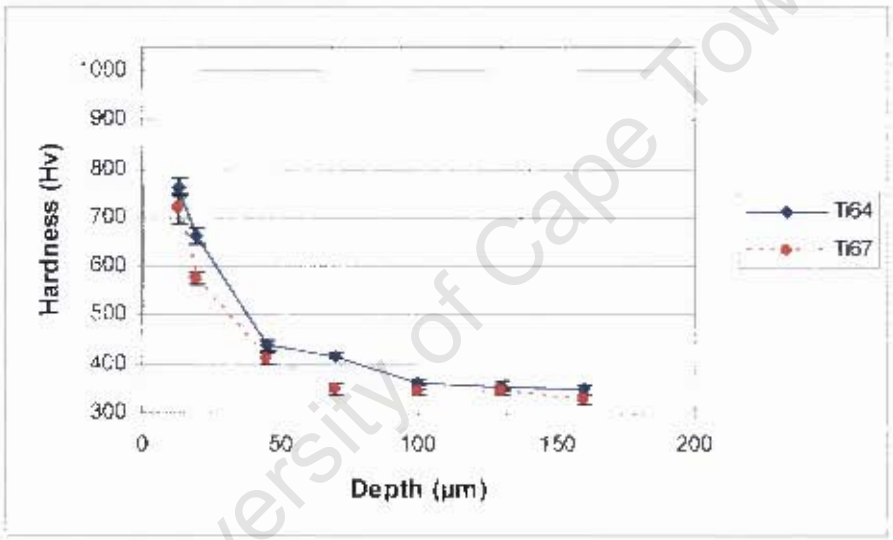

Figure 4.12: Microhardness profiles for Ti64 and Ti67 - Oxidation at 850°C for 30 minutes followed by heat-treatment in argon at 750°C for 20 hours.

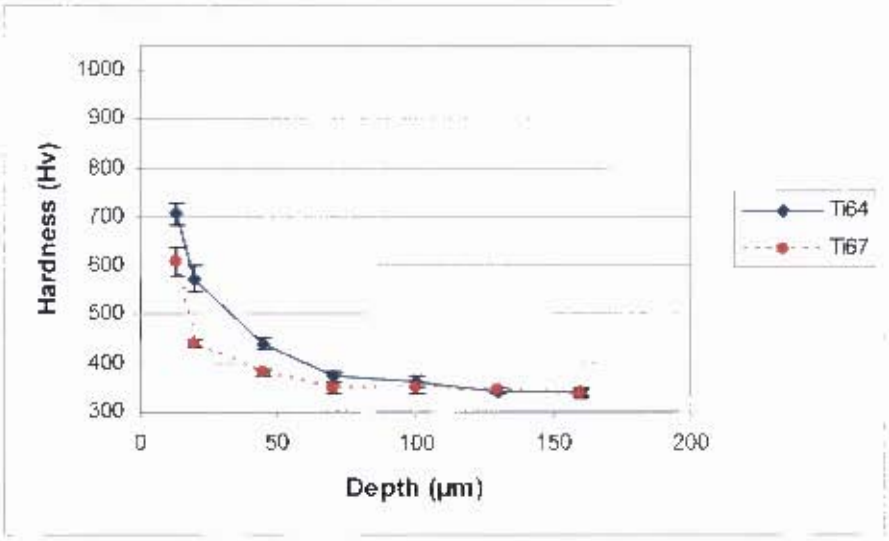

Figure 4.13: Microhardness profiles for Ti64 and Ti67 - Oxidation at 750°C for 45 minutes followed by heat-treatment in argon at 750°C for 20 hours.

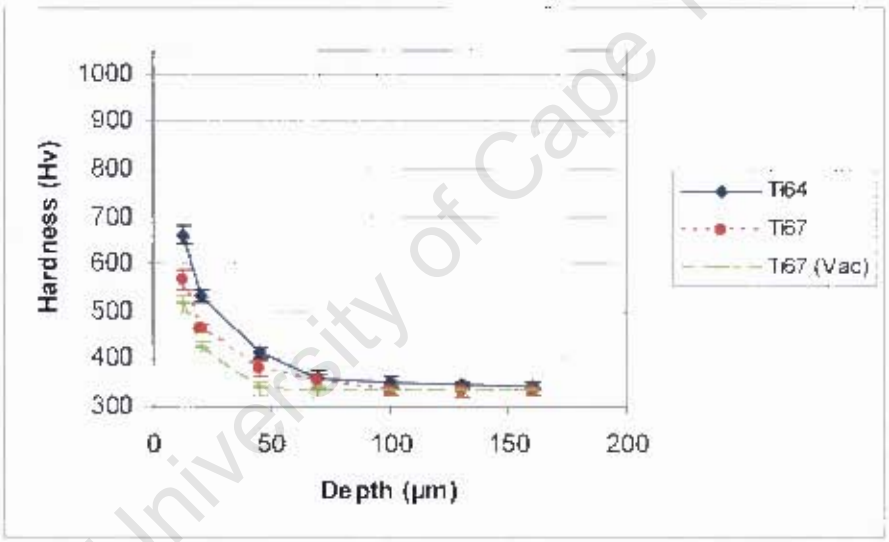

Figure 4.14: Microhardness profiles for Ti64 and Ti67 - Oxidation at 600°C for 20 hours followed by heat-treatment in argon at 750°C for 20 hours with the Ti67 alloy that has been heat-treated the same way but further diffusion heat-treated in vacuum overlaid for comparison.

An increased hardness on the surface which gradually decreases from the surface into the bulk of the test piece is shown on the hardness results plotted above. It is therefore clear that any high temperature inert environment facilitates the diffusion hardening during the second step. What is also notable on the hardness profiles above is that, pre-oxidised samples further heat-treated in an argon atmosphere at 750°C for

20 hours exhibit higher surface hardness and deeper hardened zone than pre-oxidised samples further heat-treated in vacuum at 750°C for 20 hours. Microhardness profile of the Ti67 alloy oxidised at 600°C for 20 hours and further boost diffusion treated in vacuum at 750°C for 20 hours has been overlaid on the microhardness profiles of the two alloys upon oxidation at 600°C for 20 hours followed by boost diffusion treatment in argon at 750°C for 20 hours in figure 4.14 for comparison.

Similarly, the pre-oxidised samples further heat-treated in an argon atmosphere at 850°C for 20 hours exhibit higher surface hardness (comparison is shown in figure 4.16) than the pre-oxidised samples further heat-treated in vacuum at 850°C for 20 hours as seen from the hardness profiles in figures 4.15-4.17.

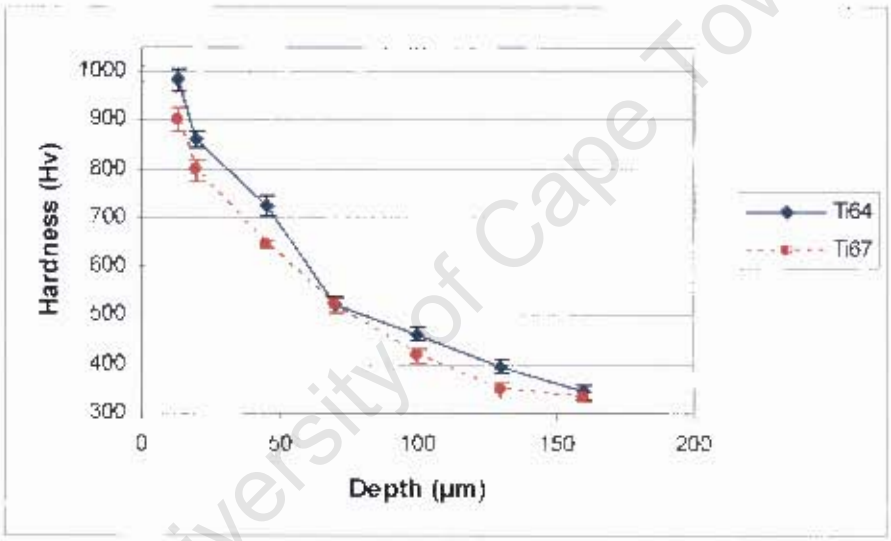

Figure 4.15: Microhardness profiles for Ti64 and Ti67 - Oxidation at 850°C for 30 minutes followed by heat-treatment in argon at 850°C for 20 hours.

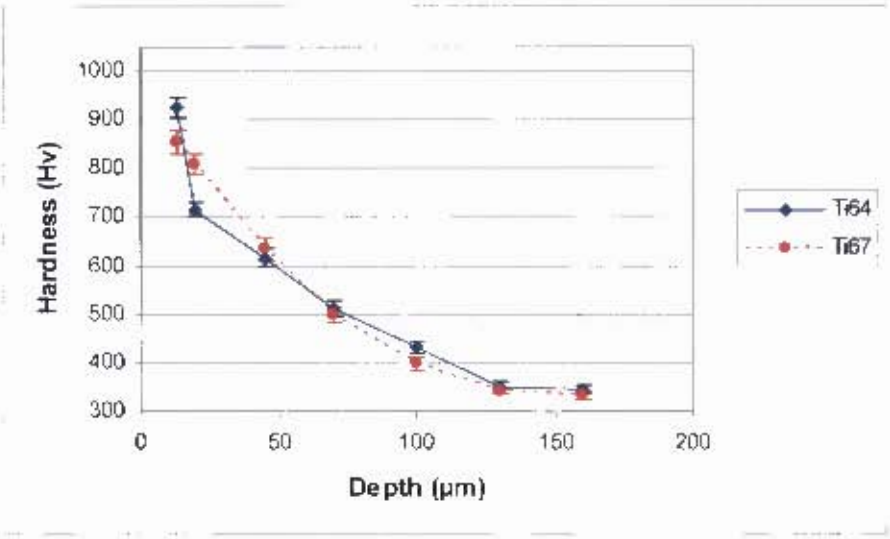

Figure 4.16: Microhardness profiles for Ti64 and Ti67 - Oxidation at 750°C for 45 minutes followed by heat-treatment in argon at 850°C for 20 hours.

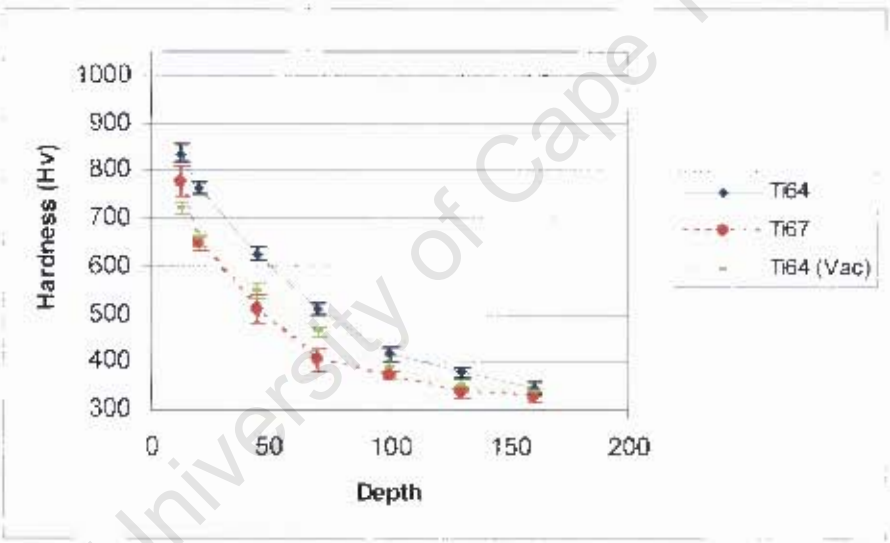

Figure 4.17: Microhardness profiles for Ti64 and Ti67 - Oxidation at 600°C for 20 hours followed by heat-treatment in argon at 850°C for 20 hours with the Ti67 alloy that has been heat-treated the same way but further diffusion heat-treated in vacuum overlaid for comparison.

As observed before, the highest surface hardness is achieved on the test pieces that were pre-oxidised at 850°C for 30 minutes in air. This suggests that there was no stratification of the oxide layer on cooling the Ti64 samples after oxidation. As expected, the surface hardness of the pre-oxidised samples that were further heat-treated in an argon atmosphere at 850°C for 20 hours is higher than the pre-oxidised

samples that were further heat-treated in an argon atmosphere at 750°C for 20 hours. The depth of the hardened zone is also thicker for the samples further heat-treated in an argon atmosphere at 850°C for 20 hours.

No reason that has been formulated to explain the increase in surface hardness that has been achieved via carrying the second step of OBDH in argon as compared to carrying it in vacuum. As stated in the second chapter the oxygen diffusion hardening process depends on three parameters namely the solute dissolved in the titanium, the temperature at which the diffusion process is carried as well as the partial pressure of oxygen in the system. Since the same alloy types were used as well as the same temperature for both vacuum and argon environments the difference in hardening can be attributed to the difference in the partial pressure of oxygen in the two systems. If we assume that the argon pumped into the furnace for the argon diffusion heat-treatment is pure then it can be concluded that the amount of oxygen in both the vacuum and argon systems is the same. The amount of oxygen in both systems is equivalent to the oxygen that is left after the vacuum is pumped until 1.33×10^{-2} Pa. The ideal gas equation can thus be used to investigate the partial pressure of the two systems:

$$PV = nRT \text{ -------- Eqn (14)}$$

where P is the pressure of the system , V is the volume of the system, n is the number of moles of gases in the system, R is the gas constant and T is the absolute temperature of the system. For the two systems the volume of the furnace used is the same, the gas constant is the same and the temperature upon which the heat-treatments were carried out is the same. Therefore the pressure of the system is proportional to the total number of moles in the system.

$$P_T \propto n_T$$

The partial pressure of oxygen in the system is proportional to the total number of moles of oxygen in the system.

$$P_{O_2} \propto n_{O_2}$$

This result is not surprising because the partial pressure of a gas is defined as the pressure the gas exerts on the system as if it was alone.

For the vacuum system: $\frac{P_{O_2}}{P_T} \propto \frac{n_{O_2}}{n_{O_2} + n_{N_2}}$ where n_{N_2} is number of moles of nitrogen (from the residual air after pumping down the vacuum) in the system.

Once the argon is purged for the argon atmosphere heat-treatments:

$$\frac{P_{O_2}}{P_T} \propto \frac{n_{O_2}}{n_{O_2} + n_{N_2} + n_{Ar}}$$ where n_{Ar} is the number of moles of argon in the system. The total pressure increase in the second system is due to the addition of argon into the furnace and the partial pressure of oxygen is the same for both systems. Therefore there is no difference in the partial pressures of the two systems.

Argon is an inert gas and therefore should not form compound with the titanium test pieces. The possible reason could be the interaction of argon with the titanium surfaces at high temperatures. It is understood that the type of inert gas used during titanium melting and casting has serious implications for the extent of porosity and the resulting mechanical properties of the cast components. Zinelis[72] concluded that specimens cast under argon show higher hardness than the ones that have been cast under krypton and xenon. The extent of solubility of inert gases in the titanium lattice remains unknown. At high enough temperatures in an argon atmosphere, argon can possible 'open-up' the surface of the titanium sample and thereby paving way for oxygen (which can bond to titanium) to diffuse further in the titanium matrix in what is referred to as the "exchange reaction". Argon is a bigger atom than oxygen and the exchange reaction between the two species would lead to porosity.

4.1.2.5 Effect of the Alloying Element on the OBDH of Titanium Alloys

All the hardness profiles have one common feature and that is the Ti64 microhardness profile always shows higher surface hardness and deeper hardened zone than the Ti67 alloy. The difference between the two alloys is that one contains vanadium and the other one contains niobium. As indicated before the Ti64 alloy forms V_2O_5 while the Ti67 alloy forms Nb_2O_5. Nb_2O_5 formed during the oxidation of Ti67 is much more stable than V_2O_5 that is formed during the oxidation of Ti64. Once the two oxides have been formed during the oxidation in air, V_2O_5 will break down quicker than the Nb_2O_5[42,43]. With the decomposition of V_2O_5 more oxygen will be made available to diffuse into the titanium matrix while less oxygen will be released in the case of the more thermally stable Nb_2O_5.

Twin cycle heat treatments were carried out on the pre-oxidised samples further heat-treated in vacuum/argon at 850°C for 20 hours.

4.1.2.6 Effect of the Number of Heat-treatment Cycles on the OBDH

Even higher surface hardness and deeper hardened zone was achieved by performing an OBDH cycle heat-treatment on the two alloys as suggested by the microhardness profiles in figures 4.18-4.23. During the OBDH heat-treatment a sample that is oxidised in air and further diffusion treated in vacuum or argon atmosphere has undergone a cycle heat-treatment. A cycle heat-treated sample that is further oxidised and diffusion treated in the same conditions as the first cycle has undergone a twin cycle heat-treatment.

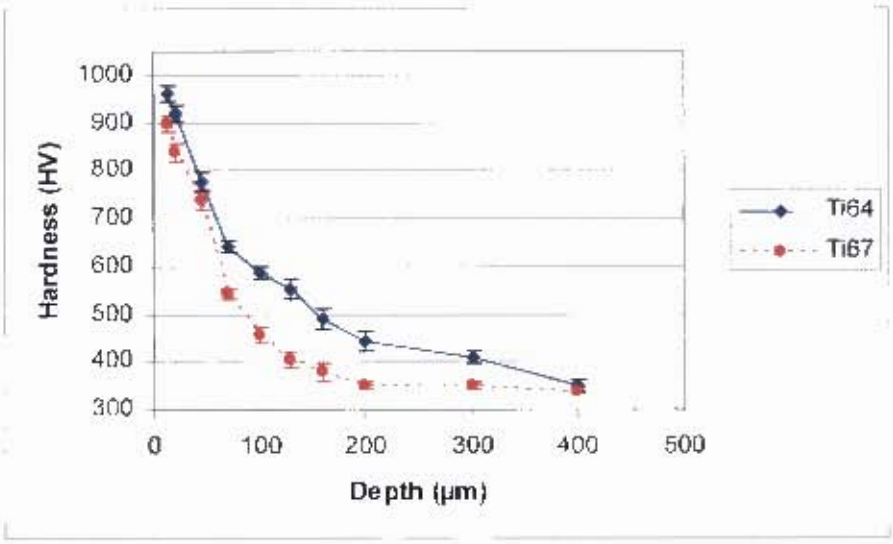

Figure 4.18: Microhardness profiles for Ti64 and Ti67 – Twin cycle oxidation at 850°C for 30 minutes followed by heat-treatment in vacuum at 850°C for 20 hours.

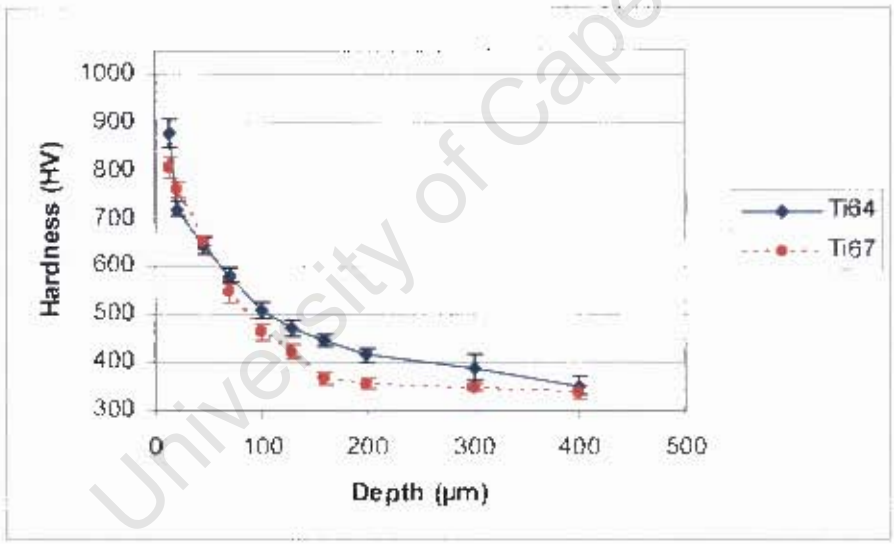

Figure 4.19: Microhardness profiles for Ti64 and Ti67 – Twin cycle oxidation at 750°C for 45 minutes followed by heat-treatment in vacuum at 850°C for 20 hours.

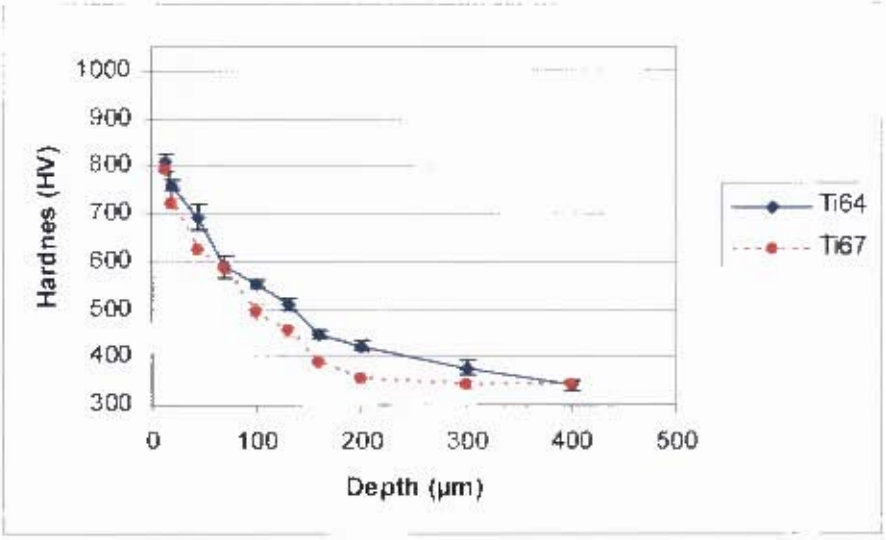

Figure 4.20: Microhardness profiles for Ti64 and Ti67 – Twin cycle oxidation at 600°C for 20 hours followed by heat-treatment in vacuum at 850°C for 20 hours.

Higher surface hardness and deeper hardened zone is achieved despite severe scaling of the samples that was observed for both alloys during the twin cycle heat-treatment. The twin cycle heat-treatment was carried out on the pre-oxidised samples that were further heat-treated in vacuum or in an argon atmosphere at 850°C for 20 hours.

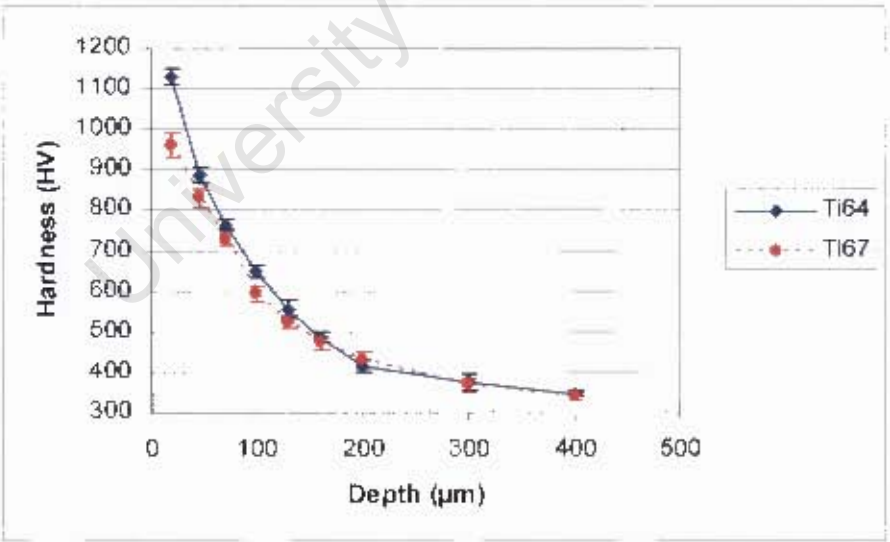

Figure 4.21: Microhardness profiles for Ti64 and Ti67 – Twin cycle oxidation at 850°C for 30 minutes followed by heat-treatment in argon at 850°C for 20 hours.

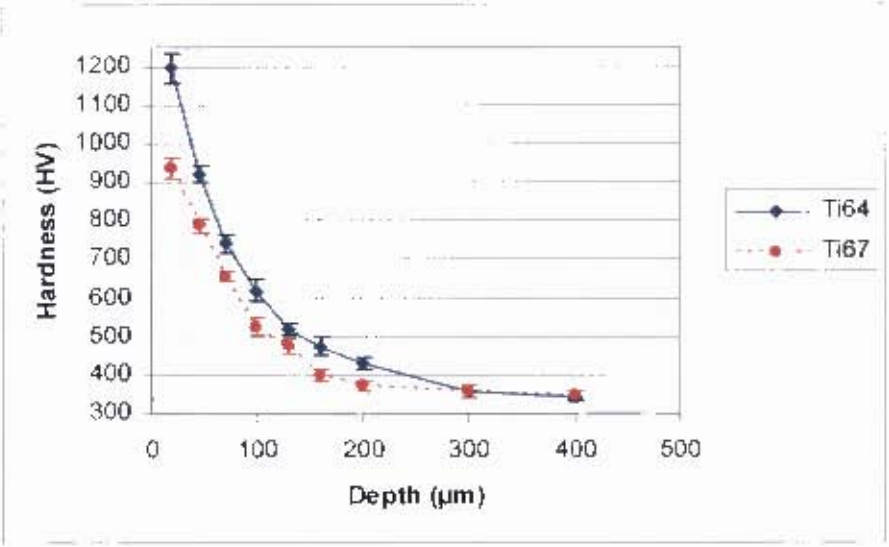

Figure 4.22: Microhardness profiles for Ti64 and Ti67 – Twin cycle oxidation at 750°C for 45 minutes followed by heat-treatment in argon at 850°C for 20 hours.

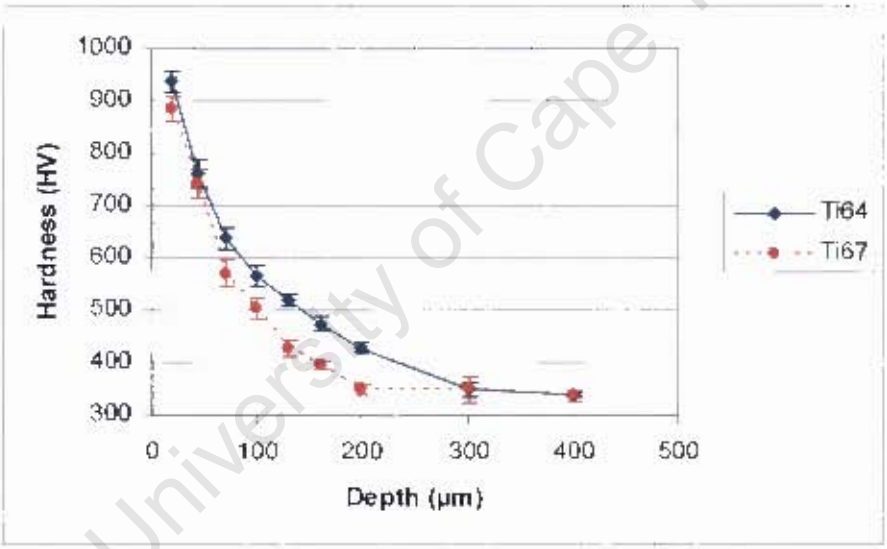

Figure 4.23: Microhardness profiles for Ti64 and Ti67 – Twin cycle oxidation at 600°C for 20 hours followed by heat-treatment in argon at 850°C for 20 hours.

The increased surface hardness and deeper hardened zone is not surprising because both steps involved in the OBDH play a vital role. The first step (oxidation) results in the formation of oxide which is the oxygen reservoir for the second step. The deficiency of oxygen and nitrides in the second step facilitates the decomposition of the oxide scale thereby releasing oxygen atoms to diffuse into the titanium matrix. The deficiency of the oxygen in the vacuum or argon environment inhibits oxidation that leads to scaling of the oxide layer. The deficiency of the nitrogen means there is

no formation of nitrides in the oxide/substrate interface which hinders the diffusion of oxygen from the oxide layer into the substrate. The pile-up of nitrogen in the form of nitrides on oxide/substrate interface of Ti64 alloy oxidised in air was detecteted by Dong et al[39]. The oxide scale which is the source of oxygen becomes depleted after the second step (diffusion in vacuum/argon) of OBDH. The twin cycle heat treatment replenishes the oxide film after the diffusion process building up an oxygen source for the second diffusion heat-treatment in an oxygen deficient environment. Therefore the twin cycle heat-treatment allows for higher oxygen content on the surface of the test piece as well as longer time for diffusion which is important for surface treatments governed by gas diffusion into the metal surface.

Key for the OBDH Samples

Example: Ti64-A,Ar-850

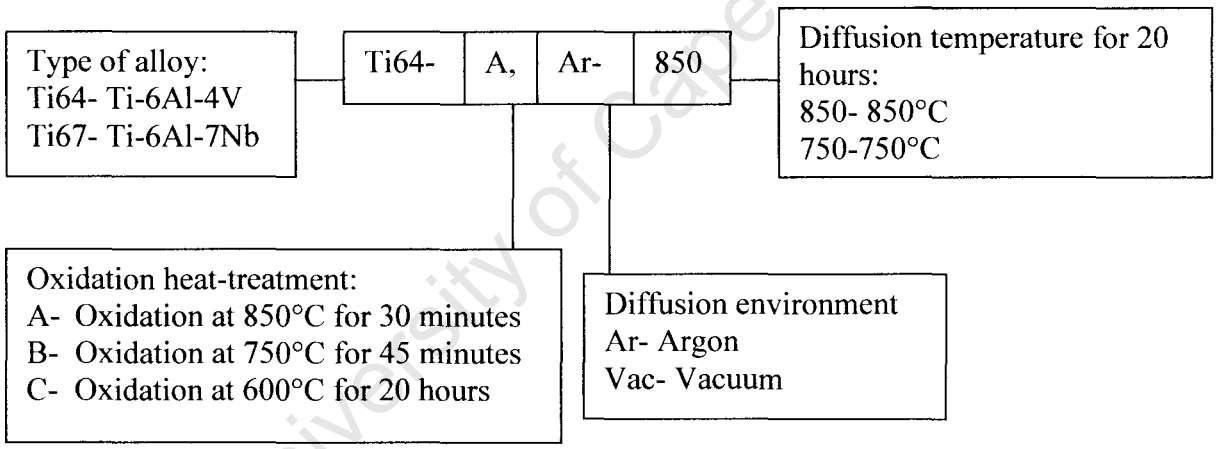

4.1.3 Microstructural Analysis

Optical micrographs for both alloys were captured to study the effect of the heat-treatments on the underlying microstructures of the two alloys. All the micrographs were captured under 50 x objective lens magnifications.

4.1.3.1 The As-received Condition

The microstructures of the two alloys in the as-received condition are shown in figure 4.24.

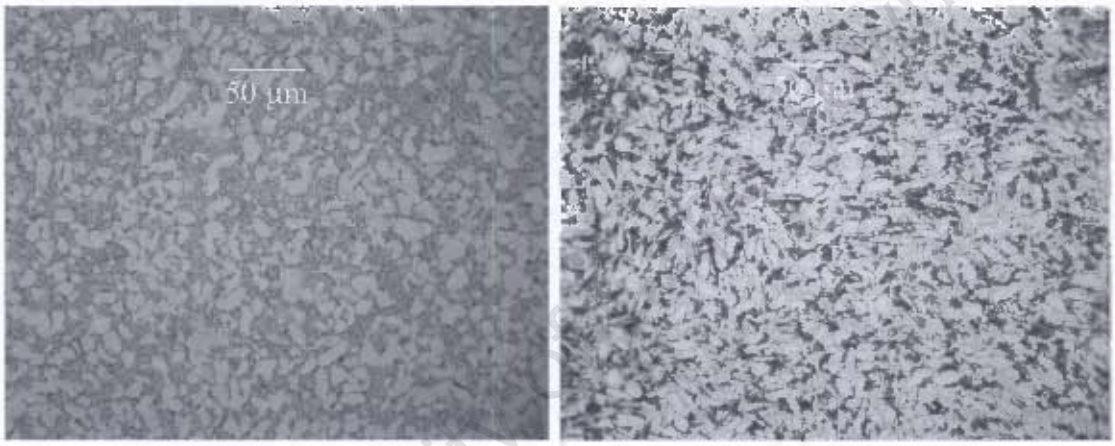

(a) Ti64 (b) Ti67

Figure 4.24: Optical micrographs showing the underlying microstructures of untreated (a) Ti64 alloy and (b) Ti67 alloy.

Both microstructures reveal a combination of the α-β grain structure as expected for the two alloys. Aluminium stabilises the α phase in both alloys while vanadium and niobium stabilises the β phases of the Ti-6Al-4V and Ti-6Al-7Nb respectively. The phase that appears light from the etching effect is the HCP α phase and the dark phase is the BCC β phase. The homogeneously dispersed equiaxed grain structure is indicative of annealed alloys. The alloys were then subjected to various ODH heat-treatments.

4.1.3.2 Water saturated Argon Environment

The microstructures of the surfaces of the samples oxygen diffusion hardened in a controlled atmosphere via the dissociation of water vapour are shown below along with the micrographs of the two alloys that were heat-treated in argon.

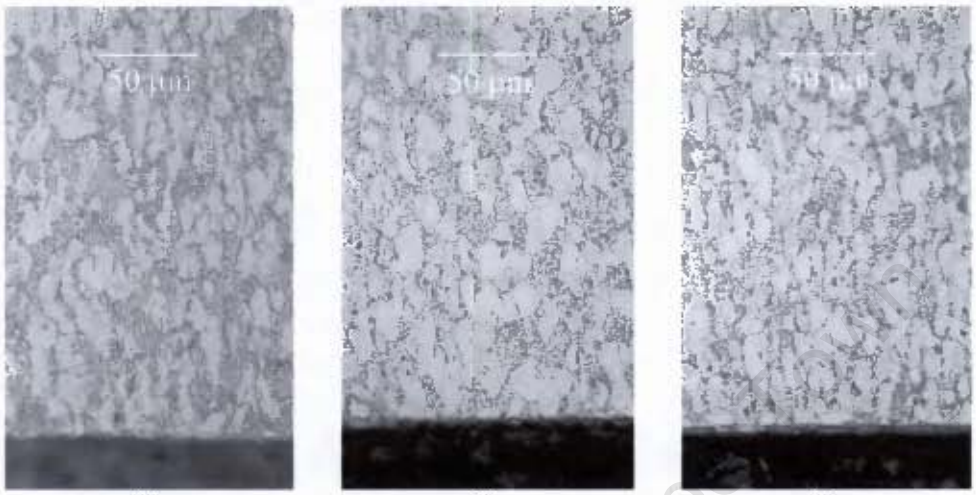

(a) (b) (c)

Figure 4.25: Cross-section optical micrographs of the Ti64 alloy after heat-treatment in (a) Argon at 700°C for 10 hours, (b) Argon saturated with water vapour at 700°C for 10 hours and (c) Argon saturated with water vapour at 700°C for 48 hours.

(a) (b) (c)

Figure 4.26: Cross-section optical micrographs of the Ti67 alloy after heat-treatment in (a) Argon at 700°C for 10 hours, (b) Argon saturated with water vapour at 700°C for 10 hours and (c) Argon saturated with water vapour at 700°C for 48 hours.

Observation on the surfaces of the two alloys upon the ODH in figures 4.25 and 4.26 shows no influence of absorption of oxygen. As an α phase stabilizer, oxygen would be expected to cause a surface layer that is depleted of the dark β phase. With hardening of the alloys that was measured up to only 13 μm it would be difficult to detect any volume fraction changes of the two phases using optical microscopy. As expected the heat-treated samples show larger grains than the untreated samples due to grain growth that occurred at elevated temperatures. There is no notable change on the surfaces of Ti64 as well as Ti67 that have undergone ODH in the controlled atmosphere at 700°C for 10 hours and 48 hours. The sample heat-treated with just purging argon into the furnace at 700°C for 10 hours exhibit similar microstructures as those samples heat-treated in controlled atmosphere of argon.

4.1.3.3 Oxygen Boost Diffusion Hardening (OBDH)

The OBDH is a surface modifying process and particular attention will be focused on studying the changes occurring on the surfaces of the two alloys upon the heat-treatment processes. The cross section of the micrographs was used to reveal the changes occurring on the surfaces of the two alloys. The microstructures of the oxidised samples (step one) are shown in figures 4.27 and 4.28.

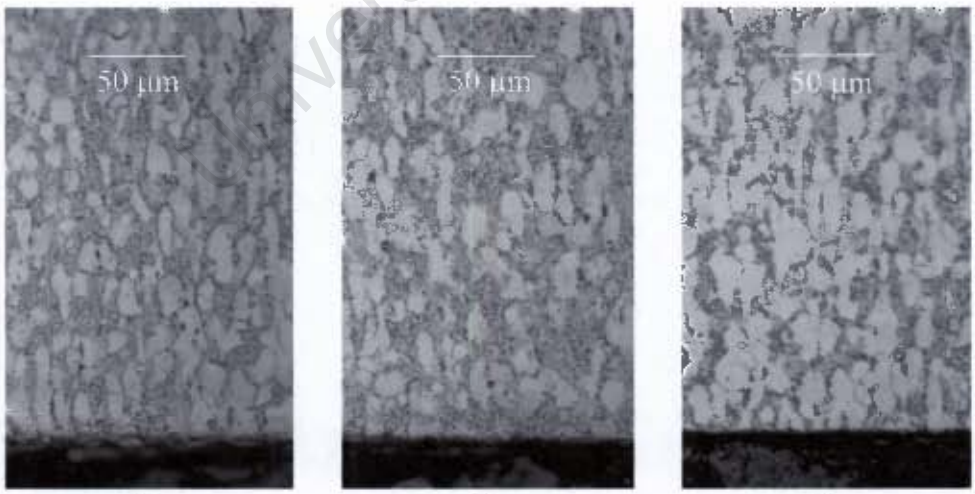

(a) (b) (c)

Figure 4.27: Cross-section optical micrographs of the Ti64 alloy oxidised at (a) 850°C for 30 minutes, (b) 750°C for 45 minutes and (c) 600°C for 20 hours.

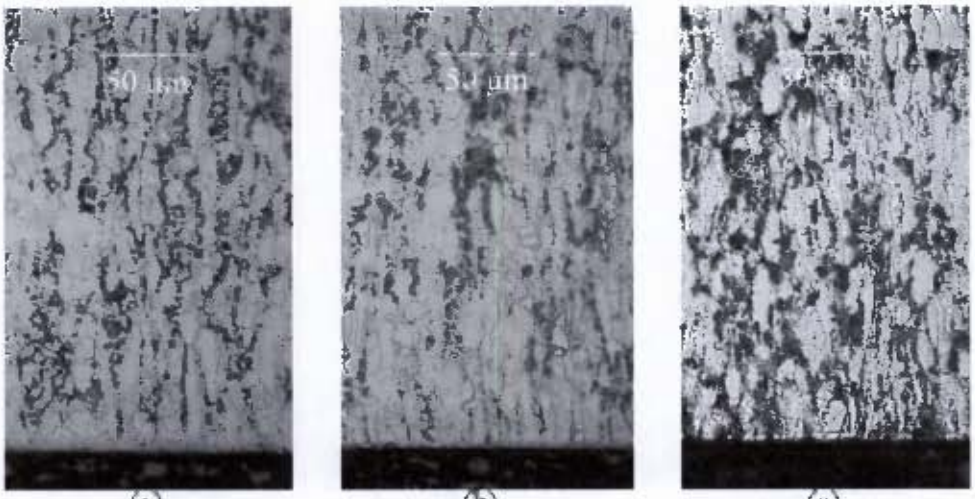

Figure 4.28: Cross-section optical micrographs of the Ti67 alloy oxidised at (a) 850°C for 30 minutes, (b) 750°C for 45 minutes and (c) 600°C for 20 hours.

There is no oxide layer that is seen on the micrographs after oxidation of the alloys. The oxide layer is thin and cannot be revealed by the magnification used for optical micrographs. The notable difference on the micrographs after oxidation is the elongation (less circular) of the grains and growth of the grains. The elongation of the grains is more pronounced for the samples oxidised at 850°C for 30 minutes and the samples oxidised at 750°C as the samples were quenched in air from a high temperature. There was not enough time allowed for the grains to spheridise and assume the circular grain structure due to air quenching. Treatment at 850°C is the highest of the three oxidation temperatures therefore samples cooled in air from this temperature will undergo the fastest cooling rate due to steep thermal gradient between 850°C and the room temperature.

There is a light band of the light phase that appears as a thin film on the surface of the Ti67 alloy oxidised at 850°C for 30 minutes is observed. This thin layer on the surface suggests the influence of oxygen as an α phase stabiliser.

The microstructures of the OBDH samples were captured for comparison with the oxidised samples.

4.1.3.3.1 Effect of the Second Step of OBDH on the Microstructures of the Two Alloys

The microstructures of the pre-oxidised Ti64 alloy samples further heat-treated in vacuum at 750°C for 20 hours reveal no significant changes in terms of volume fractions of the two phases present on the surfaces. This is despite the increase in hardness on the surfaces of this alloy after this particular heat-treatment. The optical micrographs of the 2 alloys are shown in figures 4.29 and 4.30.

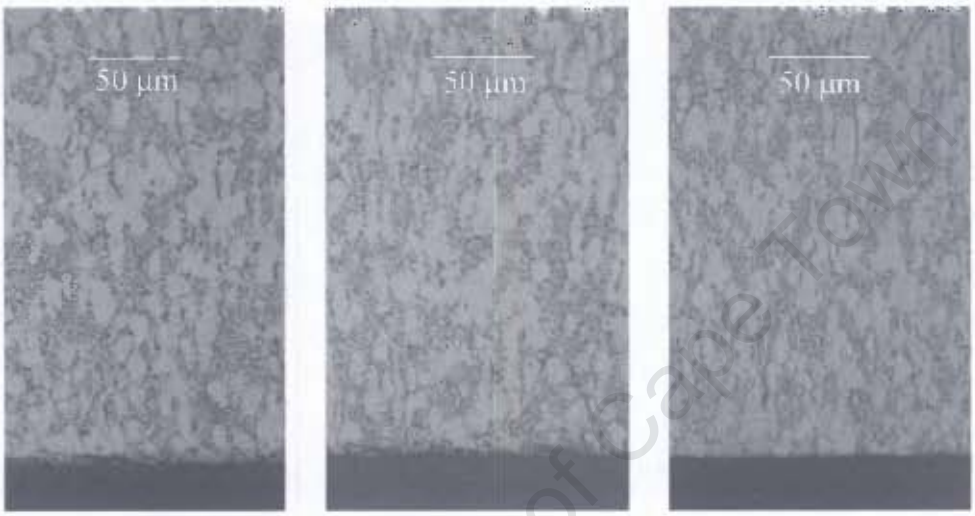

(a) (b) (c)

Figure 4.29: Cross-section micrographs of the samples (a) Ti64-A,Vac-750, (b) Ti64-B,Vac-750 and (c) Ti64-C,Vac-750.

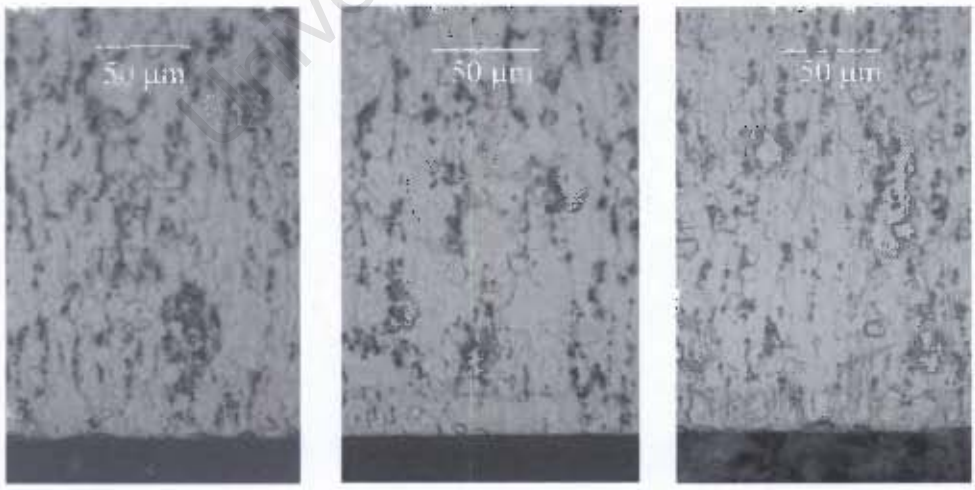

(a) (b) (c)

Figure 4.30: Cross-section micrographs of the samples (a) Ti67-A,Vac-750, (b) Ti67-B,Vac-750 and (c) Ti67-C,Vac-750.

The Ti67 alloy shows a thin zone that is depleted of the dark β phase at the surface. Oxygen is an α phase stabiliser hence a certain amount of oxygen absorbed by titanium and alloys will influence the volume fractions of the α-β system by increasing the volume fraction of the α phase at the expense of the β phase.

4.1.3.3.2 Effect of Varying the Temperature during the Second Step of OBDH on the Underlying Microstructures

Upon heat-treating the pre-oxidised test pieces at 850°C in vacuum for 20 hours a significant change on the microstructures was noticed as shown in figures 4.31 and 4.32.

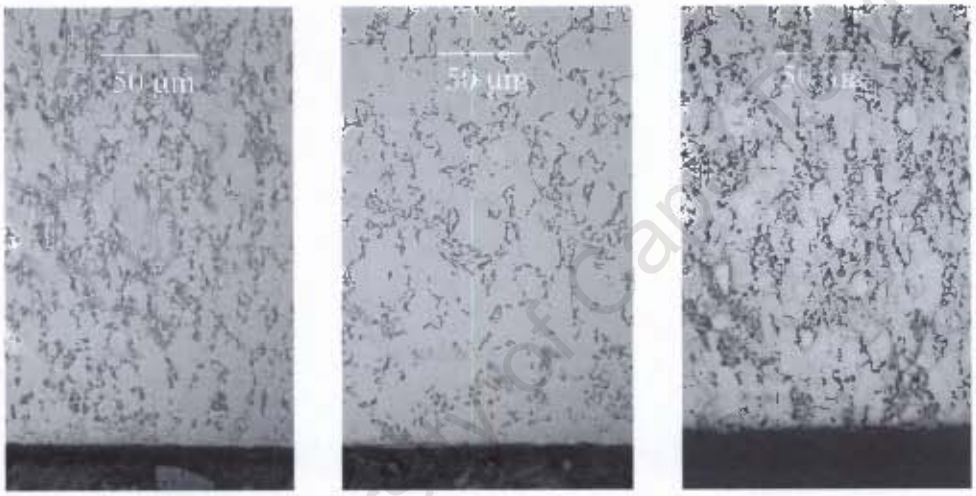

(a) (b) (c)

Figure 4.31: Cross-section micrographs of the samples (a) Ti64-A,Vac-850, (b) Ti64-B,Vac-850 and (c) Ti64-C,Vac-850.

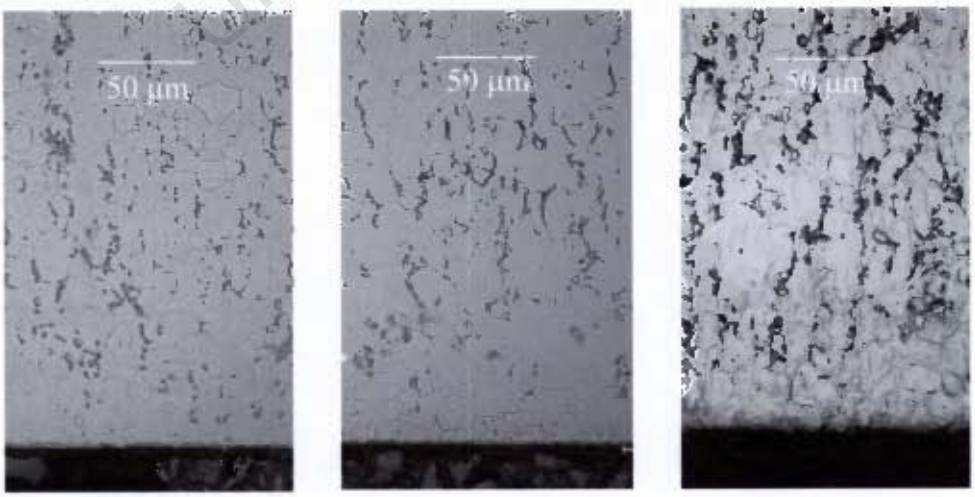

(a) (b) (c)

Figure 4.32: Cross-section micrographs of the samples (a) Ti67-A,Vac-850, (b) Ti67-B,Vac-850 and (c) Ti67-C,Vac-850.

In both alloys there is a distinct zone that is depleted of the dark β phase on the surface. Enough oxygen has diffused into the two alloys such that the α phase becomes dominant on the surfaces of OBDH samples. This modification of the microstructure is in agreement with the increased surface hardness and thicker hardened zone that is observed for the pre-oxidised samples further heat-treated in vacuum at 850°C for 20 hours than those further heat-treated in vacuum at 750°C for 20 hours. Higher temperature in vacuum causes more oxygen diffusion into the bulk which results in a thicker β depleted zone as well as higher surface hardness and deeper diffusion hardened zone.

It can be observed from the microstructures in figures 4.31 and 4.32 that the Ti67 alloy shows a more conspicuous and thicker β depleted zone than the Ti64 alloy after the same heat-treatment. This is despite the higher surface hardness for the Ti64 alloy than the Ti67 alloy after the OBDH. A conclusion can thus be drawn that, less amount of oxygen is required to influence the volume fractions of two phases in an α-β system of the Ti67 alloy than the Ti64 alloy.

After the twin cycle heat- treatment on the pre-oxidised samples further heat-treated in vacuum at 850°C for 20 hours the optical micrographs of the cross-section were captured.

4.1.3.3.3 Effect of the Number of Heat-treatment Cycles on the OBDH

The light α phase is even more pronounced on the surfaces of the twin cycle heat-treated test pieces shown in figures 4.33 and 4.34. More diffusion that is facilitated by oxygen replenishment and longer diffusion time resulted in more β depleted surfaces. A thicker diffusion zone is observed as the hardening profiles of these samples suggested.

(a) (b) (c)

Figure 4.33: Cross-section optical micrographs for twin cycle samples (a) Ti64-A,Vac-850, (b) Ti64-B,Vac-850 and (c) Ti64-C,Vac-850.

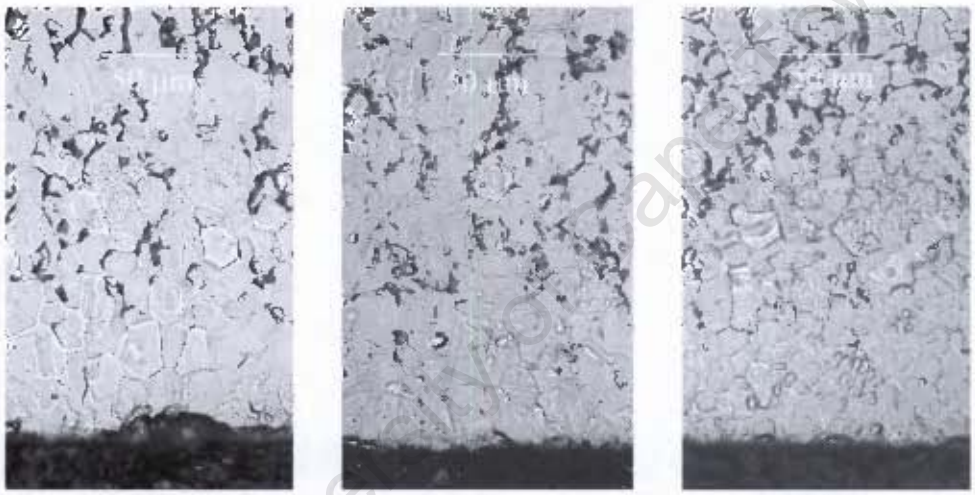

(a) (b) (c)

Figure 4.34: Cross-section optical micrographs for twin cycle samples (a) Ti67-A,Vac-850, (b) Ti67-B,Vac-850 and (c) Ti67-C,Vac-850.

What is more significant with the twin cycle heat-treated samples is the unevenness of the surface which is indicative of the severe stratification of the surfaces that occurred during the twin cycle heat-treatment. More unevenness is observed on the twin cycle heat-treated sample that was pre-oxidised at 850°C for 30 minutes which indicates that more scaling occurred during the heat-treatment of this sample.

4.1.3.3.4 Step Two: Argon Boost Diffusion

Similarly the changes that were observed on the pre-oxidised samples further heat-treated in vacuum have been observed for the pre-oxidised samples further heat-treated in an argon atmosphere shown in figures 4.35-4.38.

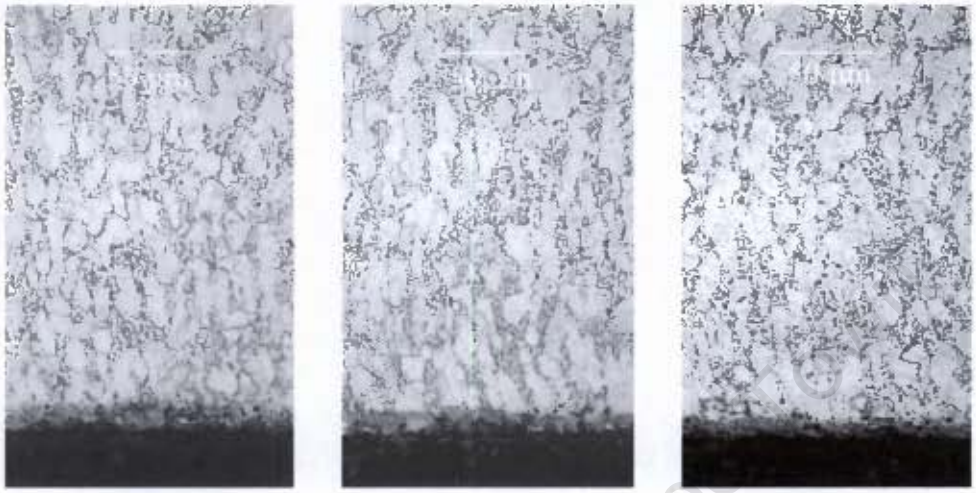

(a) (b) (c)

Figure 4.35: Cross-section micrographs of the samples (a) Ti64-A,Ar-750, (b) Ti64-B,Ar-750 and (c) Ti64-C, Ar-750.

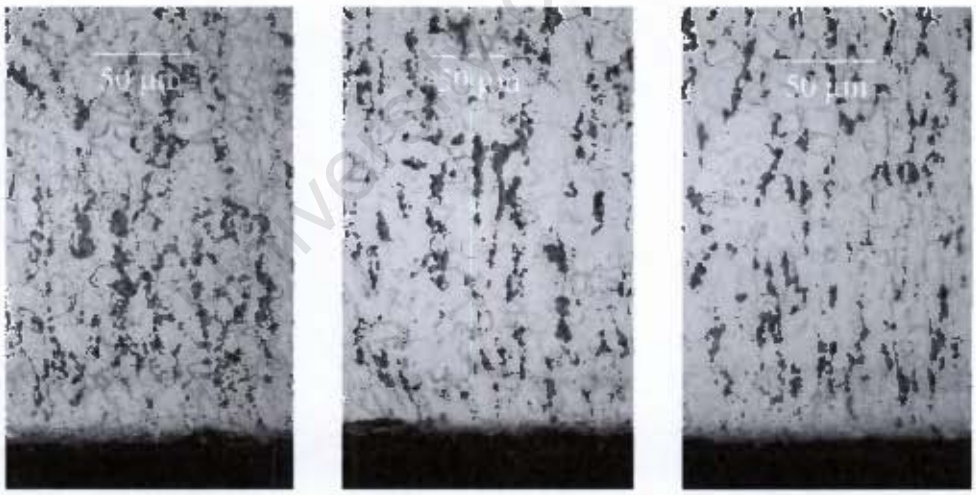

(a) (b) (c)

Figure 4.36: Cross-section micrographs of the samples (a) Ti67-A,Ar-750, (b) Ti67-B,Ar-750 and (c) Ti67-C, Ar-750.

A layer of the β depleted zone on the surfaces of the two alloys is observed on the pre-oxidised samples further heat-treated in an argon atmosphere at 750°C for 20 hours while the same depleted zone was not observed for the pre-oxidised samples further heat-treated in vacuum at 750°C for 20 hours. This is also the case with the

pre-oxidised samples further heat-treated in argon at 850°C for 20 hours showing a more conspicuous β-depleted surface than those further heat-treated in vacuum at 850°C for 20 hours. This further suggests that the argon environment enhances the diffusion of oxygen during the second step of the OBDH which is what was depicted by the hardness profiles of these samples.

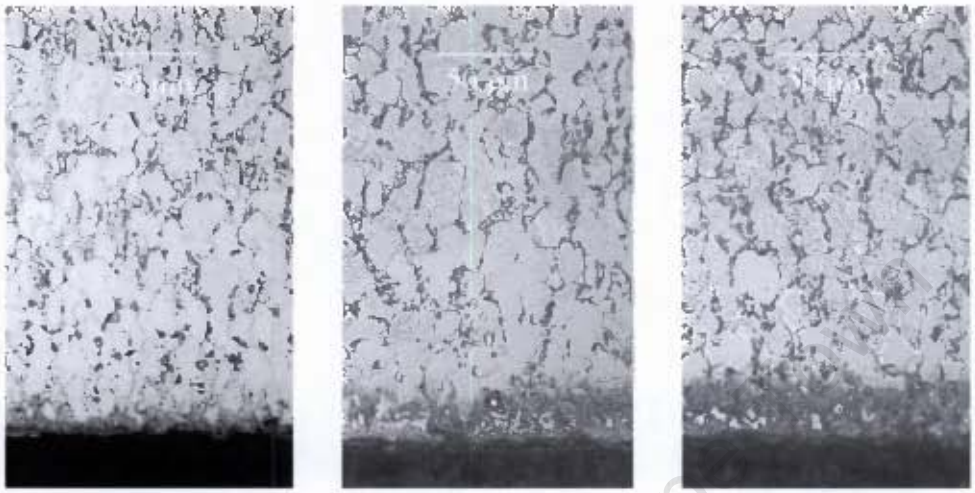

(a) (b) (c)

Figure 4.37: Cross-section micrographs of the samples (a) Ti64-A,Ar-850, (b) Ti64-B,Ar-850 and (c) Ti64-C,Ar-850.

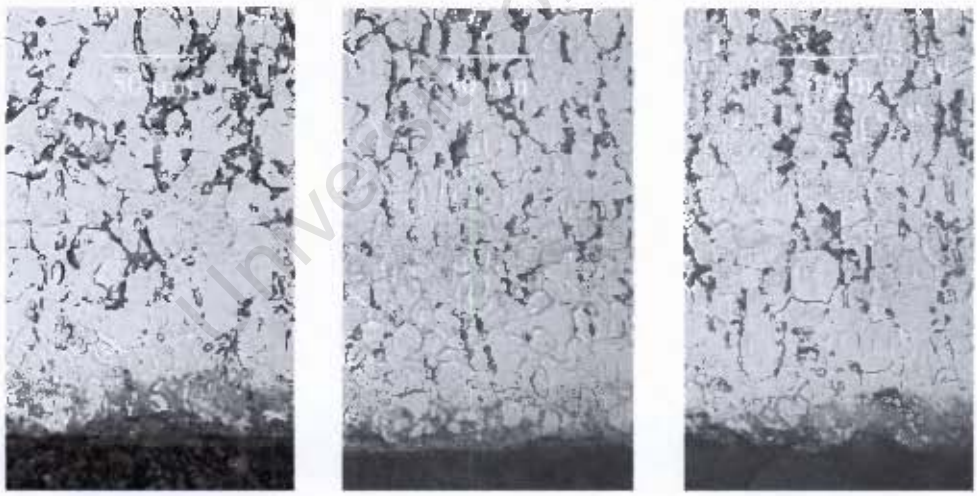

(a) (b) (c)

Figure 4.38: Cross-section micrographs of the samples (a) Ti67-A,Ar-850, (b) Ti67-B,Ar-850 and (c) Ti67-C, Ar-850.

There is powdery texture that was observed on the surfaces of the pre-oxidised samples further heat-treated in an argon atmosphere at 850°C for 20 hours as well as the cycle heat-treated samples. This may further suggest the role of argon as 'paving' way for oxygen to diffuse further resulting in a porous surface.

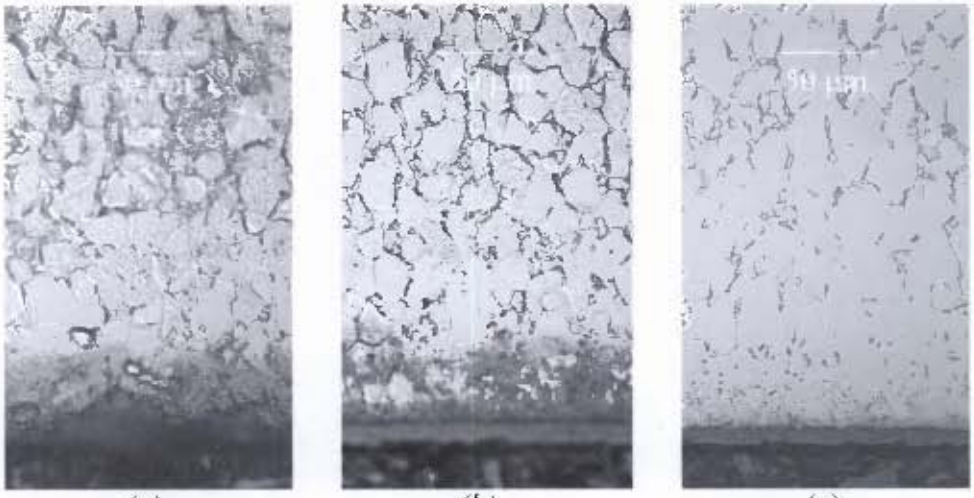

(a) (b) (c)

Figure 4.39: Cross-section optical micrographs for twin cycle samples (a) Ti64-A,Ar-850, (b) Ti64-B,Ar-850 and (c) Ti64-C,Ar-850.

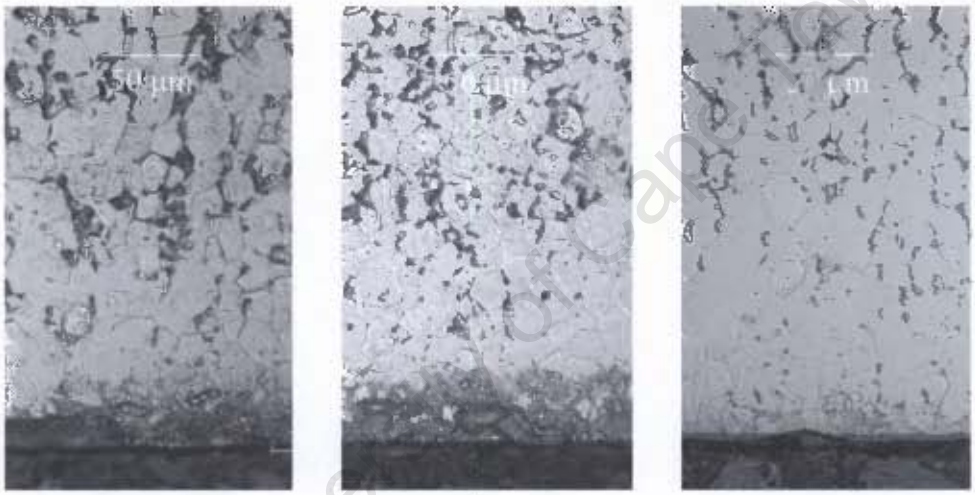

(a) (b) (c)

Figure 4.40: Cross-section optical micrographs for twin cycle samples (a) Ti67-A,Ar-850, (b) Ti67-B,Ar-850 and (c) Ti64-C,Ar-850.

Surface integrity is very important for surface treated components. Surface modification is done on net-shaped components which allow no further alterations after the heat treatment of the component. Therefore a surface heat treatment that causes undesirable effect on the surface is not only problematic due to the extra cost required to rehabilitate the component but the compromised dimensions might render the component unfit for the intended application. Heat-treatments that results in a loose crumbly oxide layer or severe scaling are therefore undesirable.

4.1.4 Surfaces of the Heat-treated Samples

The surfaces of the Ti64 alloy showed a yellow to brown colour with the increasing oxidation temperature. The Ti67 alloy surfaces showed a shiny green colour after oxidation at 600°C for 20 hours and a blue coloured surface upon oxidation at 750°C for 45 minutes and a yellow colour was observed on the surface after oxidation at 850°C for 30 minutes. According to the scale appearances observe by Morton and Baldwin[47], the colour of the surfaces suggests the formation of rutile. Rutile can appear light blue, yellow brown and dark blue depending on the oxidation heat-treatment of the titanium component[47].

After the second step of OBDH the loosely bound scale on the surfaces of the Ti64 test pieces pre-oxidised at 850°C for 30 minutes would spall off. There was restoration of the shiny metallic colour upon further heat-treatment of the pre-oxidised test pieces in vacuum at 750°C for 20 hours. This is as a result of the decomposition of the oxide layer and the release of oxygen into the bulk of the test piece. There was no observed restoration of the lustre on the two alloys upon further heat-treatment in vacuum at 850°C for 20 hours. This is despite the more diffusion that occurred during the further heat-treatment in vacuum at 850°C for 20 hours which resulted in higher surface hardness and deeper diffusion zone than the further heat-treatment in vacuum at 750°C for 20 hours.

Upon heat-treatment of the pre-oxidised samples in argon at 750°C and 850°C for 20 hours the surfaces of the two alloys assumed a greyish-white colour. All the colours may be for different types of rutile or even different oxides. Different types of rutile occur from the stoichiometric rutile to various non-stoichiometric rutile. The table summarising the surface condition upon OBDH is shown in table 4.1. Pictures showing the surface appearances of some of the heat-treated samples are shown in appendix A.

Table 4.1: Summary of the surface condition upon OBDH.

Alloy treatment	Surface colour	Surface quality	Comment
Ti64-A	Brown	Loose and crumbly	Rutile formation
Ti67-A	Yellow	Adherent	Rutile formation
Ti64-B	Yellow-brown	Adherent	Rutile formation
Ti67-B	Shiny blue	Adherent	Rutile formation
Ti64-C	Yellow	Adherent	Rutile formation
Ti67-C	Shiny green	Adherent	Rutile formation
Ti64-A,Vac-850	Dark brown	Flaky	Scaling of the surface
Ti67-A,Vac-850	Greyish-blue	Adherent	Rutile decomposition
Ti64-B,Vac-850	Brown	Slight pitting of the surface	Rutile decomposition
Ti67-B,Vac-850	Greyish-blue	Adherent	Rutile decomposition
Ti64-C,Vac-850	Yellow	Slight pitting of the surface	Rutile decomposition
Ti67-C,Vac-850	Brown	Adherent	Rutile decomposition

Key for the OBDH Samples

Example: Ti64-A,Ar-850

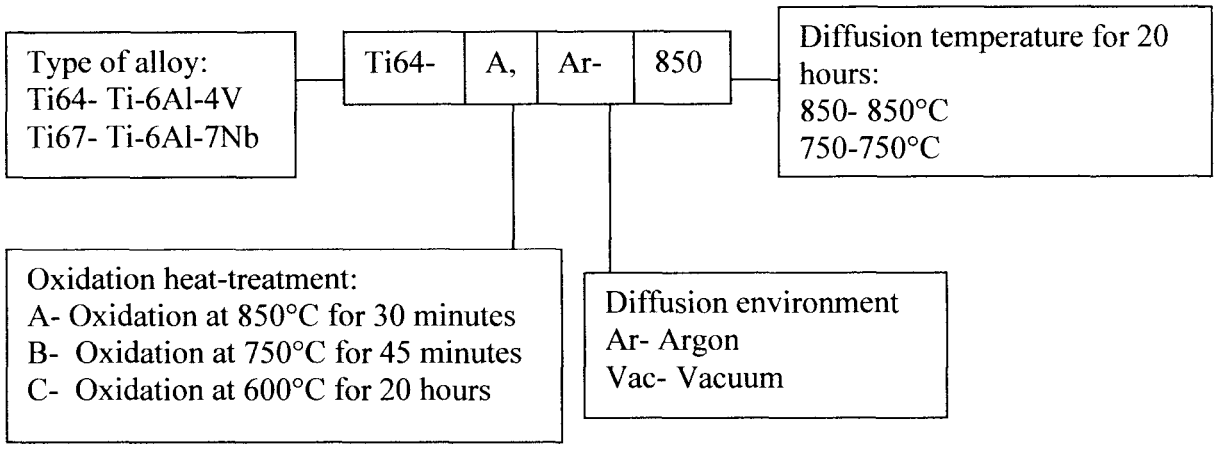

The surface colour and quality of the pre-oxidised samples further heat-treated in vacuum at 750°C for 20 hours is the same as the pre-oxidised samples further heat-treated in vacuum at 850°C for 20 hours. The difference is the more shiny appearance of the surfaces of the pre-oxidised samples further heat-treated in vacuum at 750°C for 20 hours.

All the pre-oxidised samples further heat-treated in argon exhibited a greyish-white colour. The pre-oxidised samples further heat-treated in argon at 850°C for 20 hours had a powdery surface texture.

The samples that were subjected to the twin cycle heat-treatment had a grey-coloured surface. The often flaky surfaces had a tendency to spall off.

Some of the oxygen boost diffusion hardened specimens were subjected to a two-body abrasion wear test using the automatic grinding/polishing machine. This was to ascertain if the increased surface hardness resulted in improved wear resistance. The two alloys in the as-received conditions, the pre-oxidised samples further heat-treated in vacuum/argon at 850°C for 20 hours as well as the twin cycle heat-treated samples underwent the wear testing. The weight loss of these test pieces upon wear-testing under the conditions outlined in the previous chapter was compared to the weight loss of the untreated samples.

4.1.5 Wear

The wear results of the samples are shown below in the form of weight loss as a function of heat-treatment. The present study was not aimed at performing extensive wear tests on the surface treated samples. A preliminary five minute wear test on a single surface of the heat-treated sample against 800 grit SiC paper was performed. This was done only to rank the treated samples and the untreated samples without taking into consideration the contributions of the surface, the oxygen diffusion zone and the base metal on the wear results. A more extensive approach of wear testing will provide wear loss as a function of relative sliding distance. The sliding distance should be increased to a point where the surface treated layer eventually wears away. This test will provide information about the durability of the treated surfaces as opposed to the initial wear resistance and is recommended as a future study. The wear results presented were obtained using a Struers polishing machine (section 3.4.3).

4.1.5.1 OBDH in Vacuum

Upon subjecting the samples to wear testing, the pre-oxidised samples further heat-treated in vacuum at 850°C for 20 hours exhibited lower weight losses than the untreated samples as shown in figure 4.41 below.

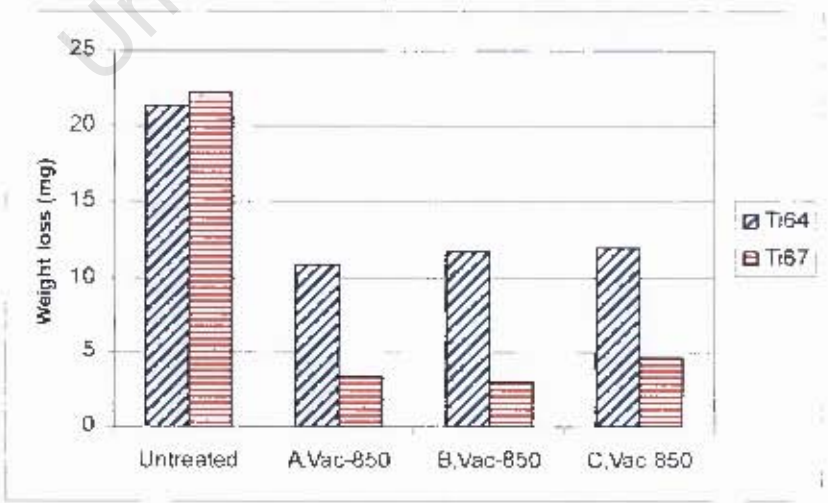

Figure 4.41: Abrasive wear resistance for oxygen boost diffusion (in vacuum) treated and untreated Ti64 and Ti67 alloys.

The OBDH Ti64 alloy shows a reduced weight loss producing an improvement between 71 and 89% over the untreated alloy. The Ti64 alloy pre-oxidised at 850°C for 30 minutes shows the least weight loss, followed by the sample pre-oxidised at 750°C for 45 minutes and then the sample pre-oxidised at 600°C for 20 hours.

A similar trend in terms of pre-oxidation temperature and improved mass loss resistance for the boost diffusion treated Ti67 alloy is observed. The Ti67 alloy shows even more improved mass loss reduction after abrasive wear against 800 grit SiC paper. The weight loss has been reduced by the oxygen boost diffusion hardening heat-treatment, producing an improvement of more than 100% over the untreated alloy for the Ti67 alloy.

Despite the higher surface hardness that was measured for the OBDH Ti64 alloy compared to theTi67 alloy, the OBDH Ti67 exhibits more improved weight loss reduction under the two-body abrasive wear testing that was conducted. The oxide layer that is formed on the surface of the Ti67 alloy during oxidation is more stable and more adherent to the substrate hence the more improved wear for the Ti67 alloy than theTi64 alloy following the boost oxygen diffusion heat-treatment.

4.1.5.2 OBDH in Argon

Following the abrasive wear testing of the pre-oxidised samples further heat-treated in an argon atmosphere at 850°C for 20 hours the weight loss of the samples was compared to the untreated samples in figure 4.42.

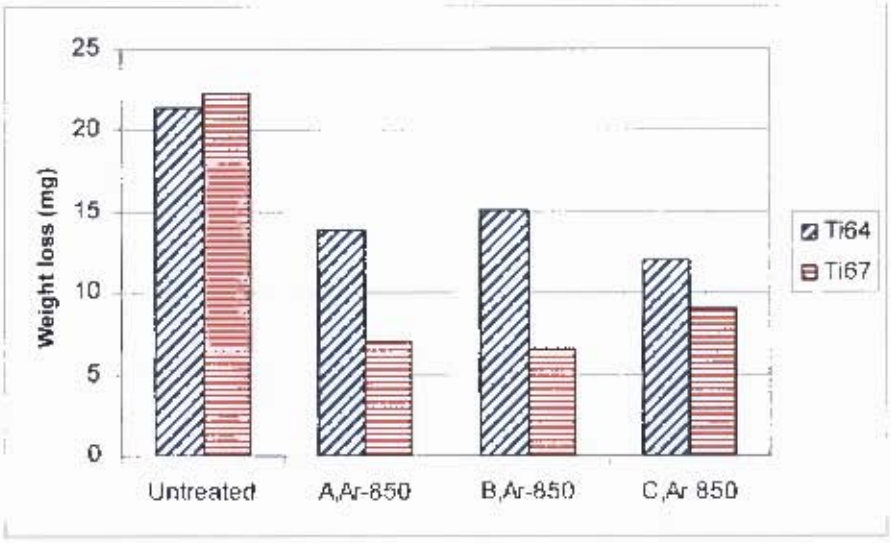

Figure 4.42: Abrasive wear resistance for oxygen boost diffusion (in argon) treated and untreated Ti64 and Ti67 samples.

It can be seen from the figure 4.42 that the weight loss has been reduced upon heat-treating the pre-oxidised samples in an argon atmosphere at 850°C for 20 hours. The Ti64 alloy shows an improved weight loss between 35 and 70% upon the three boost diffusion heat-treatments. As was the case with the pre-oxidised samples further heat-treated in vacuum, the Ti67 alloy shows more improved weight loss reduction than the Ti64 alloy.

Although the pre-oxidised samples further heat-treated in argon measured higher surface hardness they have undergone higher weight loss than the pre-oxidised samples further heat-treated in vacuum against the 800 grit SiC paper. The porosity observed on the surfaces of samples boost diffusion treated in argon has resulted in less improvement on the wear resistance. The interaction of argon gas atoms with the alloy surfaces results in porosity and the less dense porous layer does not improve the tribological properties as much as the boost diffusion heat-treatment that is carried out in vacuum.

4.1.5.3 Twin Cycle OBDH

Performing the twin cycle heat-treatments on the pre-oxidised test pieces further heat-treated in vacuum at 850°C for 20 hours has produced the weight loss profiles depicted by figure 4.43.

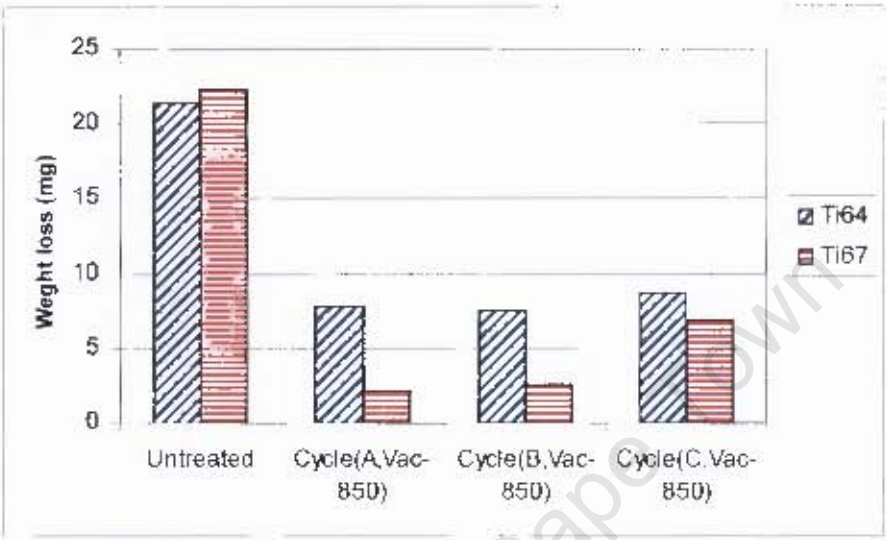

Figure 4.43: Abrasive wear resistance for cycle oxygen boost diffusion (in vacuum) treated and untreated Ti64 and Ti67 samples.

Even more improved weight loss reduction is achieved by performing the twin cycle heat-treatments as suggested by the figure 4.43. This is despite severe scaling of the test pieces upon the twin cycle heat- treatment. More than 100% improvement in weight loss over the untreated material is achieved when abraded by 800 grit SiC paper. The Ti67 alloy still shows higher wear resistance than the Ti64 alloy when abraded by 800 grit SiC paper after the twin cycle heat-treatment. As indicated before, more oxygen intake occurred on the twin cycle heat-treated samples resulting in even more improved tribological properties of the two alloys.

Similarly the twin cycle heat-treatment produces more improvement in weight reduction on the pre-oxidised samples further heat-treated in an argon atmosphere at 850°C for 20 hours as suggested by figure 4.44. Twin cycle heat-treated samples that underwent diffusion in argon shows less wear resistance than the twin cycle heat-treated samples that underwent diffusion in vacuum.

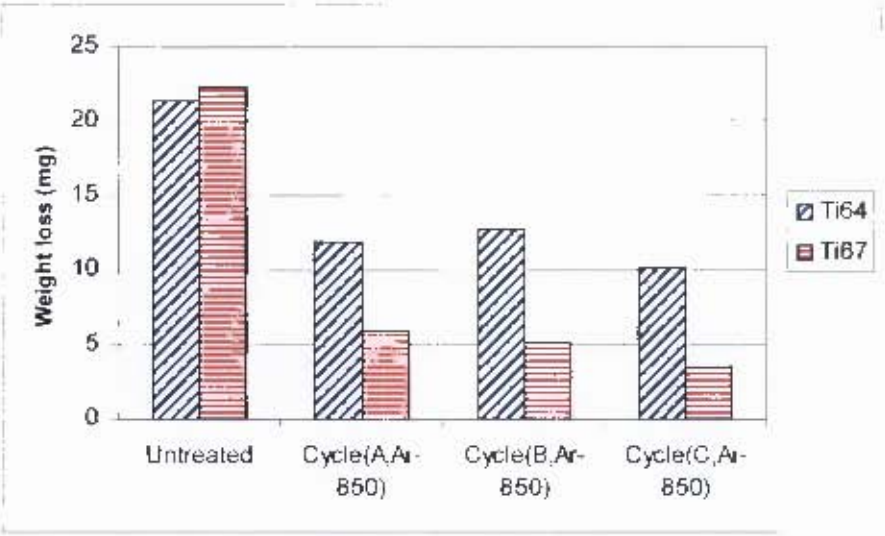

Figure 4.44: Abrasive wear resistance for cycle oxygen boost diffusion (in argon) treated and untreated Ti64 and Ti67 samples.

Chapter Five

Conclusions

Based on the results obtained during this research the following conclusions can be drawn:

- The heat-treatment practice in a controlled saturated argon environment was unsuccessful in developing a significant oxygen diffusion hardened layer.

- The OBDH process can be carried out to modify the surface properties of titanium and alloys. Both steps of this process play a vital role in achieving a thick modified layer for improved tribological properties of titanium and alloys. The first step of oxidation allows for the formation of rutile which becomes an oxygen reservoir for the second step. The second step performed in oxygen and nitrogen depleted environment causes the decomposition of rutile into the bulk material resulting in a thicker hardened zone beneath the surface of the component.

- Oxidation of the Ti-6Al-4V at 850°C for 30 minutes produces the optimal oxide for the second step of OBDH but there is a tendency for the oxide scale to peel off during the air cooling from this temperature.

- There was no peeling off of the oxide scale on the Ti-6Al-7Nb upon air cooling after oxidation at 850°C for 30 minutes which suggests that this alloy has higher thermal stability than the Ti-6Al-4V alloy.

- Performing the oxidation step of OBDH heat-treatment at higher temperatures results in higher surface hardness and deeper diffusion zone than carrying the oxidation step at lower temperatures for longer times provided there is no peeling of the oxide scale during the high temperature oxidation.

- Carrying out the second step of OBDH heat-treatment at higher temperatures increases the rate of diffusion of oxygen resulting in a thicker hardened zone.

- The Ti-6Al-4V achieves higher surface hardness than the Ti-6Al-7Nb upon the same OBDH heat-treatment.

- The second step of the OBDH can also be carried out in an argon environment instead of vacuum. Carrying out the second step in an argon atmosphere allowed for higher surface hardness and thicker hardened zone than carrying the same step in vacuum.

- The effect of OBDH on the underlying microstructures of the two alloys under investigation is the depletion of the β phase on the modified surface as a result of the diffused oxygen which stabilises the α phase. The effect of the OBDH process is more conspicuous on the microstructure of the Ti-6Al-7Nb alloy than on the Ti-6Al-4V after the same OBDH heat-treatment which indicates that less amount of oxygen is influencing the α-β system of the Ti-6Al-7Nb alloy than the α-β system of the Ti-6Al-4V.

- Although higher surface hardness was achieved for the Ti-6Al-4V alloy than the Ti-6Al-7Nb alloy after the same heat-treatment, the Ti-6Al-7Nb alloy achieved higher wear resistance due to more adherence of the oxide scale after the oxidation step.

- Despite achieving higher surface hardness and thicker hardened zone upon carrying out the second step of OBDH in an argon atmosphere than in vacuum, samples which underwent the second step of OBDH heat-treatment in vacuum exhibited higher wear resistance.

- Performing a twin cycle OBDH heat-treatment results in even higher surface hardness and higher wear resistance despite the severe scaling of the alloys upon the heat-treatments.

Chapter Six

Recommendations

Various heat-treatments have been carried out with certain variations from one heat treatment to the other. The following recommendations are made based on the outcome of the heat-treatments:

- The preferred heat-treatment will be the one that has a good combination in terms of achieving optimal tribological properties as well cost effective. A cost effective heat-treatment will be the one that is not performed at very high temperatures and does not take a very long time. Oxidation at 850°C for 30 minutes produced the most improved tribological properties and slightly less than 750°C for 45 minutes where spalling off of the oxide layer occurred during air cooling. Therefore a slower cooling rate on the Ti-6Al-4V from oxidation at 850°C for 30 minutes will result in a more adherent oxide scale.

- A higher oxidation temperature or longer oxidation time can be used on the more thermally stable Ti-6Al-7Nb to achieve an even thicker oxide and a subsequent thicker diffusion zone upon OBDH heat-treatment.

- Higher temperature or longer time than used for this research on second step of the OBDH heat-treatment can be employed for both alloys to increase the rate of diffusion of oxygen into the titanium lattice.

- Carry out the second step of the OBDH heat-treatment in another inert gas such as krypton and xenon to study the effect of these gases on the wear properties of titanium and alloys.

- Carry out the oxidation step in oxygen or a gas mixture with higher oxygen partial pressure than air to investigate the influence of oxidation concentration in the first step of OBDH heat-treatment.

- Perform more extensive wear tests that will provide weight loss as a function of relative sliding distance. The sliding distance should be increased to a point where the surface treated layer eventually wears away. This test will provide information about the durability of the treated surfaces as opposed to the initial wear resistance.

References

1. R. A. Poggie, P. Kovacs and J. A. Davidson, Materials and Manufacturing Processes, **11**, No 2, 185-197, (1996).
2. Http: www.engine.umich.edu, Biomechanics of Artificial joints, (April 2005).
3. Http: www.woke2.com, (April 2005).
4. D. W. Hoeppner and V. Chandrasekaran, Wear, **173**, 189-197 (1994).
5. P. A. Dearnerley, Proc Instn Mech Engrs, **213**, 107-135 (1999).
6. M. Long, H. J. Rack, Biomaterials, **19**, 1621-1639, (1998).
7. G. K. McKee, J Watson-Farrar, Journal of Bone and Joint Surgery, **48-B** (2), 245-259 (1996).
8. P. S. Walker, B. L. Gold, Wear, **17**,285-299 (1971).
9. J. Charnley, Clinical Orthopaedics and Related Research, **72**, 7-21(1970).
10. V. Saikko, Wear, **166**, 169-178(1993).
11. V. Saikko, Wear, **176**, 207-212(1994).
12. R. A. Buchanan, E. D. Rigney, J. M. Williams, Journal of Biomedical Materials Research, **21**, 367-377(1987).
13. C. D. Peterson, B. M. Hillberry, D. A. Heck, Journal of Biomedical Materials Research, **22**, (1988).
14. J. H. Dumbleton, Journal of Biomaterials Applications, **3**, 3-32(1988).
15. A. D. McQuillan, M. K. McQuillan Metallurgy of Rarer Metals, Vol.4 Titanium, Butterworths Publication, 1956.
16. D. R. Askerland, The Science and Engineering of Materials, 3rd S. I. Edition, 1998, Stanely Thornes Ltd, 424-430.
17. R. Venugopalan, J. J. Weimer, M. A. George, L. C. Lucas, Biomaterials, **21**, 1669-1677 (2000)

18. J. C. Keller, C. M. Stanford, J. P. Wightman, R. A. Draugn, R. Zaharias, J Biomed Mat Res, **28**, 939-946(1994).

19. E. T. den Braber, J. E. de Ruijter, H. T. Smits, L. A. Ginsel, A. F. von Recum, Journal of Biomedical Materials Research, **29**, 511-518(1995).

20. A. M. Green, J. A. Jansen, J. P. van der Waerden, A. F. von Recum, Journal of Biomedical Materials Research, **28**, 647-653(1994).

21. J. Meyle, H. Wilburg, A. F. von Recum, J Biomat Appl, **7**, 362-374(1993).

22. J. Meyle, K. Gultig, H. Wolburg, A. F. von Recum, J Biomed Mater Res, **27**, 1553-1557(1993).

23. K. T. Bowers, J. C. Keller, B. A. Randolf, D. G. Wick, C. M. Michaels, J Oral Maxillofac Implants, **7**, 302-310(1992).

24. I. Lavos-Valereto, M. C. Z. Deboni, N. Azambuja, M. M. Marques, Journal of Periontology, **73**, No 8, 900-905, (2002).

25. D. R. Askerland, The Science and Engineering of Materials, S. I. Edition, 1988, Van Nostrand (International) Co. Ltd, 338-350.

26. M. T. Jovanovic, S. Tadic, S. Zec, Z. Miskovic, I. Bobic, Materials and design, **27**,192-199, (2006).

27. Http: www.machinedesign.com, (2005/06/06).

28. V. Oliveira, R. R. Chaves, R. Bertazzoli and R. Caram, Brazilian Journal of Chemical Engineering, **15**, 1-9, (1998).

29. P. F. Barbosa and S.T. Button, Proc Instn Mech Engrs, 214, Part L, 23-32, (2000).

30. J. L. Murray, The Al-Ti (aluminium-titanium) system. Phase diagrams of binary titanium alloys, ASM, 12-24(1987).

31. Atlas of Microstructures of Industrial Alloys, Metals Handbook 8th edition, Vol. 7, 321-334 (1972).

32. R. Shivpuri, J. Hua, P. Mittal, A. K. Srivastava, Industrial, Welding and Systems Engineering, The Ohio State University, Columbus, USA, 1-4(2002).

33. W.R. Kerr, R.R. Smith, M.E. Rosenblum, F.J. Gurney, Y.R. Mahajan and L.R. Bidwell: in 'Titanium 80: Science and Technology', (ed. H.Kimura and O.Izumi), TMS-AIME, Warrendale, PA, 1980, 4, 2477-2486

34. A.A. Ilyn, B.A. Kolachev, and A.M. Mamonov: in 'Titanium '92: Science and Technology', (ed. F.H. Froes and I. Caplan), TMS, Warrendale, PA, 1993, 1, 941-947

35. J. L. Murray, The Nb-Ti (niobium-titanium) system. Phase diagrams of binary titanium alloys, ASM, 188-194(1987).

36. R. M. Streicher, H. Weber, R. Schon and M. Semlitsch, Biomaterials, 12, 125-129(1991).

37. F. Borgioli, E. Galvanetto, A. Fossati, G. Pradelli, Surface and Coatings Technology, **184**, 255-262(2004).

38. R. Venugopalan, J. J. Weimer, M. A. George, L. C. Lucas, Biomaterials, **20**, 1709-1716(1999).

39. H. Dong, and X. Y. Li, Materials Science and Engineering, **A280**, 303-310, (2000).

40. S. M. Johns, T. Bell, M. Samandi, G. A. Collins, Surface and Coatings Technology, **85**, 7-14, (1996).

41. Http//www.corrosion-doctors.org (March 2005).

42. http//www.textorgroup.ch/pdf/publications/booksmonographs/6/Chap_07.pdf.

43. H. Chuanxi, L. Bingnan: in 'Titanium '92: Science and Technology', (ed. F.H. Froes and I. Caplan), TMS, Warrendale, PA, 1993, **II**, 1981-1897.

44. G. L. Humphrey, American chemical Society, **73**, 2261(1951).

45. Dong, et al., United States Patent (6210807), April 3, 2001.

46. P. H. Morton, W. M. Baldwin, Transactions of the American Society for Metals, **44**, 1004(1952).

47. E. A. Gulbransen, F. K. Andrew, Transactions of the American Institute of Mining and Metallurgical Engineers, 185, 741(1949)

48. E. A. Gulbransen, F. K. Andrew, Transactions of the American Institute of Mining and Metallurgical Engineers, **96**, 364(1949).

49. W. L. Finlay, J. A. Snyder, Transactions of the American Institute of Mining and Metallurgical Engineers, **188**, 277(1950).

50. E. S. Bumps, H. D. Kessler, M. Hansen, American Chemical Society Metals, **45**, 1008(1953).

51. T. Tsuji, Journal of Nuclear Materials, **247**, 63-71(1997).

52. T. B. Massalski, H. Okamoto, O. R. Subramanian, L. Kacprzak, Binary alloy Phase Diagrams, 2nd Ed. (ASM International, Metals Park, OH, 1990).

53. H. Guleryuz, H. Cimenoglu, Surface & Coatings Technology, **192**, 164-170(2005)

54. R. I. Jaffee, H. R. Ogden, D. J. Maykuth, Transactions of the American Institute of Mining and Metallurgical Engineers **188**, 1261, (1950)

55. C. Boetcher, Surface Engineering, **16**, No. 2, 148-152, (2000).

56. J. Luo, Z. Zhang, H. Dong, T. Bell, J. Phys. IV France, **120**, 259-268, (2004).

57. M. Dechamps, R. Feldman, P. Lehr, "High temperature oxidation of titanium physical mathematical models", Titanium and titanium Alloys: Scientific and Technological Aspects, Third International Conference on Titanium, edited by Williams J. C. and Belov A. F., Vol 2 (Plenum Press, New York, 1980) pp. 1045-1056.

58. Z. Liu, G. Welsh, Metallurgical Transactions A, **19A**, 1121-1125(1988).

59. T. Hurlen, Journal of the Institute of Metals, **89**, 128-136(1960-1961).

60. U. Diebold, J. Lehman, T. Mahmoud, M. Kuhn, G. Leonardelli, W, Hebenstreit, M. Schmid, P. Varga, Surface Science, **411**, 137-153(1998).

61. M. A. Barteau, Chemical. Reviews, **96**, 1413(1996).

62. M. A. Barteau, Journal of Vacuum Science& Technology A, **11**, 2162(1996).

63. M. Li, W. Hebenstreit, U. Diebold, Surface Science, **414**, L951-L956(1998).

64. J. Unnam, R. N. Shenoy, Oxidation of Metals, **26**, 231-252(1986).

65. K. Haufe, Oxidation of Metals, Plenum, New York, 1965.

66. D. R. Gaskel, Introduction to Metallurgical Thermodynamics, 2nd edition, Hemisphere, Washington, 1981.

67. S. Krol, W. Grzesik, Z. Zalisz, M. Hepner, Tribology International, **37**, 633-643(2004).

68. W. C. Oliver, R. Hutchings, J. B. Pethica, Metall. Trans. A, **15**, 2221(1984).

69. D. F. Moore, Principles and Applications of Tribology, Pergamon Press, Oxford, 1975.

70. J. Crank, The Mathematics of Diffusion (Clarendon Press, Oxford, 1956).

71. C. E. Shamblen, T. K. Redden, "Air contamination and embrittlement of titanium alloys", The Science, Technology and Application of Titanium, First International Conference on Titanium, edited by R. I. Jaffee and N. E. Promisel (Pergamon Press, London, 1970) pp. 199-208.

72. S. Zinelis, The Journal of Prosthetic Dentistry, **84**, No. 5, 575-582, (2000).

Appendix A: The Appearance of the alloy Surfaces After the First as well as the Second Step of the OBDH Heat-treatment.

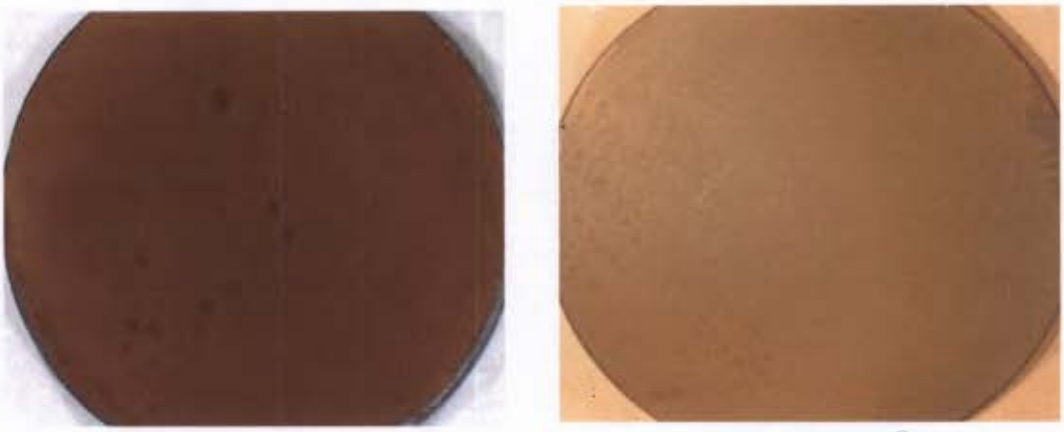

(a) (b)

(a) Ti64 and (b) Ti67 alloys after oxidation at 850°C for 30 minutes.

(a) (b)

(a) Ti64 and (b) Ti67 alloys after oxidation at 750°C for 45 minutes.

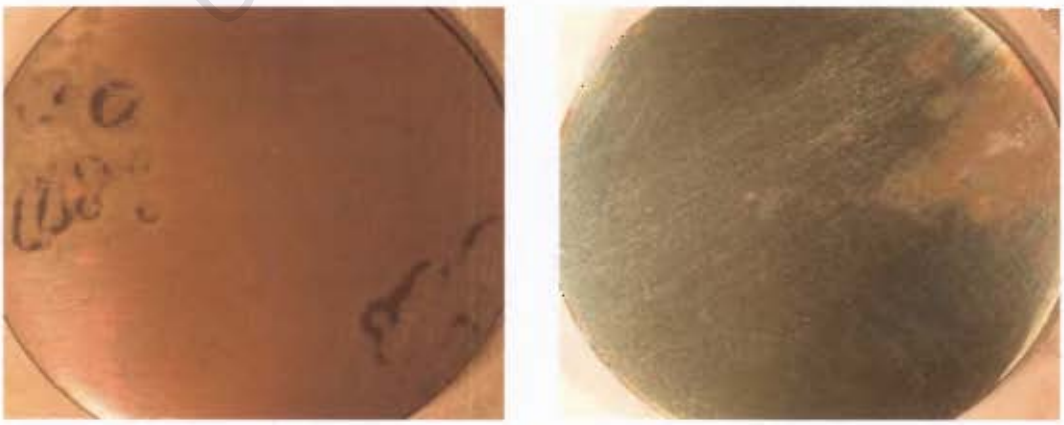

(a) (b)

(a) Ti64 and (b) Ti67 alloys after oxidation at 600°C for 20 hours.

(a) (b)

(a) Ti64 and (b) Ti67 alloys after oxidation at 850°C for 30 minutes followed by heat-treatment in vacuum at 750°C for 20 hours.

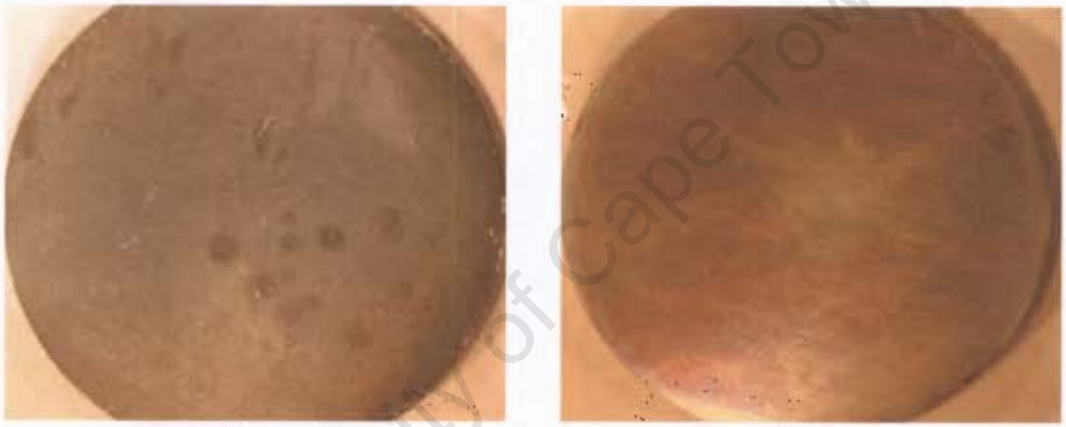

(a) (b)

(a) Ti64 and (b) Ti67 alloys after oxidation at 750°C for 45 minutes followed by heat-treatment in vacuum at 750°C for 20 hours.

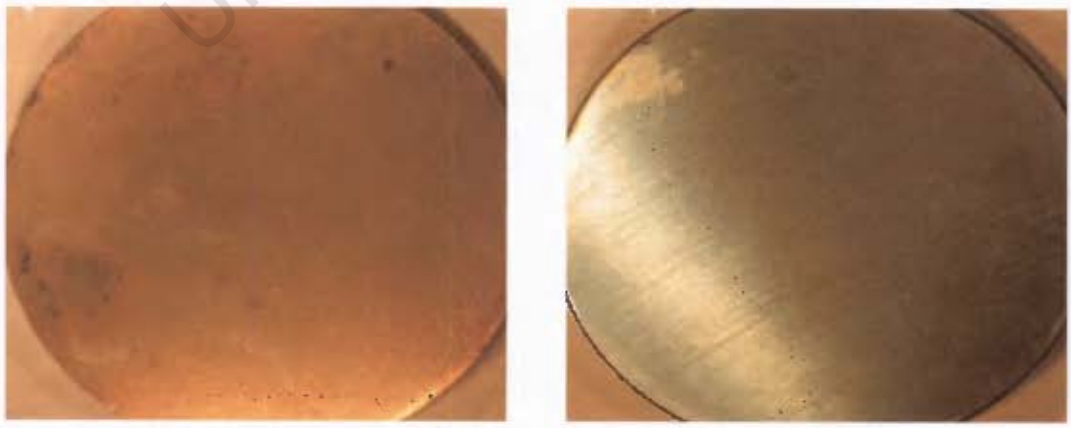

(a) (b)

(a) Ti64 and (b) Ti67 alloys after oxidation at 600°C for 20 hours followed by heat-treatment in vacuum at 750°C for 20 hours.

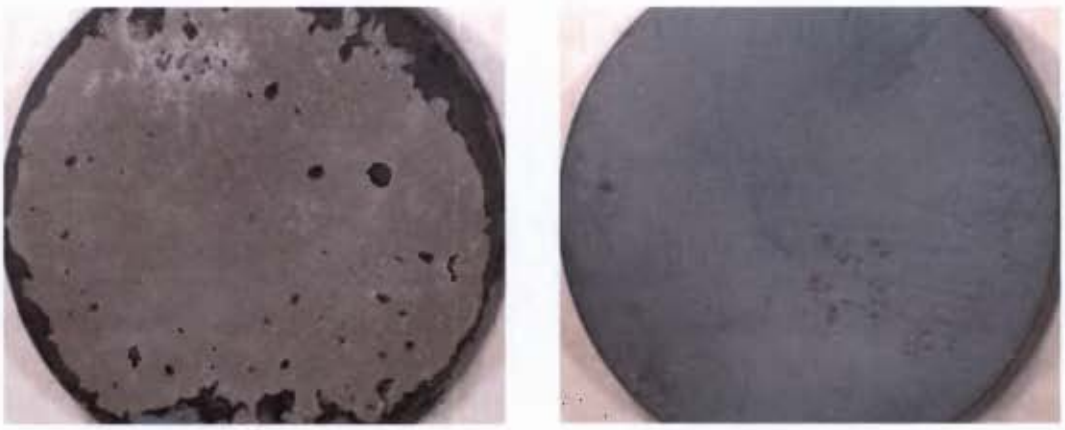

(a) (b)

(a) Ti64 and (b) Ti67 alloys after oxidation at 850°C for 30 minutes followed by heat-treatment in Argon atmosphere at 750°C for 20 hours.

(a) (b)

(a) Ti64 and (b) Ti67 alloys after oxidation at 750°C for 45 minutes followed by heat-treatment in Argon atmosphere at 750°C for 20 hours.

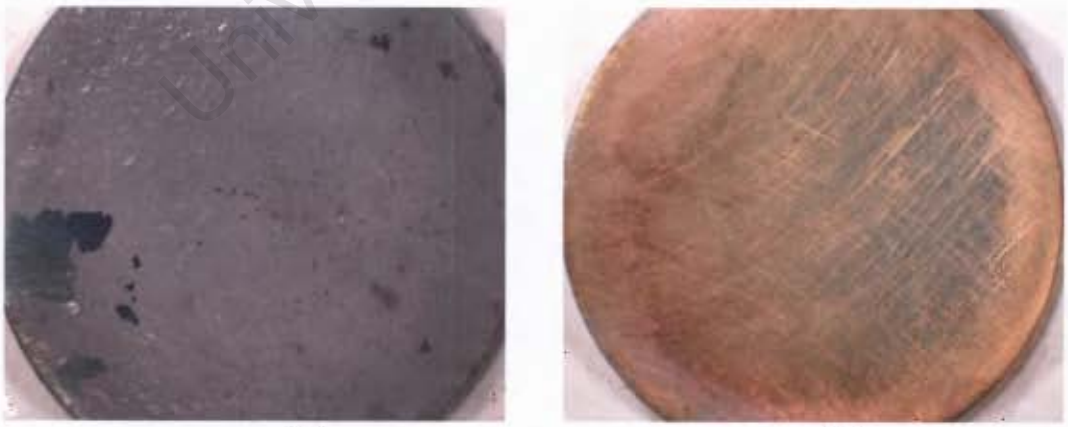

(a) (b)

(a) Ti64 and (b) Ti67 alloys after oxidation at 600°C for 20 hours followed by heat-treatment in Argon atmosphere at 750°C for 20 hours.

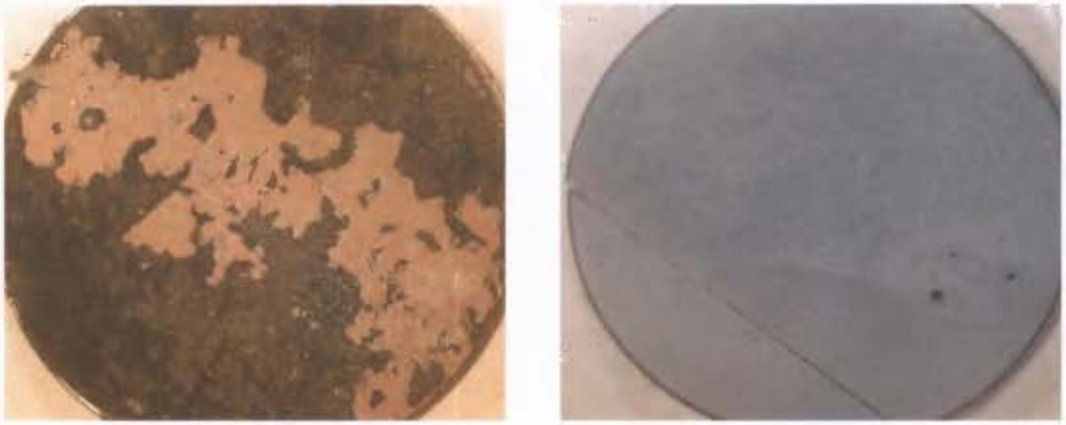

(a) (b)

(a) Ti64 and (b) Ti67 alloys after oxidation at 850°C for 30 minutes followed by heat-treatment in vacuum at 850°C for 20 hours.

(a) (b)

(a) Ti64 and (b) Ti67 alloys after oxidation at 750°C for 45 minutes followed by heat-treatment in vacuum at 850°C for 20 hours.

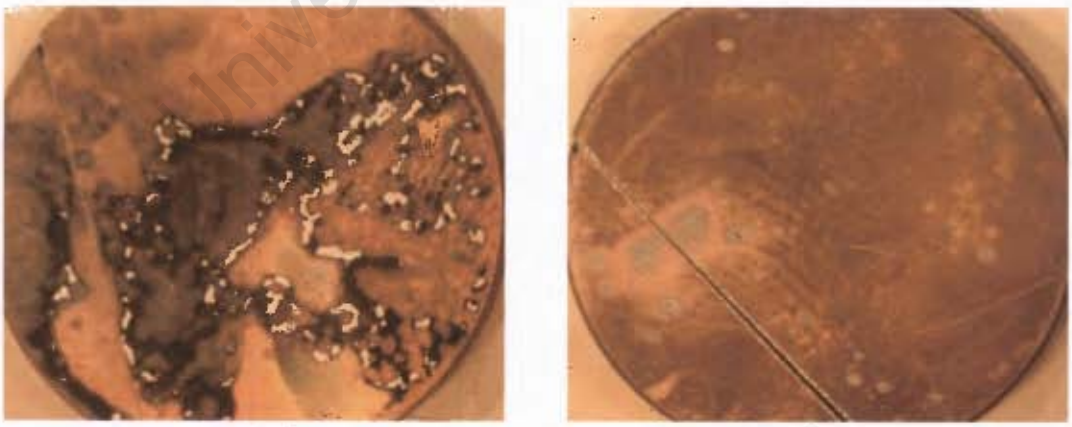

(a) (b)

(a) Ti64 and (b) Ti67 alloys after oxidation at 600°C for 20 hours followed by heat-treatment in vacuum at 850°C for 20 hours.

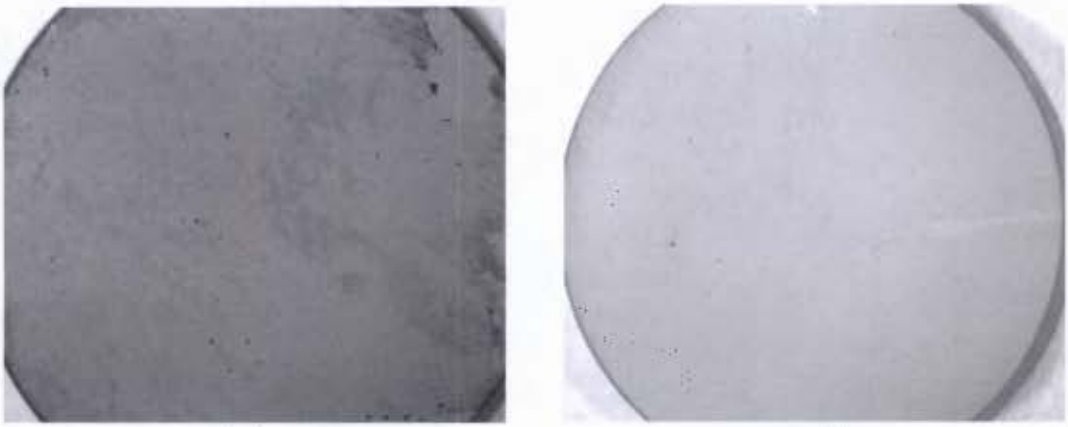

(a) (b)

(a) Ti64 and (b) Ti67 alloys after oxidation at 850°C for 30 minutes followed by heat-treatment in Argon atmosphere at 850°C for 20 hours.

(a) (b)

(a) Ti64 and (b) Ti67 alloys after oxidation at 750°C for 45 minutes followed by heat-treatment in Argon atmosphere at 850°C for 20 hours.

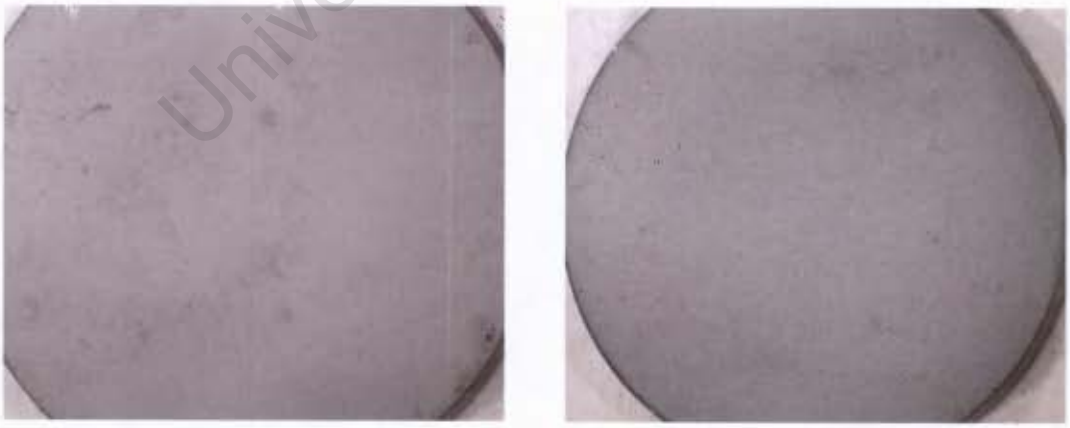

(a) (b)

(a) Ti64 and (b) Ti67 alloys after oxidation at 600°C for 20 hours followed by heat-treatment in Argon atmosphere at 850°C for 20 hours.

Appendix B: Elemental Composition Specifications and Mechanical Properties of Wrought and Cast Ti-6Al-4V Alloys.

Table 2.4a: Elemental composition specifications for wrought Ti-6Al-4V alloys[5].

Weight (%) Standard	Ti	Al	V	N	C	O	H	Fe	Y
BS 7252 Part 33: 1990 and ISO 5832-3: 1996 (E)	Balance	5.5 - 6.75	3.5 - 4.5	0.05 max	0.08 max	0.20 max	0.015* max	0.30 max	
ASTM F1472 - 93	Balance	5.5 - 6.75	3.5 - 4.5	0.05 max	0.08 max	0.20 max	0.015* max	0.30 max	0.005 max
ASTM F136 - 96	Balance	5.5 - 6.75	3.5 - 4.5	0.05 max	0.08 max	0.20 max	0.012† max	0.25 max	

* Maximum hydrogen content for billets 0.010 wt %

† Section sizes of 0.813 mm and under may have a hydrogen content up to 0.0150 wt %

Table 2.4c: Mechanical properties of wrought Ti-6Al-4V alloys[5].

Standard	Minimum Tensile strength (MPa)	Minimum 0.2% proof strength (MPa)	Minimum % elongation	Minimum % reduction on area	Hardness (Rockwell C)
ASTM F136 - 96*	860	795	10‡	25‡	Unspecified
ASTM F1472 - 93	930	860	10	20 – 25	Unspecified
BS 7252: Part 3: 1990†	860	780	10	25	Unspecified
ISO 5832 - 3: 1996 (E)	860	780	10	Unspecified	Unspecified

* For sizes (diameter or thickness) between 4.75 and 44.45 mm in the annealed condition.

† For bar diameter or thickness up to 75 mm.

‡ In the longitudinal direction of the test bar.

Appendix C: Values for the Pilling-Bedworth ratio, R of various metal oxides[41].

Protective oxides	Non-protective oxides
Be 1.59	K 0.45
Cu 1.68	Ag 1.59
Al 1.28	Cd 1.21
Cr 1.99	**Ti 1.95**
Mn 1.79	Mo 3.40
Fe 1.77	Hf 2.61
Co 1.99	Sb 2.35
Ni 1.52	W 3.40
Pd 1.60	Ta 2.33
Pb 1.40	U 3.05
Ce 1.16	V 3.18